CRITICAL REVIEWS IN SOLID STATE AND MATERIALS SCIENCES
2022, VOL. 47, NO. 1, 1–45
https://doi.org/10.1080/10408436.2021.1886042

Taylor & Francis
Taylor & Francis Group

REVIEW

A review on friction stir-based channeling

Kush P. Mehta[a,b] and Pedro Vilaça[a]

[a]Department of Mechanical Engineering, School of Engineering, Aalto University, Espoo, Finland; [b]Department of Mechanical Engineering, School of Technology, Pandit Deendayal Energy University (formerly known as Pandit Deendayal Petroleum University), Gandhinagar, Gujarat, India

ABSTRACT

Friction stir-based channeling is a solid-state processing encompassing the friction stir channeling (FSC) and its variants. In one manufacturing action, the FSC delivers a subsurface internal closed channel in a monolithic plate with no length limitation. The unique characteristics of theses internally closed channels produced with FSC can fit the demand from several industrial fields, namely lightweight structurally stiffened panels and applications where high power density requires highly efficient thermal management systems, such as power electronics and electric vehicles-based transportation. This first review on the FSC and its variants encompasses a systematic and comprehensive understanding on physical properties, including thermal performance and channel manufacturability applied to different engineering materials. The discussion is emphasized on working principle of channel formation, tool design, influence of process parameters, geometrical characterization, mechanical properties, hardness field and microstructural features correlated with mechanical properties. It can be summarized that novel processing of channels by FSC enhances the thermal performance compared to conventional fabrication techniques. FSC can produce complex path channels with various sizes, shapes and surface finishing. Precise control on process parameters and material flow governs the channel formation that subsequently influences thermal and mechanical performances of the channels. FSC has been applied to different range of thermal management systems and has potential for many demanding existent applications and enabling new high-performance products. From the initial FSC concept based on a shoulder-workpiece clearance, to the most recent solutions, such as the stationary shoulder FSC, and the no-tilt-angle and no-shoulder-workpiece clearance, allowing the manufacturing of large size channels, leaving the processed surface at its original quota and ready to be used. A significant leap is introduced with the Hybrid FSC enabling simultaneous welding and channeling, of similar and dissimilar metal components, and therefore, enhancing design opportunities for even more competitive solutions.

KEYWORDS

Review; friction stir channeling; microstructures; properties; solid-state; tool design; thermal management

Table of contents

CONTACT Pedro Vilaça pedro.vilaça@aalto.fi

1. Introduction

Friction-based manufacturing has acquired remarkable success in the field of manufacturing due to be an highly sustainable processing, via high efficiency and low energy consumption, usage of minimum resources typically discarding the demand for shielding gas and filler metal or machining of special beveled joint preparation, negligible emission of radiation and fumes. Other appreciated benefits are low distortion, cost saving, multimaterial manufacturing ability and typically good metallurgical properties typical from high quality solid state forging operations.[1,2] Friction-based manufacturing works on solid-state physical domain with thermo-mechanical activation, wherein the plastic deformation of base materials is obtained under a complex dynamic action of multiaxial compression and heat that subsequently lead materials into visco-plastic behavior.[2–5] In friction-based manufacturing, the heat is mostly generated from dissipation of energy during bulk plastic deformation of the work-pieces being processed, but also from friction inherent to the rubbing action between the components, with or without using external nonconsumable tool.[6–8] Based on these process fundaments, various techniques exist and are being developed envisaging distinct applications encompassing a wide range of different engineering materials. Some of the most popular inventions of friction-based manufacturing are presented in Figure 1.

Friction stir channeling (FSC) is a type of friction stir-based manufacturing technique, derived from the process principle of friction stir welding and processing (FSWP).[9] The FSC produces internal closed free path of channel along with capabilities to govern shape and size of channel, within a single manufacturing step. The unique characteristics of the channels produced with FSC can fit the demand from several potential industrial fields namely electronics, electric vehicles-based transportation (e.g. automotive and aeronautic industries) and chemical industries. Specific FSC applications are manufacturing of compact heat exchangers, fabrication of composites with channels, channels with metallic structures for cables path, nondestructive testing (NDT) wires' path, power generation structures, aerospace/transport structures, embedded instrumentation, lubrication networks, fluid storage/hydraulics, fabricating hollow panels and structures for light weight assemblies, condensers and evaporators in air-conditioned and refrigeration and aircraft oil-coolers.[10,11] FSC of different thermal management systems are popular and promisingly applied to produce inbuilt cooling path and different size of heat exchangers. Figure 2 shows some of the interesting applications of FSC for thermal management systems, such as heat exchanger by Nippon light metal, heat sink component for ABB semiconductors, water cooled engine blocks and radiators of automobile engines, water cooled vacuum chamber by Kurt J Lesker, panel for pre-pressing of fish blocks before quick freezing, cooling system solution for batteries of electric vehicles and helical coil heat exchangers.[12] The complex cooling path of channels by FSC with different size, shape and internal surface features is especially appropriate for manufacturing of compact heat exchangers FSC. The classification of heat exchangers are presented by Kandlikar and Grande[14]

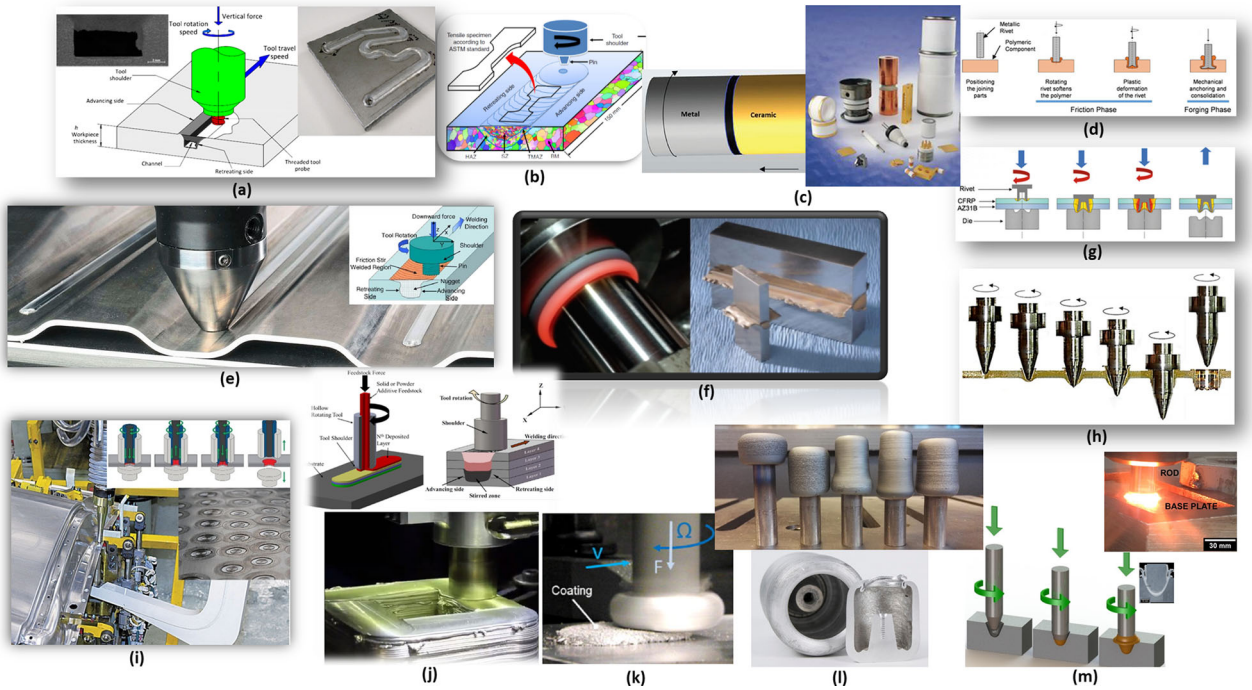

Figure 1. Popular friction-based manufacturing processes: (a) Friction stir channeling[43, 44]; (b) Friction stir processing[92]; (c) Friction brazing[93, 94]; (d) Friction riveting[95]; (e) Friction stir welding[96, 97]; (f) Friction welding[98, 99]; (g) Friction self-piercing riveting[100]; (h) Friction drilling[101]; (i) Friction stir spot welding[102]; (j) Friction stir additive manufacturing[103-105]; (k) Friction surfacing[5]; (l) Friction flash to tube[106]; (m) Friction hydro pillar processing[107].

and Mehendale et al.[15] (summarized in Table 1) based on the channel's size (i.e. equivalent hydraulic diameter). The hydraulic diameter is an equivalent dimension used in the analysis of flow fluids in non-circular channel shapes. It is defined as the ratio of four times the area of the cross-section to the wetted perimeter of the channel.[16] Manufacturing process of these channels influences the performance of the heat exchanger. FSC can produce compact, mesosized and microsized heat exchangers. FSC is observed as better as compared to drilling, milling and electro discharge machining in terms of heat transfer capabilities, surface roughness and channel path variations, low cost processing, higher production rate and a single step manufacturing.

The fast development pace of the FSC technique encompasses already different friction stir-based channeling techniques, such as, FSC with and without shoulder-workpiece clearance, stationary shoulder FSC and hybrid FSC. Ongoing progress brings bigger channels, with improved process stability, and enabling welding and channeling simultaneously, as a one-step manufacturing solution. There is no literature yet, with a comprehensive overview and analysis on this friction stir-based processing for obtaining functional channels and corresponding properties. Because the amount of studies involving the friction stir-based channeling are now significant, it is worth to collect and process the information toward guidelines envisaging further developments and applications. The present review provides detailed information on working principle of friction stir-based channeling, influence of process parameters, channel formation characterization, microstructural features, variations in mechanical properties and channel capabilities.

2. Process development and description

The concept of channeling using friction-based processing techniques is grown from a tunnel (also known as extension of wormhole defect) to a dedicated channel formation. The main distinguishable process variants can be classified among the following groups: FSC with shoulder-workpiece clearance (with or without tilt-angle); FSC without shoulder-workpiece clearance with rotary shoulder; Stationary shoulder FSC (without shoulder-workpiece clearance); and Hybrid FSC. The development of these FSC variants, with the historic milestones, is shown in Figure 3.

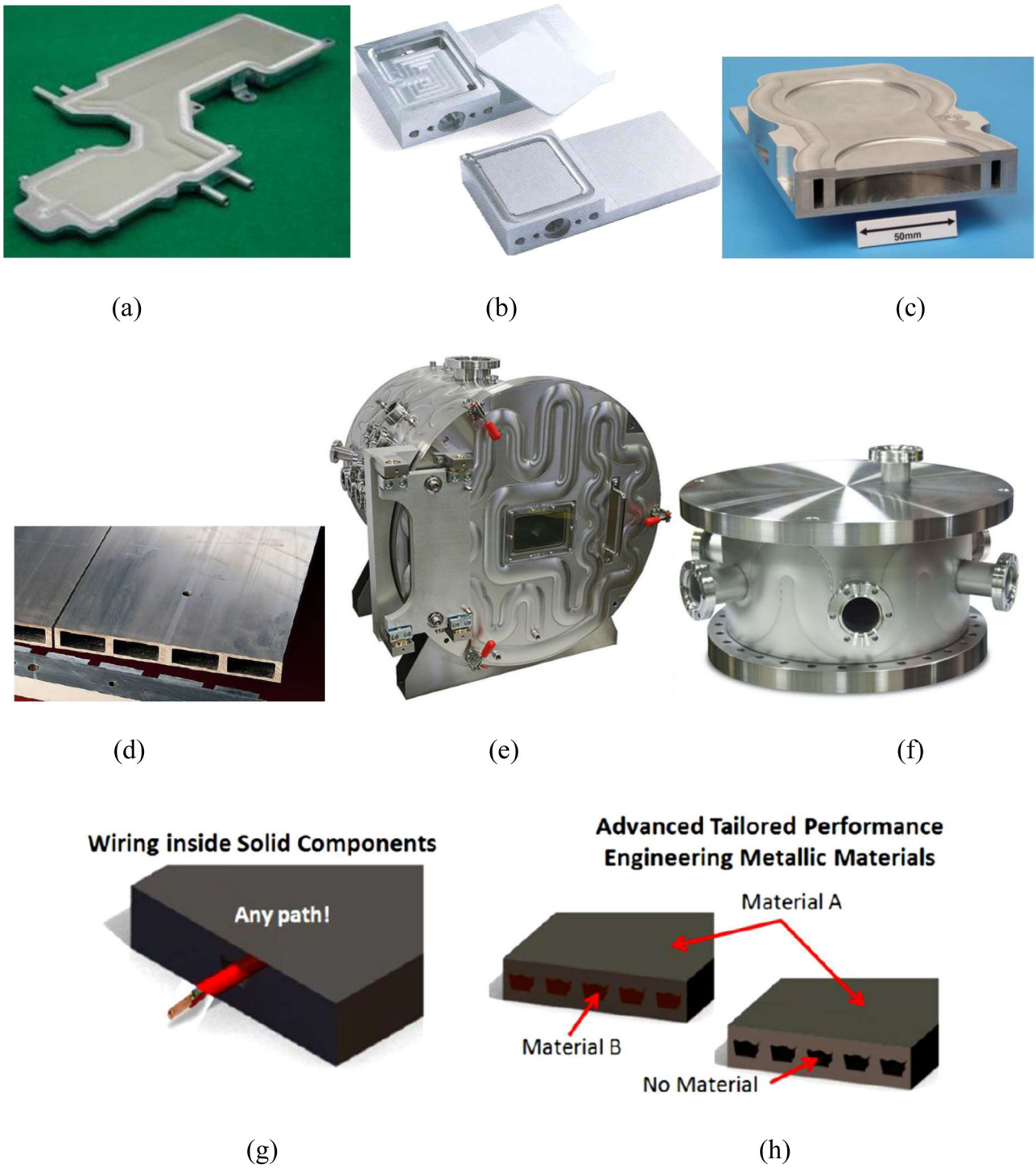

Figure 2. Applications of FSC, (a) Heat exchanger,[12] (b) Heat sinks for semiconductors,[12] (c) Water cooled engine block,[12] (d) Panel for pre pressing of fish blocks before quick freezing,[12] (e, f) Cooling channels in the wall chamber[13] (g) Wiring inside solid component and (h) Metallic core composites made with channels.[9]

2.1. Friction stir channeling with shoulder-workpiece clearance

In case of FSWP, the nonconsumable rotating tool (consists of probe and shoulder) is plunged into the workpiece, to obtain viscoplastic behavior surrounding to the probe.[17–20] The stirring effects and subsequent recrystallization lead weld formation in case of friction stir welding (FSW) between two workpieces[21–24] while alter the microstructures and properties in case of friction stir processing (FSP) for monolithic workpiece.[25–29] The stirring process is governed by the tool geometric features, rotational and travel speeds,

Table 1. Heat exchanger classification based on hydraulic diameter.

Classification by Kandlikar and Grande[14]		Classification by Mehendale et al.[15]	
Conventional channels	$D > 3$ mm	Micro-heat exchangers	$D = 1 - 100\,\mu$m
Mini channels	$3\text{ mm} \geq D > 200\,\mu$m	Meso-heat exchangers	$D = 0.0001 - 1$ mm
Microchannels	$200\,\mu\text{m} \geq D > 10\,\mu$m	Compact heat exchangers	$D = 1 - 6$ mm
Transitional channels	$10\,\mu\text{m} \geq D > 0.1\,\mu$m	Conventional heat exchangers	$D > 6$ mm
Transitional microchannels	$10\,\mu\text{m} \geq D > 1\,\mu$m		
Transitional nano-channels	$1\,\mu\text{m} \geq D > 0.1\,\mu$m		
Molecular nano-channels	$0.1\,\mu\text{m} > D$		

D is hydraulic diameter of the channel.

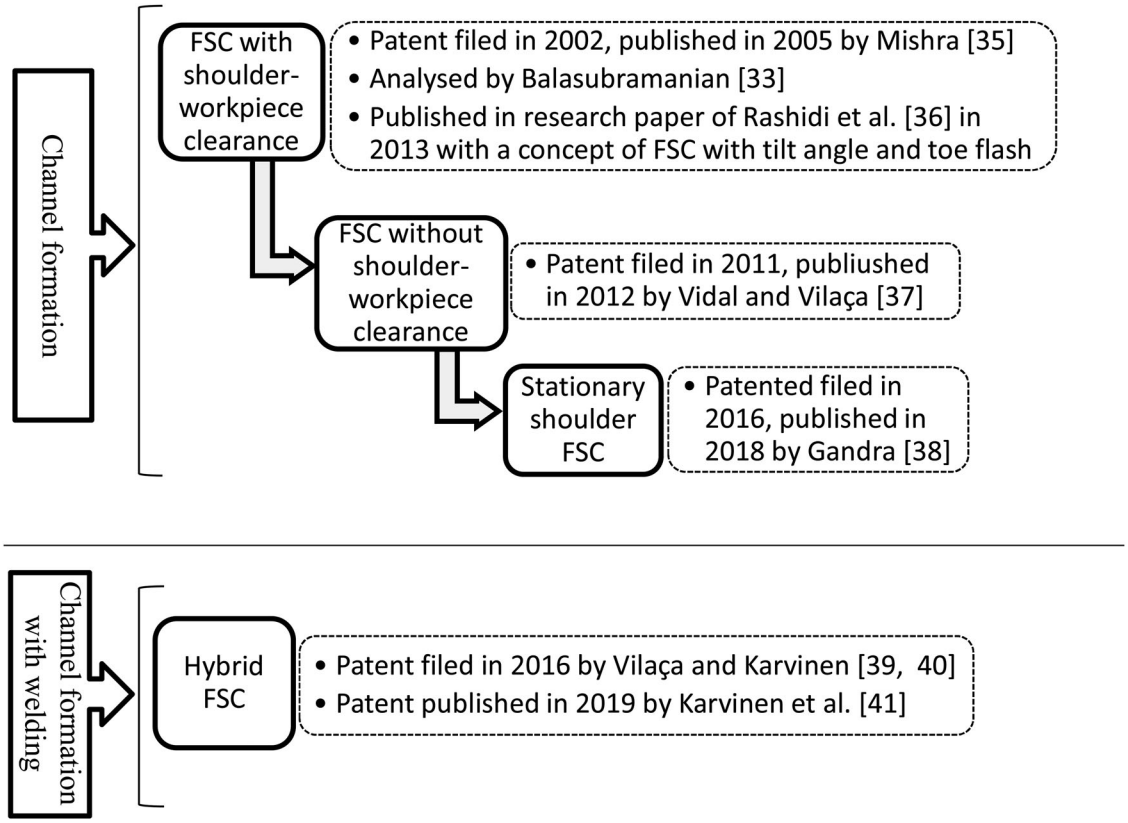

Figure 3. Classification of main FSC process variants and historic milestones.

tool tilt angle, downward force, tool position, equipment, process control, fixture design and properties of base materials.[17–23] Improper processing conditions influence viscoplastic material flow that in turn produces defects.[30–32] Formation of wormhole (i.e. cavity within the stir zone) is one of such defects that is caused due to improper material flow caused by processing parameters.[33–37] Utilizing this defect formation concept, that occurs in FSW as well as in FSP, Mishra[38] introduced FSC patented in year 2002 and published in 2005, with an extension of worm-hole defect throughout the path of tool's travel.

To obtain channel, Mishra[38] applied shoulder-workpiece clearance as shown in Figure 4b with combination probe's threaded direction and tool's rotation direction, the material from the workpiece flows toward the shoulder-workpiece clearance. This material extraction from workpiece and deposition in-between shoulder-workpiece clearance subsequently forms cavity within the stirred zone region. The material extraction from the workpiece can either be obtained by combination of left-hand threaded probe with anticlockwise tool's rotation direction or right-hand threaded probe with clockwise tool's rotation direction. The subsurface channel is produced by the continuous process of material extraction from workpiece and consequent deposition within the shoulder-workpiece clearance along the movement of tool.

2.2. Friction stir channeling with tilt angle and toe flash

FSC with tilt angle and flash is tested by Rashidi et al.,[40] wherein the tool consists of thread-less

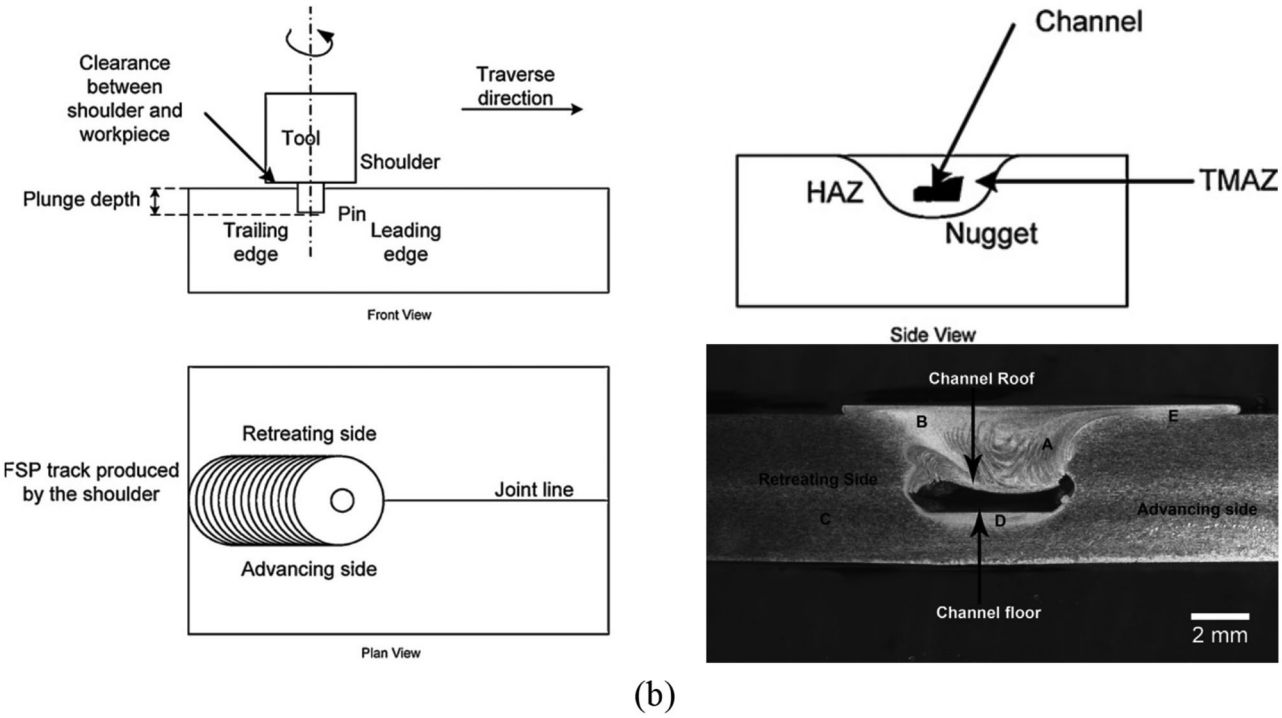

Figure 4. Process description of Friction stir channeling with shoulder-workpiece clearance.[39]

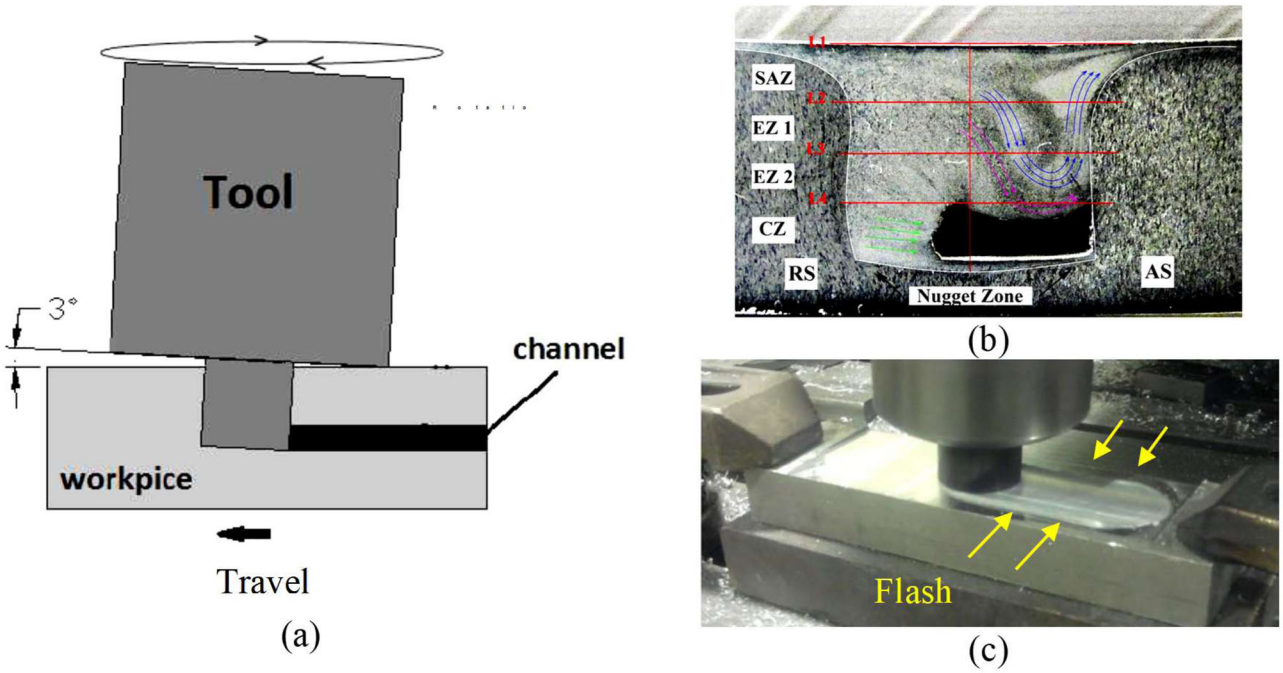

Figure 5. FSC with tilt angle and toe flash (a) process description, (b) channel formation and (c) toe flash effect.[41]

cylindrical or conical probe that makes a contact by shoulder's trailing edge with the workpiece using higher tool tilt angle such as 2° to 3°. Figure 5a shows this approach, named as modified friction stir channeling, but in fact there is no modification from FSC, but only using the classical FSW approach with lack of contact pressure applied by the shoulder on the surface being processed, creating a defect previously reported as tunnel defect. So, in practice the authors have an FSC approach depositing the material in the shoulder-workpiece clearance left empty by the tilt angle. In this approach, the thread less probe and high tool tilt angle result in reversal of vertical material flow toward the direction of shoulder from the processed area, which in turn produces channel with extracted material left as overthickens and increased

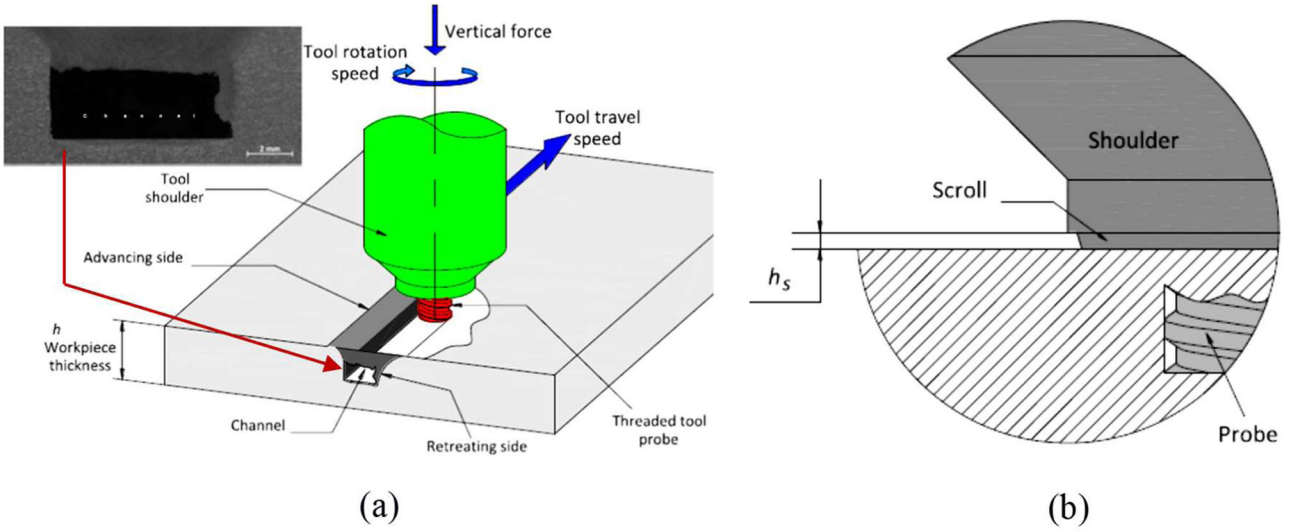

Figure 6. Friction stir channeling without shoulder-workpiece clearance (a) process description[43] and (b) scroll feature of the shoulder making contact with the workpiece surface.[44]

flash on the surface of the workpiece. Other non-consubstantiated claims, such as that the step defect of FSC with shoulder-workpiece clearance can be greatly eliminated are presented in Refs. [40, 41]. In fact, the extracted material is presented as non-self-extractable toe flash, as can be seen from Figure 5c, or as a step over the processed surface, as discussed later in subsection 3.5. This extracted material needs to be removed with post-processing step, as in the original FSC concept. Also, the claim that with hotter conditions, the great fluidity of material leads to better extraction is pending on demonstration as the material domain in viscoplasticity, and sensitive to the tool action, reduces in volume with the inherent lower viscosity.

2.3. Friction stir channeling without shoulder-workpiece clearance

FSC without shoulder-workpiece clearance is invented by Vidal and Vilaça,[42] wherein the customized channel can be obtained with larger size and better control of the shape, as compared to the previous FSC variants. A specially designed tool consisting of threaded probe and a scroll shoulder feature is inserted into the workpiece as shown in Figure 6a. During the FSC processing, the scrolled shoulder is at the original workpiece surface quota and in permanent low pressure contact with the workpiece surface as shown in Figure 6b. The channel fabricated by FSC without shoulder-workpiece clearance, can produce large size channels because the volume of material extracted from the workpieces, to produce the channel, is fully removed from the processing zone, and there is a permanent forging pressure applied by the shoulder, that closes the subsurface channel. In the previous FSC variants, it is not possible to produce large size channels, at least in height, because there is the need to increase the shoulder workpiece clearance, to receive that larger volume of extracted material, and it is not possible to apply the necessary forging pressure to close the channel along the full path with increasing the shoulder workpiece clearance.

With this FSC without shoulder-workpiece clearance variant, the larger tailored channels enable new applications such as composite fabrication, embedded instrumentation and hollow structures fabrication. The threads on the probe are designed with large pitch as compared to the probes' threads used in case of FSWP, FSC with shoulder-workpiece clearance and FSC with tilt angle and toe flash. Conversely, a special scroll feature on shoulder with a passage to extract material in form of self-detachable flash is designed that subsequently avoids imperfections, such as the step or sticky surface toe flash, observed in case of FSC with shoulder-workpiece clearance and FSC with tilt angle and toe flash.[9,43–58] The extracted material is collected in the form of self-detachable flash that can be reused with a separate processing technique, e.g. Friction Extrusion Process.[59,60] The FSC without shoulder-workpiece clearance is recommended to perform with cold conditions to produce effective self-detachable flash. FSC without shoulder-workpiece clearance leads to the benefits such as low forces on tool with shoulder-workpiece contact, better surface finish on the top surface of the workpiece with detachable flash, large and enhanced channel features and better

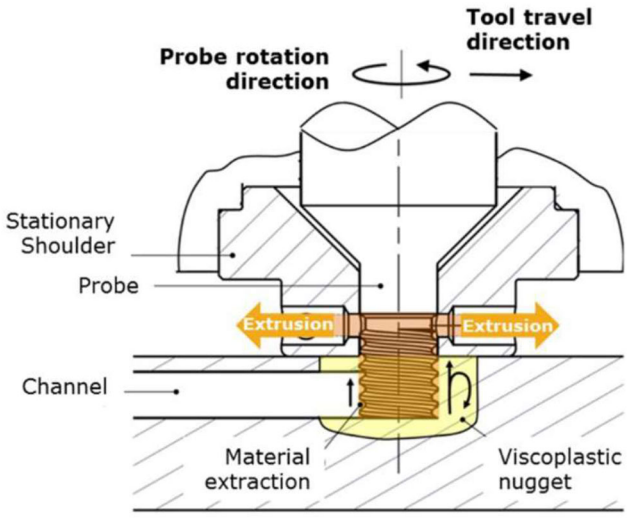

Figure 7. Schematic representation of the stationary shoulder friction stir channeling (SSFSC).[61]

forging for channel ceiling effect as compared to previously mentioned FSC variants.

2.4. Stationary shoulder friction stir channeling

Stationary shoulder friction stir channeling (SSFSC) is patented by Gandra,[61] wherein the viscoplastic material from the stir zone is extracted through the threads on the tool's probe and subjected out from the processed zone through internal passage of stationary shoulder as shown in Figure 7. The shape of the internal passage within the stationary shoulder is circular that converts extracted material in form of wire that can be used for any other purpose. In this SSFSC, only the probe rotates for stirring action inside of the workpiece, while the shoulder is making contact with the top surface of workpiece and remains stationary. As the shoulder is stationary, it offers better heat input toward cold conditions as compared to the FSC made with conventional rotative shoulder.[11] In this SSFSC, the heat is mostly generated within the stirring region from the interaction between tool's probe and workpiece and plastic deformation of material that causes viscoplastic behavior around the probe, enabling material flow toward extraction between the probe and the shoulder, or through the stationary shoulder. Besides, the stationary shoulder contributes less to the heat generation but, is majorly responsible for forging action on the top surface of the workpiece. SSFSC claims advantages of improved surface finish, minimal surface undercut and reduced surface heat input. SSFSC eliminates disadvantages of FSC with shoulder-workpiece clearance such as step effect and smaller channel size along with advantages of excellent repeatability, better surface finish and design flexibility in configuration.[11,61]

2.5. Hybrid friction stir channeling

The Hybrid friction stir channeling (HFSC), a novel solution represented in Figure 8,[62] enables simultaneous welding and channeling of multiple metal components from similar or dissimilar materials and geometries. The HFSC process creates a weld and a subsuperficial channel, in one action, which is not possible with other known techniques. This technique opens new possibilities to manufacture components with optimized physical and chemical performance, for high demanding applications requiring continuous channels along a free path. The HFSC tool probe consists of distinct features such as channel formation features and welding features. The more detailed details on tool profiles are explained in subsection 3.1. The metallurgically sound bonding can be established between multiple base-materials activating joining mechanisms similar to the ones present in FSW. In HFSC, the self-detachable flash is generated and received out from the tool similar like FSC without shoulder-workpiece clearance.

Therefore, it can be said that the HFSC technique combines the best of FSC and FSW processes, in a distinct single processing action with its own challenges, namely including parameters inherent to the integration of the integrated actions of channeling and welding, just like in other hybrid solutions such as laser-MIG hybrid welding integrating different power sources.[63] HFSC opens a new dimension in engineering design for thermal management, by using channels in lightweight materials, such as aluminum alloys, that can be used as small width and thick ribs, welded to thin and large width sheet metal of high density and expensive materials with high thermal performance, such as Cu and its alloys, as depicted in Figure 8b. Wherein combination of Al-Cu system enhances heat extraction capacity and reduces overall weight.[58,64–66]

3. Process parameters

The most important parameters related to friction stir-based channeling are tool design, shoulder-workpiece clearance, rotational speed, travel speed, torque and forces on tool, tilt angle, processing path and equipment (machine and fixture).[9] These parameters

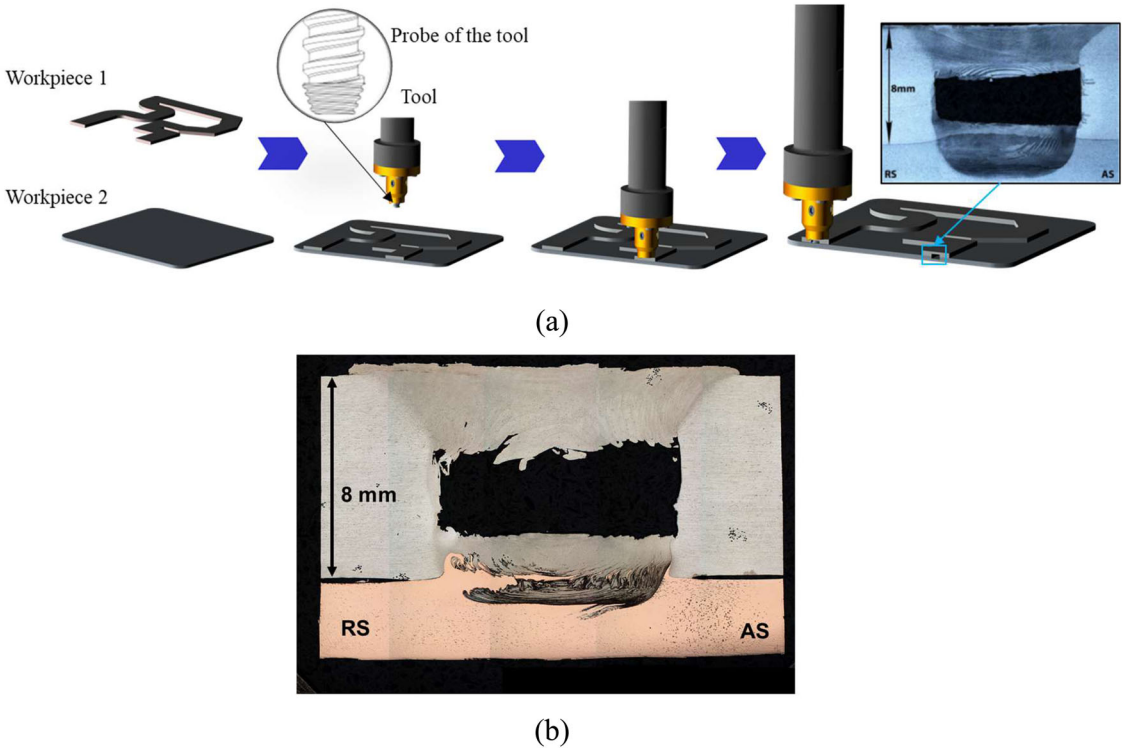

Figure 8. Hybrid friction stir channeling (HFSC) (a) process schematic description and (b) macrograph of the HFSC to Al-Cu system.

contribute to heat input conditions that subsequently affects channel processing through viscoplastic material flow. Adequate heat input is required to obtain suitable processing condition to fabricate large and uniform channel throughout the path of the tool's travel. Suitable processing condition provides well controlled viscoplastic material flow to fabricate subsurface channel with regulated material extraction from the workpiece material. Variations in heat input can be performed with change in process parameters that in turn influences the channel formation characteristics. Different processing conditions studied in published literature are summarized in Table 2 wherein investigated process parameters and recommended processing conditions are quantitatively summarized. Individual explanation on each parameter is presented as under.

3.1. Tool design

In friction stir-based channeling, a nonconsumable tool consists of probe and shoulder is used for materials processing. The most important parameters of tool design are tool material, shoulder diameter, probe diameter, shoulder to probe diameter ratio, shoulder surface geometry, probe surface geometry and probe shape that govern viscoplastic material flow characteristics with an influence on heat input conditions.[1,2,20–23] The heat generation is governed by combination of friction between tool-workpiece interactions and plastic deformation of workpiece, wherein the probe's geometrical features and dimensions are most influencing factors. In FSC, the probe of the tool significantly contributes to the frictional heating, shear deformation and viscoplastic material movement for material extraction. The shoulder mainly contributes to material forging action on surface of the workpiece to close the channel through material consolidation. Different variants of friction-based channeling are consisting of specific tool design that is suitable to produce channel with respective processing conditions of individual variant. Detailed summary on investigated tool design and recommended tool design for different variants of friction stir-based channeling are presented in Table 2 from the published literature. The discussion on tool design for different variants of friction stir-based channeling is presented as under.

3.1.1. FSWP tools and shoulder-workpiece clearance

In case of FSC with shoulder-workpiece clearance, the tool design applied is similar like FSWP tools, wherein the tunnel defect or worm hole defect (typically found in FSWP) is extended throughout the path of tool's travel. Mishra,[38] Balasubramanian et al.[16] and Pandya et al.[70] applied conventional tool designs of

Table 2. Summary on friction stir-based channeling.

Sr. No.	Workpiece material and dimension	Investigated parameters and tool design	Recommended parameters and tool design	Obtained properties and observations with remarks	References
Friction stir channeling with shoulder-workpiece clearance					
1	6061 Al alloy, thickness 6 mm	Process parameters: TTS 0.4 m/s to 2.8 m/s, TRS 10–20 rps, PD 2.8, 3.0 mm, TRD counterclockwise, SWC 0.2 mm to 1.2 mm, TTA 0° Tool design: SD 16 mm, TPD 5 mm, PL 4 mm, TPP Cylindrical profile with three tools of Tool 1 thread pitch of 1.25 mm with a thread angle of 60° and a depth of cut of 0.4 mm, Tool 2 threaded pitch of 1.25 mm with threaded angle of 60° and a depth of cut of 1 mm and Tool 3 thread pitch of 1.25 mm with a thread angle of 75° and a depth of cut of 1.6 mm	Process parameters: TTS: 0.4 m/s to 2 m/s, TRS: 10–12 rps, PD 3 mm, TRD counterclockwise, SWC 1 mm, TTA 0° Tool design: SD 16 mm, TPD 5 mm, PL 4 mm, TPP Tool 2 threaded pitch of 1.25 mm with 60° and a depth of cut of 1 mm and Tool 3 thread pitch of 1.25 mm with a thread angle of 75° and a depth of cut of 1.6 mm (recommendation based on hydraulic diameter)	hydraulic diameter: 0.2 mm to 1.2 mm, Tensile strength: 171 MPa (of channel closing region), Yield strength: 117 MPa (of channel closing region), Maximum elongation: 12 % (of channel closing region), Channel surface pitch: 0.032 mm/rot to 0.107 mm/rot, Channel shape: Elliptical	[16, 67]
2	6061-T6 Al alloy, thickness 5 mm	Process parameters: TTS 2.17 and 2.96 mm/s, TRS 1000, 1100, 1200 rpm, PD 3.2 mm, TRD counterclockwise, SWC 0.8 mm, TTA 0° Tool design: SD 16 mm, TPD 5 mm, PL 4 mm, TPP: Cylindrical profile with three tools of Tool 1 thread pitch of 1.25 mm with a left-hand thread angle of 60° and a depth of cut of 0.2 mm, Tool 2 threaded pitch of 1.25 mm with left-hand thread angle of 60° and a depth of cut of 0.5 mm and Tool 3 thread pitch of 1.25 mm with a thread angle of 75° and a depth of cut of 0.8 mm		The existence of channel in stir region is correlated with resultant force acting between retreating side and trailing edge of probe. Magnitude of forces reduces with an increase in heat index. The processing pattern/bands are depended on pitch of tool run. Channel shape: Elliptical	[16, 39]
3	6061-T6 Al alloy, thickness 6 mm	Process parameters: TTS 1.69 m/s, TRS 1000, 1100, 1200 rpm, PD 3.0, 3.1, 3.2 mm, Tool design: SD 16 mm, TPD 5 mm, PL 4 mm, TPP: Cylindrical profile with a left-hand thread angle of 75° and a depth of cut of 0.8 mm	Process parameters: TTS 1.69 m/s, TRS 1100 rpm, PD 3.0 mm,	The peak temperature during FSC is linearly correlated with specific energy of the process. Cross-section of channel decreases with increase in specific energy. Maximum obtained cross-section of channel: 4.125 mm, Maximum surface temperature: 182 °C, 5 mm away from shoulder and specific energy of 1,851,700,000 J/m at 11 rpm, 1.69 m/s and 3.2 mm of PD, Channel shape: Elliptical	[16, 68]
4	6061-T6 Al alloy, thickness 6.3 mm	Process parameters: TTS 1.69, 2.12. 2.96 m/s, TRS 1050, 1200 rpm, PD 3.1 mm, TTA 0°	Process parameters: TTS 1.69 m/s, TRS 1200 rpm, PD 3.1 mm, TTA 0° (recommendation based on hydraulic diameter)	hydraulic diameter: 1 mm to 2 mm, roughness height: 0.08 mm to 0.17 mm, Reynolds number: 550 to 2240, Smallest hydraulic diameter resulted in largest pressure drop, Irregular shape of channel and rough channel surface increases pressure drop. Channel shape: Elliptical	[16, 69]
5	6061-T6 Al alloy, 150 mm × 100 mm × 6 mm	Process parameters: TRS 1000 rpm to 1500 rpm, TTS 20 mm/min to 100 mm/min, SWC 0.5 mm to 0.9 mm, TTA 0° Tool design: TPD 6 mm to 10 mm, SD 12 mm to 24 mm, PL 5 mm to 6.5 mm	Process parameters: TRS 1200 rpm, TTS 40 mm/min, SWC 0.4 mm, TRD clockwise direction, TTA 0° Tool design: TM high speed steel tool, TPD 6 mm, SD 18 mm, PL 5.8 mm, TPP cylindrical probe profile with right-hand threads of 60°, 1 mm pitch and 1 mm depth of cut	Material extraction from advancing side to SWC leads in four sides of channel. Distinct zone around channel: probe influenced and shoulder influenced regions that contributes in formation of channel. The probe influenced material Channel shape: rectangle	[70]
6	6061-T6 Al alloy, 197 mm × 160 mm × 10 mm	Process parameters: TRS 800 rpm, TTS 31.5 mm/min, TRD clockwise direction, TTA 0° Tool design: TM AISI-H13 steel, TPP Eight different profiles such as nonthreaded cylindrical, left-hand threaded cylindrical, right-hand threaded cylindrical, bidirectional threaded tool, right-	Process parameters: TRS 800 rpm, TTS 31.5 mm/min, TRD: clockwise direction, TTA 0° Tool design: TM AISI-H13 steel, TPP bidirectional diamond shape threaded, TPD root 4 mm, middle 6 mm and tip 4 mm,	Channel area: 10.90 mm^2, Channel periphery: 18.72 mm, hydraulic diameter: 2.33 mm, Nusselt number: 2.303, average surface roughness: 6.11 micron (wall 0.74 micron, root 2.88 micron and roof 14.70 micron), conduction thermal resistance: 2.06 mm, Highest score of 14.25 for channel produced by bidirectional diamond shaped profile based on laminar flow resistance, turbulence flow resistance, laminar thermal convection	[71]

(*Continued*)

Table 2. Continued.

Sr. No.	Workpiece material and dimension	Investigated parameters and tool design	Recommended parameters and tool design	Obtained properties and observations with remarks	References
		hand taper threaded, bidirectional diamond shape threaded, double start right-hand threaded and triple start right-hand threaded investigated, TPD 4 mm to 6 mm, SD 16 mm and 18 mm	(based on overall thermal performance of channel)	resistance, turbulence thermal convection resistance and thermal conduction resistance	
7	6061-T6 Al alloy, 150 mm × 100 mm × 6 mm	Process parameters: TRS 1200 rpm, TTS 40 mm/min, TRD clockwise direction, TTA 0° SWC 0.7 mm Tool design: TM high-speed steel tool TPD 6 mm TPP right-hand threaded cylindrical TPD 18 mm TPL 5.8 mm		Channel area: 6.80 ± 0.35 mm^2, Channel perimeter: 14.02 ± 0.68 mm, hydraulic diameter: 1.93 ± 0.19 mm, Channel length: 100 ± 1.76 mm Channel width: 5.31 ± 0.22 mm Channel height: 1.42 ± 0.27 mm Channel surface roughness (average): 0.052 mm Channel's heat transfer surface area: 1402 ± 72.82 mm^2 Reynolds number: 500 to 2100 The heat transfer is significantly affected by axial wall conduction effect, Heat transfer rate is higher in mini channels, The wall temperature is nonuniformly distributed along the length of the channel, Surface roughness of mini channels affects thermo-hydraulic performance	[72]
Friction stir channeling with tilt angle and toe flash					
1	6061 Al alloy, thickness 10 mm	Process parameters: TRS 1000 rpm, TTS 25 mm/min, TTA 3°, TWC Zero, PL 0 mm Tool design: TM AISI-H13 steel, TPP nonthreaded cylindrical, TPD 8 mm, SD 25 mm, TPL 7.8 mm	Process parameters: TRS 1000 rpm, TTS 25 mm/min, TTA 3° TWC Zero, PL 0 mm	Cross-section area of channel: 16.48 mm^2, Average channel height: 2.62 mm, Channel width: 6.82 mm, ratio of cross-section area of channel to longitudinal cross-sectional area of tool probe: 0.27, Channel shape: Rectangular	[73]
2	5083 Al alloy, thickness 10 mm	Process parameters: TRS 630 and 800 rpm, TTS 12 and 31.5 mm/min, TTA 3° TWC Zero Tool design: TM AISI-H13 steel, TPP nonthreaded cylindrical, TPD 8 mm, SD 25 mm, TPL 7.8 mm, TSP concave 5° without scroll	Process parameters: TRS 800 rpm, TTS 12 mm/min, TTA 3° TWC Zero	Width of the channel: 75 % of the tool probe diameter, Different regions around channel: stir zone, channel roof, area of channel, remaining material zone at the side of channel Channel shape: closer to rectangular	[40]
3	5083 Al alloy, 200 mm × 60 mm × 10 mm	Process parameters: TRS 630, 800, 1000 rpm, TTS 12 and 25 mm/min, TTA 2°, 2.5° and 3° TWC Zero Tool design: TM AISI-H13 steel, TPP nonthreaded cylindrical, TPD 8 mm, SD 25 mm, TPL 7.8 mm, TSP concave 5° without scroll	Process parameters: TRS 800 rpm, TTS 12 mm/min, TTA 2°, 2.5° and 3°, TWC Zero (based on obtained channel dimensions, TTA of 3° resulted in closer to rectangular channel)	Stir zone dimensions across above the channel from the center line: *X*1: 4 mm, *X*2: 2.76 mm, *X*3 2.24 mm, stir zone dimension at the side of channel *X*4: 2.16 mm, Distinct zones around channel: nugget zone, shoulder affected zone, extrusion zone 1 and 2, and channel zone Increase in rotational speed increases channel dimensions. Channel shape: Trapezoidal and close to rectangular	[41]
4	5083 Al alloy, 300 mm × 300 mm × 10 mm and 300 mm × 150 mm × 10 mm	Process parameters: TRS 800 and 1000 rpm, TTS 12 and 31.5 mm/min, TTA 3° for cylindrical TPP and 0° for upward conical TPP, TWC 0.5 mm and 0.8 mm, TRD clockwise and counterclockwise, Tool design: TM AISI-H13 steel, TPP nonthreaded cylindrical and nonthreaded upward conical with 6° conic angle, TPD 8 mm for cylindrical TPP and	Process parameters: TRS 800 rpm, TTS 12 mm/min, TTA 0° with upward conical TPP, TWC 0.8 mm, TRD clockwise (based on uniformity of channel), Tool design: TM AISI-H13 steel, TPP nonthreaded upward conical with 2° conic angle, TPD 7 mm root diameter and 8 mm tip diameter for upward conical TPP,	Upward conical TPP is better than cylindrical TPP in terms of increase in height, hydraulic diameter and more stable shape of the channel that eliminates step inside the channel, average channel area: 16 mm^2, average hydraulic diameter of channel: 3.4 mm, The size and shape of the channel vary with serpentine curvature path, Channel shape: Trapezoidal	[74, 75]

(*Continued*)

Table 2. Continued.

Sr. No.	Workpiece material and dimension	Investigated parameters and tool design	Recommended parameters and tool design	Obtained properties and observations with remarks	References
		7 mm root diameter and 8 mm tip diameter for upward conical TPP, SD 25 mm, TPL 7.8 mm, TSP concave 5° without scroll	SD 25 mm, TPL 7.8 mm, TSP concave 5° without scroll		
Friction stir channeling without shoulder-workpiece clearance					
1	5083-H111 Al alloy, 15 mm	Process parameters: Vertical force 420 Kg, TTS 100 mm/min, TRS 400 rpm, TRD counter clockwise, plunge speed 0.1 mm/s, dwell time 5 s, Control mode: vertical force control, SWC Zero Tool design: TPP conical 5 mm root diameter with left-hand threads, SD outer diameter of 20 mm and inner diameter of 9 mm, TSP plane shoulder with two spiral striates scrolls of 360° angle		Nonconventional testing methods are required to evaluate the performance of the channel produced by FSC., Helium leak test, hydraulic pressure test, macro indentation, free four point bend resistance, geometrical stability across complex path by macro examination are suggested for successful assessment of channel's assessment after FSC.	[48]
2	5083-H111 and 5083-O Al alloy, 15 mm and 26 mm	Process parameters: Vertical force 420 Kg and 500 kg, TTS 100 mm/min, TRS 400 rpm and 600 rpm, TRD counter clock wise, plunge speed 0.1 mm/s, dwell time 5 s and 8 s, Control mode: vertical force control and position control, SWC Zero Tool design: TPP cylindrical left-hand threaded, TPD 8 mm SD outer diameter of 20 mm and inner diameter of 9 mm, TSP plane shoulder with two spiral striates scrolls of 360° angle		The rough surface of channel can enhance the heat transfer from channel to outer surface. FSC has adequate potential for the cooling systems in mold industries including injection molding and open molding techniques. FSC has higher productivity compared to alternative channel fabrication techniques.	[76]
3	5083-H111 Al alloy, 15 mm	Process parameters: Vertical force 4 kN and 2 kN, TTS 50 mm/min and 80 mm/min, TRS 1100 rpm, TRD counter clockwise, TTA 0° Control mode: vertical force control, SWC Zero Tool design: TPP cylindrical left-hand trapezoidal threads with thread pitch of 3 mm and depth of cut of 0.7 mm, TPD 8 mm, TPL 6 mm, SD 19 mm, TSP plane shoulder with one spiral of 0.7 mm and two different spiral pitch of 2 and 1.	Vertical force 2 KN, TTS 80 mm/min, TRS 1100 rpm, TRD counter clockwise, TTA 0° Control mode: vertical force control, SWC Zero Tool design: TPP cylindrical left-hand trapezoidal threads with thread pitch of 3 mm and depth of cut of 0.7 mm, TPD 8 mm, TPL 6 mm SD 19 mm, TSP plane shoulder with one spiral of 0.7 mm and spiral pitch of 1. (based on channel's dimension)	Channel dimensions: height 3.7 mm, width 8 mm and ceiling height 1.6 mm, Channel shape: rectangular, Fatigue resistance of channel geometries decreases at elevated temperature (of 120 °C and 200 °C) when subjected with four point bending, Fracture occurs at advancing side in the channel/TMAZ interface when subjected with four point bending.	[44, 54]
4	5083-H111 Al alloy, 15 mm	Process parameters: Vertical force 1.5 kN, 2 kN and 4 kN, TTS 50 mm/min and 80 mm/min, TRS 1100 rpm, TRD counter clockwise, TTA 0° Control mode: vertical force control, SWC Zero Tool design: TM tool steel H13 TPP cylindrical left-hand trapezoidal threads with thread pitch of 3 mm and depth of cut of 0.7 mm, TPD 8 mm, TPL 6 mm and 8 mm SD 19 mm, TSP plane shoulder with one spiral of 0.7 mm, two different spiral pitch of 2 and 1 and two different spiral height of 0.7 mm and 1 mm.	Vertical force 1.5 kN, TTS 50 mm/min, TRS 1100 rpm, TRD counter clockwise, TTA 0° Control mode: vertical force control, SWC Zero Tool design: TM tool steel H13 TPP cylindrical left-hand trapezoidal threads with thread pitch of 3 mm and depth of cut of 0.7 mm, TPD 8 mm, TPL 8 mm SD 19 mm, TSP plane shoulder with one spiral of 0.7 mm, spiral pitch of 1 and spiral height of 1 mm.	Channel dimensions: height 4.6 mm, width 8 mm and ceiling height 2.7 mm, Channel shape: rectangular, Channel's fatigue strength is lower than the unprocessed zone, Fatigue resistance of channel geometries decreases at elevated temperature (of 120 °C and 200 °C) when subjected with four point bending, Fracture occurs at advancing side in the channel/TMAZ interface, and mix fracture of intergranular decohesion and trans granular cracking is observed when subjected with four point bending.	[43,44]
5	5083-H111 Al alloy, 15 mm	Process parameters: Vertical force 1.5 kN, TTS 50 mm/min, TRS 1100 rpm,		Channel dimensions: height 4.6 mm, width 8 mm and ceiling height 2.7 mm, Channel shape: rectangular, A thicker closing layer increases fatigue crack	[44, 52]

(*Continued*)

Table 2. Continued.

Sr. No.	Workpiece material and dimension	Investigated parameters and tool design	Recommended parameters and tool design	Obtained properties and observations with remarks	References
		TRD counter clockwise, TTA 0° Control mode: vertical force control, SWC Zero Tool design: TM tool steel H13 TPP cylindrical left-hand trapezoidal threads with thread pitch of 3 mm and depth of cut of 0.7 mm, TPD 8 mm, TPL 8 mm SD 19 mm, TSP plane shoulder with one spiral of 0.7 mm, spiral pitch of 1 and spiral height of 1 mm.		propagation time, the crack propagation time is residual when compared with number of cycles, The fatigue crack propagation life obtained in the computational simulations represents a maximum of 70 % of the experimental life.	
6	5083-H111 Al alloy, 15 mm	Process parameters: Vertical force 1.5 kN, 2 kN, 2.2 kN and 4 kN, TTS 50 mm/min, 80 mm/min and 100 mm/min, TRS 400 rpm and 1100 rpm, TRD counter clock wise, TTA 0° Control mode: vertical force control, SWC Zero Tool design: TM tool steel H13 TPP cylindrical threaded with three different pitch, TPD 8 mm, TPL 6 mm and 8 mm SD 19 mm, TSP plane shoulder with one spiral with three different dimensions	Vertical force 1.5 kN, TTS 50 mm/min, TRS 1100 rpm, TRD counter clockwise, TTA 0° Control mode: vertical force control, SWC Zero, (based on channel's dimensions)	Channel dimensions: height 4.6 mm, width 8 mm and ceiling height 2.7 mm (maximum ultimate bending strength of 283 MPa for this channel), Channel shape: rectangular, Highest ultimate bending strength of 400 MPa obtained with smallest channel area (for channel dimensions: height 3 mm, width 6 mm and ceiling height 1.5 mm) having largest elongation, Uneven shape of channel leads to quick crack propagation during four point bending test while channel having thick closing layer with rectangular shape contributes to longer fatigue crack propagation time.	[44, 53]
7	7178-T6 Al alloy, 13 mm	Process parameters: TTS 80 mm/min and 150 mm/min, TRS 600 rpm and 800 rpm, TRD counter clockwise, TTA 0° Control mode: vertical position control, SWC Zero Tool design: TPP conical left-hand threaded, TPD 5 mm tip diameter, TPL 5.5 mm, SD 20 mm outer diameter and 9 mm inner diameter, TSP plane shoulder with two spiral striates scroll angle of 360 °C.	TTS 150 mm/min, TRS 600 rpm, TRD counter clockwise, TTA 0° Control mode: vertical position control, SWC Zero (based on channel area)	Channel area: 14.01 mm^2 (sustained 40 bar internal pressure with one leaking location), Maximum sustained bending load transverse to channel condition: 72.44 (for channel with area 13.49 mm^2), fracture occurred at advancing side of channel when subjected to bending test, Channel's bottom zone is more resistance to bending than ceiling zone of same.	[44, 47]
8	7178-T6 Al alloy, 13 mm	Process parameters: TTS 80 mm/min and 150 mm/min, TRS 600 rpm and 800 rpm, TRD counter clockwise, TTA 0° Control mode: vertical position control, SWC Zero Tool design: TPP conical left-hand threaded, TPD 5 mm tip diameter, TPL 5.5 mm, SD 20 mm outer diameter and 9 mm inner diameter, TSP plane shoulder with two spiral striates scroll angle of 360 °C.	TTS 150 mm/min, TRS 600 rpm, TRD counter clockwise, TTA 0° Control mode: vertical position control, SWC Zero (based on channel area)	Channel area: 14.01 mm^2, Thickness of closing layer: 2.3 mm, shear angle at retreating side: 12°, Ceiling surface and retreating side surface of channel are roughest, Height roughness of 161 HV in the ceiling zone around the channel, The shape, size and integrity of the channel can be controlled by processing conditions.	[44, 50]
9	5083-H111 Al alloy, 15 mm	Process parameters: Vertical force 3920 N, TTS 50 mm/min, TRS 1100 rpm, TRD counter clockwise, TTA 0°, PD 5.5 mm Control mode: vertical force control, SWC Zero Tool design: TM tool steel H13 TPP cylindrical left-hand threaded, TPD 8 mm, TPL 6 mm, SD 19 mm, TSP straited plane shoulder.		Tensile strength of stir zone: 352 MPa, Yield strength of stir zone: 170 MPa, Elongation of stir zone: 16 %, Maximum bending load before fracture: 20 KN	[44, 55]
10	5083-H111 Al alloy, 15 mm	Process parameters: Vertical force 1.5 KN, 2 KN, 2.2 KN and 4 KN, TTS 50 mm/min, 80 mm/min and	Vertical force 1.5 KN, TTS 50 mm/min, TRS 1100 rpm, TRD counter clockwise,	Channel dimensions: height 4.6 mm, width 8 mm and ceiling height 2.7 mm, Channel shape: rectangular, Higher rate of plastic deformation on	[44, 49]

(*Continued*)

Table 2. Continued.

Sr. No.	Workpiece material and dimension	Investigated parameters and tool design	Recommended parameters and tool design	Obtained properties and observations with remarks	References
		100 mm/min, TRS 400 rpm and 1100 rpm, TRD counter clock wise, TTA 0° Control mode: vertical force control, SWC Zero	TTA 0° Control mode: vertical force control, SWC Zero, (based on channel's dimensions)	advancing side compare to retreating side observed in microstructural features, Hardness in the ceiling zone is observed lower than the base material, however higher than the TMAZ and HAZ, The fatigue strength in the vicinity of channel is observed as 50 MPa (68.75% lowered compared to base material), Fracture of the channel occurs at TMAZ and ceiling zone/stir zone interface on advancing side, Mix fracture modes of intergranular and trans granular with and without fatigue striations.	
		Tool design: TM tool steel H13 TPP cylindrical trapezoidal threaded with threaded pitch of 3 mm and depth of cut of 0.7 mm, TPD 8 mm, TPL 6 mm and 8 mm SD 19 mm, TSP plane shoulder with spiral with different spiral height of 0.7 mm and 1 mm and different spiral pith of 1 and 2	Tool design: TM tool steel H13 TPP cylindrical trapezoidal threaded with threaded pitch of 3 mm and depth of cut of 0.7 mm, TPD 8 mm, TPL 6 mm and 8 mm SD 19 mm, TSP plane shoulder with spiral with spiral height of 1 mm and spiral pith of 1		
11	5083-H111 Al alloy, 15 mm	Process parameters: Vertical force 3920 N, TTS 50 mm/min and 100 mm/min, TRS 1000 rpm and 1100 rpm, TRD counter clock wise, TTA 0°, PD 5.5 mm Dwell time 3 s, plunge speed: 0.1 mm/s Control mode: vertical force control, SWC Zero Tool design: TPP cylindrical left-hand threaded, TPD 8 mm, TPL 6 mm, SD inner diameter of 8 mm and outer diameter of 19 mm, TSP plane shoulder with one spiral striates scrolling angle of 360°	Vertical force 3920 N, TTS 50 mm/min, TRS 1100 rpm, TRD counter clockwise, TTA 0° Control mode: vertical force control, SWC Zero (based on four-point bending test)	Maximum bending strength 310 MPa, Maximum hardness of 117 HV observed at the bottom of the channel in stir zone, fatigue limit at room temperature: 40 MPa, at 120 °C: 30 MPa and at 200 °C: 20 MPa, Fracture of specimen occurred at advancing side between channel and TMAZ	[44, 45]
12	5083-H111 Al alloy, 15 mm	Process parameters: Vertical force 1500 N, TTS 80 mm/min, TRS 400 rpm, TRD counter clock wise, TTA 0°, PD 8.3 mm Dwell time 3 s., plunge speed: 0.1 mm/s Control mode: vertical force control, SWC Zero Tool design: TPP cylindrical left-hand threaded, TPD 8 mm, TPL 6 mm, SD inner diameter of 8 mm and outer diameter of 19 mm, TSP plane shoulder with one spiral striates scrolling angle of 360°		Tensile and fatigue tests carried out along the channel, Channel shape: Trapezoidal, Yield strength of channel: 140 MPa, Ultimate tensile strength of channel: 150 MPa, longitudinal crack initiation followed by transverse propagation observed under uniaxial tension/compression and axial/torsional loading, Crack initiation starts from corner of material deposition in trapezoidal channel.	[44, 46]
13	5083-H111 Al alloy, 10 mm	Process parameters: Vertical force 3.1 KN, TTS 70 mm/min, TRS 500 rpm, TRD counter clockwise, TTA 0°, Control mode: vertical force control, SWC Zero Tool design: TM H13 tool steel, TPP cylindrical left-hand threaded, TPD 8 mm, TPL 7 mm, SD 20 mm, TSP plane shoulder with one spiral striates scrolling angle of 360°		Channel area: 15 mm^2, Sustained pressure of 380 bar for 1.5 h without failure, surface roughness Ra: 466 at the surface of channel's ceiling side, FSC has enhanced cooling power and heat transfer capacity relative to milled channels, Maximum hardness observed at ceiling zone and lowest at HAZ.	[77]

(*Continued*)

Table 2. Continued.

Sr. No.	Workpiece material and dimension	Investigated parameters and tool design	Recommended parameters and tool design	Obtained properties and observations with remarks	References
14	5083-H111 Al alloy, 15 mm	Process parameters: Vertical force 1.5 KN, 2 KN and 2.2 KN, TTS 50 mm/min, 80 mm/min and 100 mm/min, TRS 400 rpm and 1100 rpm, TRD counter clock wise, TTA 0° Control mode: vertical force control, SWC Zero	Vertical force 1.5 kN, TTS 50 mm/min, TRS 1100 rpm, TRD counter clockwise, TTA 0° Control mode: vertical force control, SWC Zero	Channel shape: rectangular, Maximum hardness 92 HV at stir zone toward retreating side, Lowest hardness observed at TMAZ, Surface roughness: advancing side 12 μm, retreating side 66 μm, channel's top: 115 μm and channel's bottom 10 μm,	[44, 57]
		Tool design: TPP cylindrical left-hand trapezoidal threads with two different profiles such as thread pitch of 2 mm and 3 mm, depth of cut of 0.7 mm and width of 0.5 mm and 1 mm, TPD 8 mm, TPL 6 mm and 8 mm, SD 19 mm, TSP plane shoulder with three different profiles such as scroll pitch 1, 2 and 3 having one scroll and two different threads such as (1) 0.2 mm width at tip and 1 mm width at root, and 0.7 mm height, and (2) 0.3 mm width at tip with 45° thread angle	Tool design: TPP cylindrical left-hand trapezoidal threads with thread pitch of 3 mm, depth of cut of 0.7 mm and width of 1 mm, TPD 8 mm, TPL 8 mm, SD 19 mm, TSP plane shoulder with three different profiles such as scroll pitch 1 having one scroll and 0.3 mm width at tip with 45° thread angle (based on channel shape, surface features and obtained hardness)		
15	6082-T6 and 5083-H111 Al alloys, 10 mm	Process parameters: TTS 90 mm/min and 100 mm/min, TRS 800 rpm and 1000 rpm, TRD counter clockwise, TTA 0°, Control mode: vertical position control and vertical force control, SWC Zero	Process parameters: TTS 120 mm/min, TRS 800 rpm, TRD counter clockwise, TTA 0° Control mode: vertical position control, SWC Zero (based on channel area)	Channel size increases by increasing travel speed and decreasing rotation speed, Channel area: 30.66 mm^2 Position control system is better for flash removal and subsequently for enhanced top surface of workpiece, Produced channel sustained 100 bar pressure during pressure leak test without any leakage, FSC is better compare to conventional drilling, milling, electro discharge machining with little disadvantages.	[78]
		Tool design: TM tool steel H13, TPP cylindrical with special trapezoidal threads having 4 mm pitch, 1.5 mm thread width, radius of 0.5 mm at bottom of thread and 0.2 mm at top of thread and 0.7 mm height, TSD inner diameter of 8 mm and outer diameter of 20 mm, TPD 8 mm, TPL 13 mm TSP plane shoulder with three different profiles such as scroll pitch 1, 2 and 3 having one scroll and threads such as 0.3 mm width at tip and 1.55 mm width at root, and 0.75 mm height with 45° thread angle	Tool design: TM tool steel H13, TPP cylindrical with special trapezoidal threads having 4 mm pitch, 1.5 mm thread width, radius of 0.5 mm at bottom of thread and 0.2 mm at top of thread and 0.7 mm height, TSD inner diameter of 8 mm and outer diameter of 20 mm, TPD 8 mm, TPL 13 mm TSP plane shoulder with scroll pitch 2 having one scroll and threads such as 0.3 mm width at tip and 1.55 mm width at root, and 0.75 mm height with 45° thread angle		
16	5083-H111 Al alloy, 10 mm	Process parameters: Vertical force 3.1 KN TTS 70 mm/min, TRS 500 rpm, PD 7 mm		Channel's area: 15 mm^2, length of channel: 100 mm, Surface roughness of channel: ceiling surface 466 μm, retreating side surface 98 μm, advancing side surface 54 μm and bottom surface 12 μm, FSC has enhanced cooling power and heat transfer capacity relative to milled channels	[78]
		Tool design: TM H13 tool steel, TSD 20 mm, TPD 8 mm			
17	5083-H111 Al alloy, 15 mm	Process parameters: TTS 100, 150, 160, 180, 200, 250, 300, 350 mm/min, TRS 600, 720, 800, 1000, 1200, 1400 rpm, Process pitch 0.25 mm/rev, TRD counter clockwise, TTA 0°, Control mode: vertical position control and vertical force control, SWC Zero Process parameters:		The vertical forces are not stable during travel of tool (i.e. channeling phase) in case of vertical position control, The vertical position is not significantly affected in case of vertical force control, The tool is subjected to severe loading at the plunge phase, Maximum recorded temperature is 350 °C, 5 mm near to shoulder.	[56]

(*Continued*)

Table 2. Continued.

Sr. No.	Workpiece material and dimension	Investigated parameters and tool design	Recommended parameters and tool design	Obtained properties and observations with remarks	References
		Tool design: TM tool steel H13, TPP cylindrical with special trapezoidal threads having 0.5, 1 and 1.5 mm thread width, 0.7 mm thread height, TSD inner diameter of 8 mm and outer diameter of 20 mm, TPD 8 mm, TPL 6 and 8 mm TSP scroll type profile three different features			
Hybrid Friction stir channeling					
1	5083-H111 Al alloy, 8 mm top plate and 5 mm bottom plate	Process parameters: TRS 300 rpm, 350 rpm and 400 rpm, TTS 30 mm/min, 90 mm/min, 120 mm/min and 150 mm/min, TTA 0°, SWC Zero Tool design: TM tool steel H13, TPP cylindrical threaded with two different features of channeling (Right-Hand Thread with pitch of 4 mm and depth of 1 mm) and welding (left-hand taper threads with pitch of 1.25 mm and depth of 0.32 mm with three different welding tip lengths of 3 mm, 4 mm and 5 mm), TPD 10 mm (channel feature diameter), 11 mm diameter at interface between channeling and welding 30° angle up to tip (welding feature), TSP nine different shoulder profiles (flat and scroll shoulder profiles with different scroll dimensions)	Process parameters: TRS 350 rpm, TTS 150 mm/min, TTA 0°, SWC Zero (based on channel's dimensions) Tool design: TM tool steel H13, TPP cylindrical threaded with two features of channeling (Right-Hand Thread with pitch of 4 mm and depth of 1 mm) and welding (left-hand taper threads with pitch of 1.25 mm and depth of 0.32 mm with welding tip length of 3 mm), TPD 10 mm (channel feature diameter), 11 mm diameter at interface between channeling and welding 30° angle up to tip (welding feature), TSP flat and scroll shoulder profiles	The surface roughness of the channel increases with increase in TTS, The shear angle of the retreating side decreases with increase in TTS, Channel's area: 23.65 mm^2, ceiling length: 3.33 mm, welding length: 4.74 mm, ceiling shear angle: 2.14°, angle at welding-channeling interface: 7.01°	[51]
2	AA5754-H111, 8 mm top plate and 5 mm bottom plate	Process parameters: Control mode: position control, TRS 350 rpm, TTS 70 mm/min, PD 9.8 mm, TPL 10.5 mm Tool design: Not mentioned		Channel length: 450 mm, The increased hardness observed at the bottom and ceiling of the channel relative to the base material, Enhanced heat transfer with HFSC for conformal cooling applications.	[79]
3	5083-H111 Al alloy, 8 mm top plate and 5 mm bottom plate	Process parameters: TRS 200 rpm to 1000 rpm, TTS 30 mm/min to 500 mm/min, TTA 0°, SWC Zero, TRD clockwise Tool design: TM H13 tool steel, TPD 10 mm, TPP cylindrical threaded for channel feature (right-hand threaded with a pitch of 0.4 times the probe diameter, thread depth of 1/4) and taper for welding feature (30° tapered left-hand threads pitch of 1/8 of the probe diameter, thread depth of 1/4 of the thread pitch, and length of welding tip varies from 1/3 of the probe diameter to 1/2 of the probe diameter)., TSD 24 mm (2.2 times the TPD), TSP Single scroll ribbed feature with flat shoulder surface (width and height of the rib are 0 .068 and 0.045 times the shoulder diameter, respectively)	Process parameters: TRS 300 rpm, TTS 90 mm/min, TTA 0°, SWC Zero, TRD clockwise	Welding and channeling performed together on similar and dissimilar materials with self-detachable flash, Channel shape: rectangular	[80]
Stationary shoulder friction stir channeling					
1	6082-T4 Al alloy	Process parameters: Applied vertical force: 18 KN, TTS 50 mm/min, TRS 600 rpm, dwell time: 5 s, TRD clockwise		Special outlets in form of are provided vents in the tool to extract the material from workpiece, Enhanced surface finish on top of workpiece, Improved process stability for complex path such as serpentine path and rotary path	[61]
2	AA6082-T6 (15 mm) and AA1050-H14 (20 mm)	Not mentioned.		Channel area: 5–40 mm^2, linear, curved and helicoidal trajectories can be produced.	[81]

TTS: tool travel speed; TRS: tool rotational speed; SWC: shoulder workpiece clearance; PD: plunge depth; SD: Shoulder diameter; TPP: tool probe profile; TPD: tool probe diameter; TRD: tool rotation direction; TTA: tool tilt angle; rps: revolution per second; rpm: revolution per minute; TM: tool material; TPL: tool probe length; TSP: tool shoulder profile.

FSWP to produce channel, with an additional process parameters of shoulder-workpiece clearance and reverse tool rotation direction as compared to FSWP. This combined effect of tool's rotation and direction of probe's threads causes material extraction. The shoulder-workpiece clearance helps in deposition of

extracted material within the shoulder-workpiece clearance to produce closed channel. This deposited material acts as an extraction layer at the top of the workpiece (i.e. reported as discontinuity known as step effect on top of workpiece[38]). Conventional FSWP tool design consists of cylindrical shape of probe with small threaded pitch on tool's probe (such as 1 mm to 1.5 mm) and flat surface profile of tool's shoulder, that are applied in case of FSC with shoulder-workpiece clearance (refer Table 2). The size of the channel is limited in this variant of FSC with shoulder-workpiece clearance because of limited material extraction by small threaded pitch on tool's probe. In FSC with shoulder-workpiece clearance, the deposition of extracted material is also limited by volume between shoulder-workpiece clearance. To deposit large amount of material within shoulder-workpiece clearance, the large clearance gap is required, which can increase the size of the channel. But, the large clearance of shoulder-workpiece adversely affects increased stresses on tool's probe that may lead to failure of the tool's probe. Overall, it can be said that the features on the tool's probe and shoulder-workpiece clearance are correlated with each other for material extraction in case of FSC with shoulder-workpiece clearance. The tool's probe diameter must be larger enough to sustain stresses generated on it, as the shoulder surface is not in contact with workpiece in case of FSC with shoulder workpiece clearance.

The upward conical tool's probe profile is used with shoulder-workpiece clearance, wherein the conic angle is given toward the shoulder surface as shown in Figure 9c.[74,75] This conic angle provides upward swirling action to the plastically deformed material around the probe, which in turn extracts material toward the clearance between shoulder and workpiece to produce channel. In this case, nonthreaded tool's probe with conical profile is used for material extraction. It is claimed that the channel formation is better with parameters of conic tool's probe features and shoulder-workpiece clearance when compared with cylindrical nonthreaded profile of probe processed with tilt angle.[74,75] However, no quantitative comparison is presented. Also, the life of the tool and reliable tool design considerations are also not considered. The conic profile of tool's probe suggested in Refs. [74, 75] can create large amount of stresses during plunging phase and retraction phase and that increases chances of failure.

Different threaded probe profiles are investigated by Salimi et al.[71] for channel formation characteristics as shown in Figure 9d–k. The orientation of the threads on the probes is varied with eight different profiles (Figure 9d–k), which are consequently responsible for the distinct material flow. Out of eight different tool probe profiles, the bidirectional threads (as shown in Figure 9f,h,k) resulted in enhancement of channel's depth with a separation of material flow from the center of the probe. The reverse tapered threaded probe (Figure 9g) can provide smooth and uniform material extraction. However, in case of reverse tapered shape of probe, the stress concentration could be more on root side that is consisting of small diameter, which increases the chances of failure, mainly during plunging phase and retracting phase. Salimi et al.[71] claimed that the bi-directional threads (i.e. left-hand threads at bottom tip and right-hand threads above that of it), with diamond-shaped probe profile of tool (Figure 9h), is suggested for channel formation suitable for better thermal performance and fluid flow characteristics relative to other investigated tool designs. It can be summarized that the probe diameter and shape, type of threads, threaded pitch on tool's probe, orientation of threads, geometry, single directional threads and bidirectional threads of tool's probe must be considered during tool design, because these parameters of tool's probe govern channel formation characteristics in case of friction stir-based channeling.

Besides of material extraction using tool's probe threads, another way of material extraction is reported in Rashidi et al.[73] and Rashidi and Mostafapour,[74,75] wherein the tool's probe consisting of cylindrical nonthreaded probe (see Figure 9b) and upward conical nonthreaded probe (see Figure 9c) are used. The tool designs of cylindrical and conic nonthreaded tools are also commonly used in FSWP especially when the hardness of the tool's material is very high. In case of cylindrical nonthreaded probe for channel manufacturing used for FSC with tilt angle and toe flash, the plastically deformed material is extracted with an approach of tilt angle having large plow force to the viscoplastic material in front of tool's probe (see Figure 5). In case of FSC with tilt angle and toe flash, the extracted material is transported to the outside of the shoulder on the workpiece in a form of toe flash effect, as the shoulder surface is making contact to the workpiece from one edge. The straight and flat surfaces on tool's probe require large fluidity of the material (i.e. low viscosity of plastically deformed material, which is caused by large heat input conditions), to produce material extraction. Therefore, high

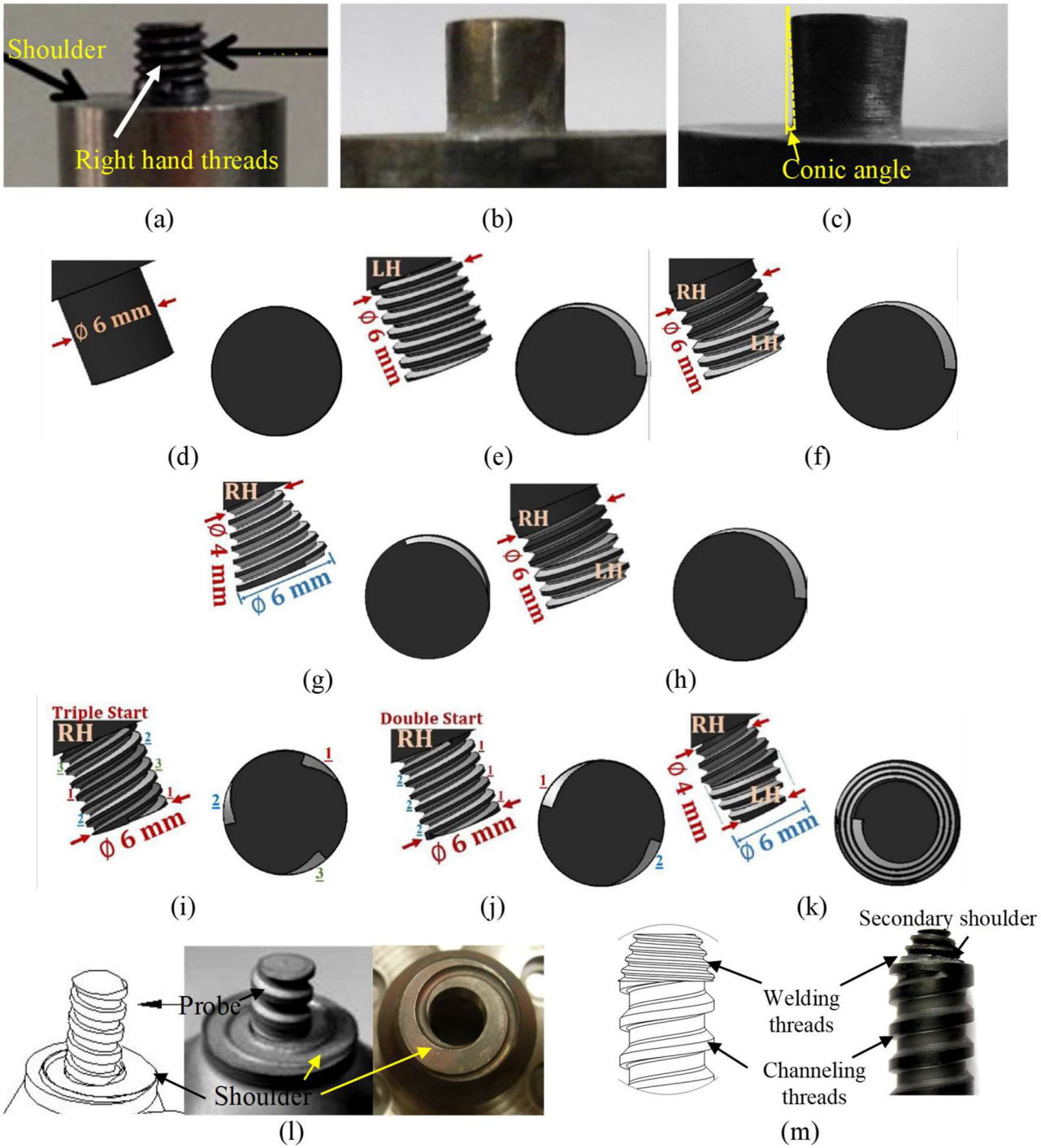

Figure 9. Tool design for friction stir-based channeling (a)[70] FSC with shoulder-workpiece clearance, (b, c) FSC with tilt angle and toe flash,[74] (d–k) various features of probe used in Ref. [71] (l) FSC without shoulder-workpiece clearance[51,76] and (m) HFSC.[51]

heat input is recommended for an effective operation with nonthreaded cylindrical probe of tool, in case of FSC with tilt angle and toe flash.[73–75] However, flat surfaces of tool's probe are less effective as compared to the threaded probe's profile due to the fact of limitation on material extraction capabilities (such as flat surfaces cause limited material extraction as compared to threaded probe features).

3.1.2. FSC tools with scroll shoulder

FSC tools with scroll shoulder features are advanced tool features to produce dedicated channel without shoulder-workpiece clearance. Vidal and Vilaça[42] developed FSC without shoulder-workpiece clearance using a scroll shoulder feature, to keep optimum forging with large material extraction capacity through large threaded pitch on tool's probe. With these tools,

larger channel volume is obtained with an elimination of step effect or surface toe flash effect on workpiece. The size and shape of the channel can be effectively governed by these tools as they are consisting of specially designed large threaded pitch on tool's probe and scrolled features on tool's shoulder. These features provide better material extraction as compared to previous tools. Figure 9l shows FSC tool designed for channel formation without shoulder-workpiece clearance, wherein combined profiles of buttress and square threads are used as features of tool's probe threads along with larger threaded pitch as compared to the threaded pitch used in case of FSC with shoulder-workpiece clearance and FSC with tilt angle and toe flash. The shoulder-workpiece clearance is not required in this tool, wherein the single sided scrolled shoulder feature is making contact with workpiece surface, as can be seen from Figure 9l. Another side of scrolled feature is designed in such a way that send extracted material away from tool-workpiece interactions in the form of self-detachable flash. In addition to self-detachable flash advantage, the rest part of the shoulder's surface forges material downward limited to specific depth, which in turn provides channel closing. Dimensions on tool's probe threads (such as thread thickness, thread width, threaded pitch, threaded angles) and tool's shoulder scrolled design (such as height of scroll feature, angle of scroll, scroll length, area covered by scroll feature and taper on scroll profile) are considered as an important parameters in this variant, because these features govern material extraction and self-detachable flash. These special features provide great control on material extraction that subsequently govern the size and shape of the channel more effectively as compared to previous tool designs.

3.1.3. HFSC tools

The HFSC tool design is shown in Figure 9m, wherein two different manufacturing processes of channeling and welding are performed simultaneously.[62,80,82] There are two different features of threads on tool's probe (such as channel formation threads and welding threads) provided on the probe along with special feature of scroll shoulder profile. The secondary welding features are provided toward the tip of the tool's probe according to the intended weld zone formation. The direction of the threads for the welding are designed in coordination to rotation direction of tool, to create downward movement of material toward workpiece, opposite to channeling threads. The base of the channeling features of the probe acts as a secondary shoulder for the welding that subsequently helps in forging-stirring effects required for welding. The welding features consisting of taper shape toward workpiece that helps in vertical material flow toward workpiece. Additionally, the threaded pitch of welding features on tool's probe is designed smaller as compared to the pitch of channeling threads that in turn promotes materials mixing. The channeling threaded features are designed similar to previously described tool in section of FSC tools with scrolled shoulder, but the combined features of channeling and welding create new challenges during processing.

3.1.4. SSFSC tools

SSFSC tool consists of stationary shoulder and rotating probe, wherein shoulder is contacting the workpiece. The tool's probe extracts the material toward shoulder from workpiece, whereas the shoulder consists of bore from the surface adjacent to the probe up to the outer surface of the shoulder (as shown in Figure 7), wherein the plasticized material flows through it that results in material extruded like wire (in place of self-detachable flash that occurs in case of FSC tools with scrolled shoulder).[61] SSFSC suggests that different probe features can be designed to vary channel formation characteristics. However, the details on tool design for SSFSC is not revealed and publications related to SSFSC tool design are lacking. In case of SSFSC, as the shoulder is not rotating, the wear resistance coating or special surface treatments on surface of the shoulder are recommended to be done, to improve wear resistance properties of tool's shoulder.

3.2. Rotational and travel speeds

The heat input conditions are also governed by the combined effect of rotational and travel speeds that subsequently governs viscoplastic behavior of the material underneath the tool's shoulder.[83,84] As discussed, the direction of tool's rotation is a major contributor for material extraction. The viscoplastic effect of material can be produced in a range with specific window of heat index using combination of rotation speed and travel speed. The heat index can be calculated as ratio of the rotational speed's square to travel speed. The fluidity and viscosity of the deformed material are greatly influenced by this heat index. It is claimed by Balasubramanian[16] that, the larger heat index and small processing pitch (i.e. distance traveled per rotation or ratio of travel to rotational speeds) is recommended to produce stable and large channels in case of FSC with shoulder-workpiece clearance (as

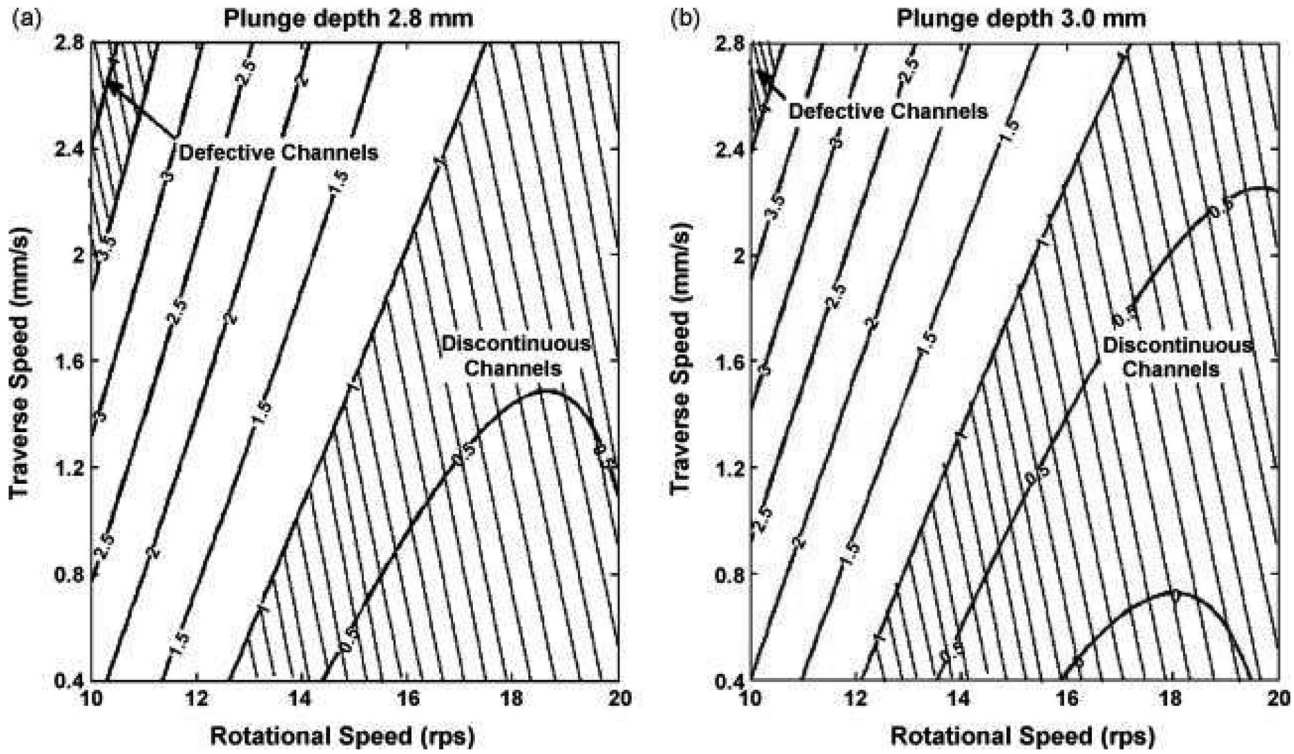

Figure 10. Effect of rotational speed, travel speed on channel formation for two different plunge depths of (a) 2.8 mm and (b) 3.0 mm, in case of FSC with shoulder workpiece clearance.[67]

shown in Figure 10). Figure 10 shows specific combination of rotational speed and travel speed provides continuous channel formation. It also shows that very high rotational speed results to discontinuous channel formation throughout the path of tool's travel, whereas very high travel speed results into formation of improper and defective (i.e. open) channels. Additionally, Figure 10 shows that the variation in plunge depth changes combination of rotational speed and travel speed for continuous channel formation. In case of FSC with shoulder-workpiece clearance, improper channel formation is resulted from very cold conditions (i.e. extremely low rotational speed or very high travel speed or combination of both). Figure 11 shows differences in shape and internal area of channel formation caused due to different combinations of rotational speed and travel speed, wherein higher rotational speed and lower travel speed resulted with larger area of channel with oval shape of channel.

Rashidi et al.[74] suggested that the larger heat index is required for the enhancement of the hydraulic diameter of channel with nearly uniform channel's size and shape, in case of FSC with tilt angle and toe flash. The higher heat index conditions can be caused by increasing rotational speed or decreasing travel speed or combined variation of increased rotational speed and decreased travel speed, that subsequently increases fluidity within plastically deformed material, which in turn helps in material extraction and causes improvement in channel's size and shape, especially when the pitch on the threads of probe is small or the probe is thread-less. However, the material extraction is still limited and not well controlled when performed with this variant of FSC with tilt angle and toe flash. Additionally, higher rotational speed can cause large differences in microstructural zones such as larger dynamically recrystallized zone, HAZ and TMAZ, due to higher heat input conditions and strong stirring action. Conversely, smaller heat index increases the viscosity of the plastically deformed material that in turn increases sticking effect to enhance the material extraction, especially when the pitch of the threads on the probe is larger. Therefore, combination of parameters for larger heat index and small processing pitch only works in case of FSC with shoulder-workpiece clearance and FSC with tilt angle and toe flash. FSC tools consisting of larger threaded pitch is recommended to be operated with smaller heat index to increase the extraction capabilities with effective viscoplastic conditions.[43–50,52–55,57] In case of FSC without shoulder workpiece clearance and HFSC, the stability of channel and higher volume of material extraction can be

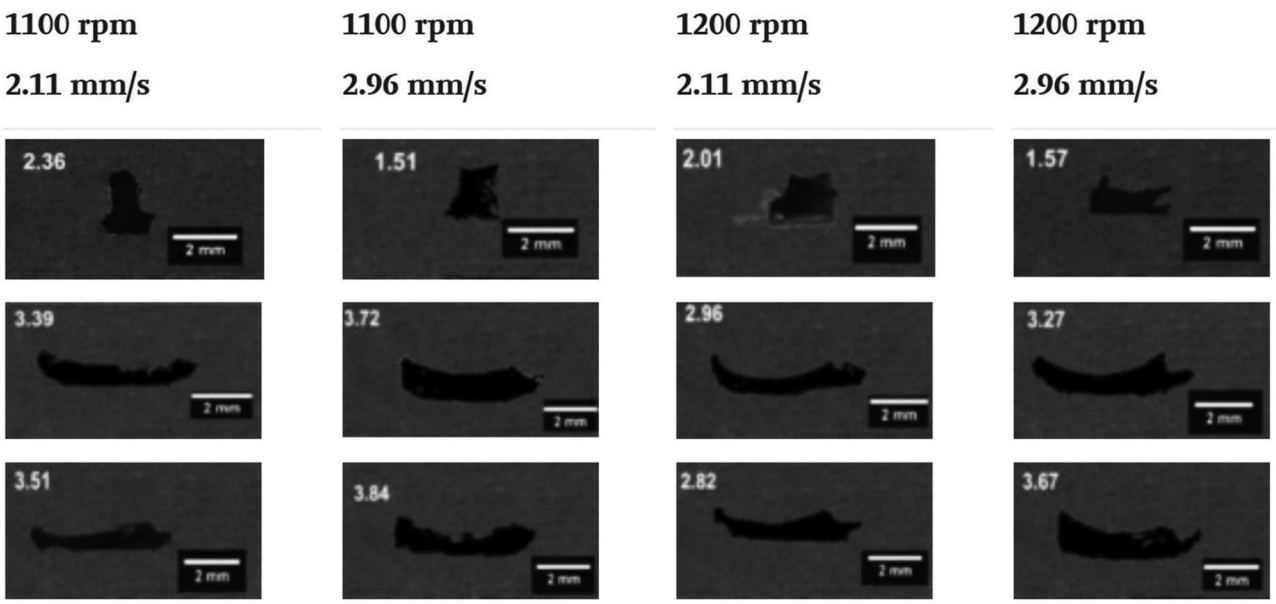

Figure 11. Variations in shape and size of the channel with respect to different combinations of rotational speed and travel speed (value in each image except scale bar shows area in mm^2).[39]

resulted from the low heat input conditions (i.e. lower rotational speed or higher travel speed or combination of lower rotational speed and higher travel speed). Nevertheless, extremely low rotational speed or extremely high travel speed can lead to probe failure due to increased stresses through large amount of forces and torque resulted on tool's probe. In addition to combination of rotational speed and travel speed, all other parameters and conditions that influence viscoplastic material flow with solid state processing must be considered to determine the suitable conditions for uniform channel formation using material extraction.

3.3. Forces and torque during processing

The forces and torque acting during friction stir-based processing influence the channel formation characteristics and durability of tool. The forces acting in three different directions such as vertical axial direction of tool (i.e. axial direction), horizontal axis parallel to the tool's travel direction (i.e. longitudinal direction) and horizontal axis perpendicular to the tool's travel direction (i.e. transverse direction) govern friction stir-based channeling.[39] During processing of channel formation, these forces are continuously varying as can be seen from Figures 12 and 13 for FSC with shoulder-workpiece clearance and FSC without shoulder workpiece clearance, respectively. The axial force (i.e. forging force) is mainly influenced by axial position of tool in case of FSC through parameter of shoulder-workpiece clearance or scrolled feature of shoulder or stationary shoulder. The higher penetration of tool's shoulder into workpiece increases forging force on workpiece, whereas reduction in penetration of tool's shoulder into workpiece decreases forging force on workpiece. However, the axial position of tool and forging force are difficult to keep constant during processing phase because of continuous changes in thermal conditions of workpiece. The processing phase of friction stir-based channeling is recommended to be operated with position control mode as compared to force control mode, as it maintains constant position of tool with respect to workpiece. This constant position of tool allows well controlled flash removal with uniform material extraction. However, in case of position control mode, the forging force variations are more. Figure 13 shows an example of variations in forging force with respect to time for processing phase under position control and force control. In case of position control mode, the variations in forging force are more unstable variation in initial times, which becomes stable at later stage, whereas the force control mode resulted with small variations in forging force. In case of friction stir-based channeling, sufficient forging force is required to obtain effective consolidation for channel ceiling zone, whereas very high forging force causes restriction for material extraction. In case of FSC without shoulder-workpiece clearance, the surface of the shoulder's scrolled features is making contact with workpiece that in turn results in higher forging force on workpiece, as compared to the ones where shoulder is not making full contact with workpiece

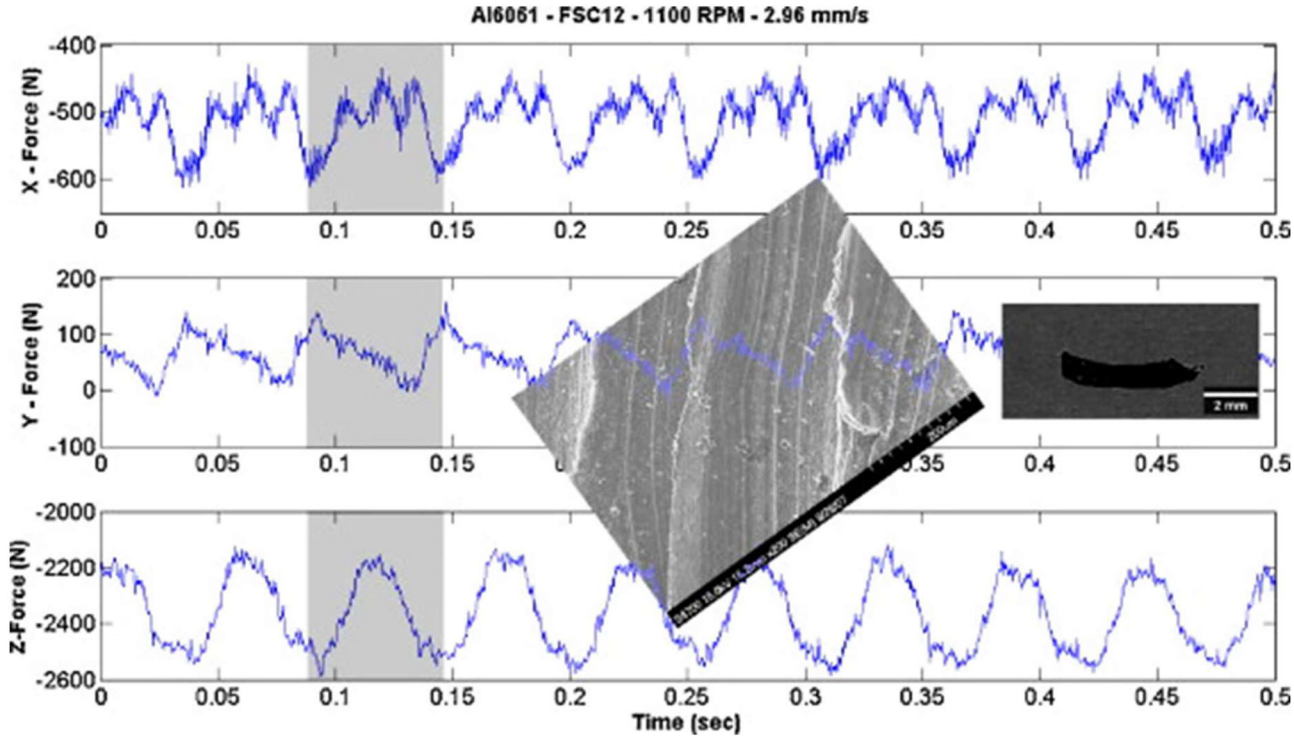

Figure 12. Forces in three different directions (longitudinal, transverse and vertical) acting on tool's probe during channel processing phase, with superimposed SEM image of channel and macrograph (highlighted region shows one complete rotation).[39]

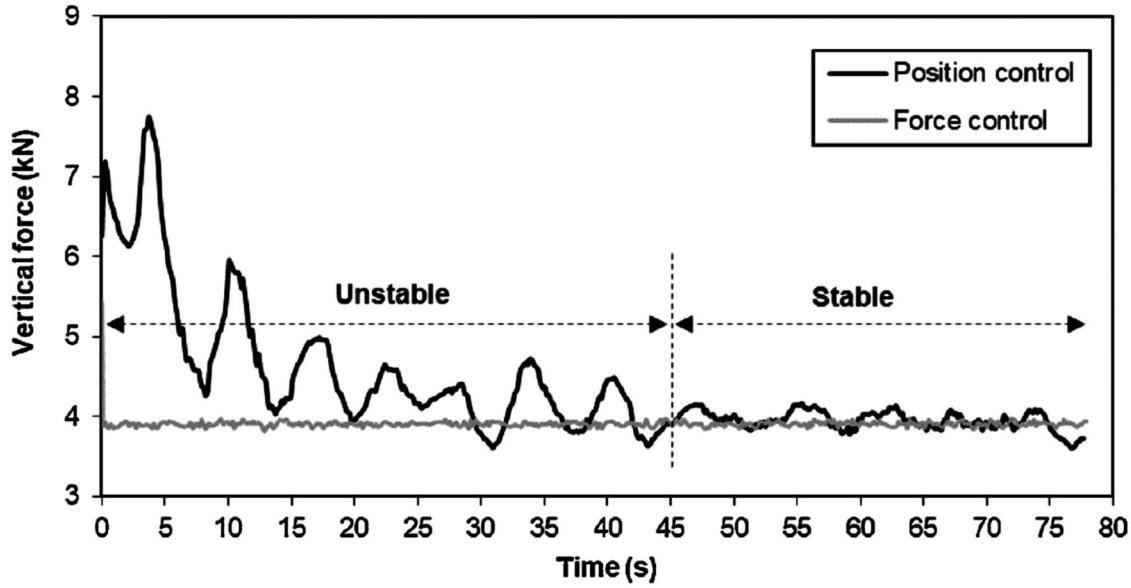

Figure 13. Variations in vertical force acting on tool's probe during channel formation phase for position control mode and force control mode.[56]

(i.e. FSC with shoulder-workpiece clearance and FSC with tilt angle and toe flash). The longitudinal and transverse forces are higher in case of FSC with shoulder-workpiece clearance, because the channel processing is performed keeping shoulder-workpiece clearance. Besides, the axial forging force is lower in case of FSC with shoulder-workpiece clearance as compared to FSC without shoulder-workpiece clearance. As the clearance between shoulder and workpiece increases, the longitudinal and transverse forces are increases, wherein the material behind the probe is extracted upward during processing. This increase in forces in longitudinal and transverse directions consequently increases the chances of probe failure due to

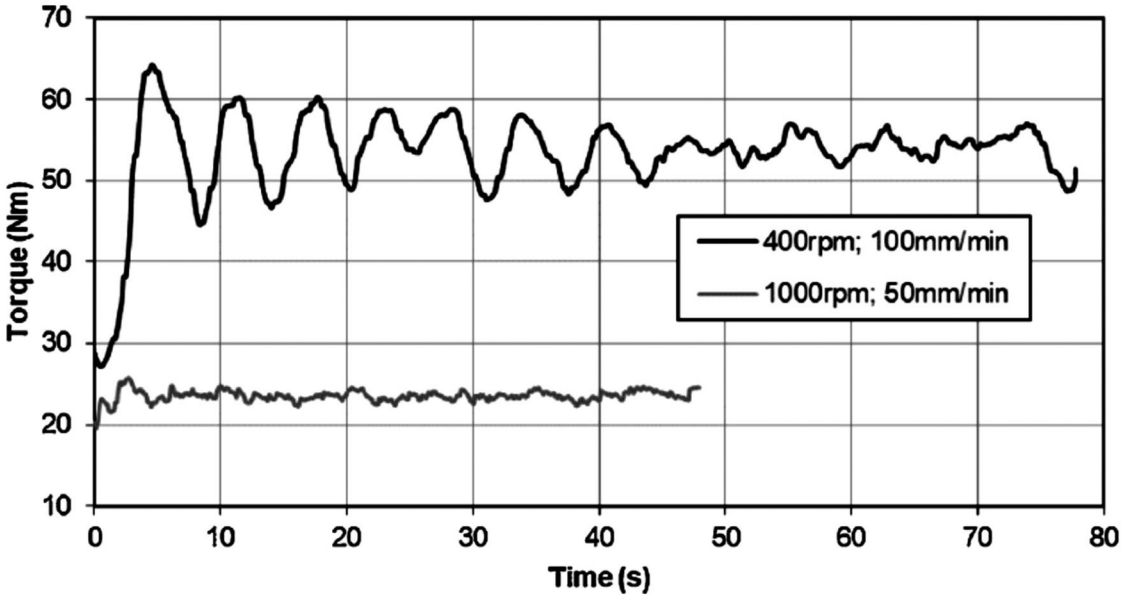

Figure 14. Variations in torque acting on tool's probe during channel formation phase for two different combinations of rotational speed and travel speed.[56]

increased stress concentration on probe (that acts as cantilever beam without shoulder's support). For example, Pandya et al.[67] reported that the tool's probe is failed during channel processing phase when subjected with shoulder-workpiece clearance. In case of FSC with shoulder workpiece clearance, the forging action is improper that in turn adversely affect the consolidation of material to close the channel. Smaller forging force leads to improper forging action that in turn results in open channel formation or voids in channel ceiling region or improper bonding in ceiling zone.

The huge amount of axial force using higher penetration of shoulder's surface into workpiece causes excessive toe flash from the workpiece that consequently lead to thinning with materials waste (subjected with post processing steps such as grinding and finishing). Increased axial force also increases chances of failure of tool's probe. The failure of tool's probe is reported by Rashidi et al.,[40] wherein higher tilt angle is used with higher penetration of shoulder's surface into workpiece. However, the tool is failed due to increased forces on tool through cold conditions subjected by rotational speed and travel speed along with applied conditions of higher tilt angle and higher penetration of shoulder's surface into workpiece.

The torque capacity of equipment used for friction stir-based channeling must be higher enough to provide an effective transport of materials for controlled extraction. Higher heat input conditions require less torque, whereas lower heat input conditions require higher torque (the example can be seen from Figure 14). In case of FSC without shoulder workpiece clearance, the required torque is very high as compared to FSC with tilt angle and toe flash and FSC with shoulder workpiece interface, due to recommended cold processing conditions.

3.4. Tilt angle

The tilt angle of the tool is very much useful in case of FSWP with threaded tool, which helps to enhance the material flow downward toward workpiece's bottom surface, by increasing vertical swirling action toward workpiece from tool that in turn enhances stirring process.[19,85] The tilt angle is kept as zero in case of FSC with and without shoulder-workpiece clearance,[16,38,39,45–49,52–55,57,67–70] whereas the tilt angle is suggested to keep as high as 2° to 3° in case of FSC with tilt angle and toe flash.[40,41,73–75] The FSC with tilt angle and toe flash is performed with thread less probe, wherein the tilt angle helps to bring material upward toward tool side from the workpiece, and consequently results in material extraction with hot conditions. However, the effective and controlled material extraction can be performed with threaded tool's probe with zero tilt angle (i.e. without tilt angle), as these threads on the probe direct the material flow, that in turn results with larger, rectangular and more uniform channel as compared to nonthreaded tool with tilt angle. The zero tilt allows more stable material extraction across the thickness in the horizontal and vertical directions within workpiece, which in turn provides larger and wider channel formation with more uniform shape throughout the channel's path.[40,41,73–75]

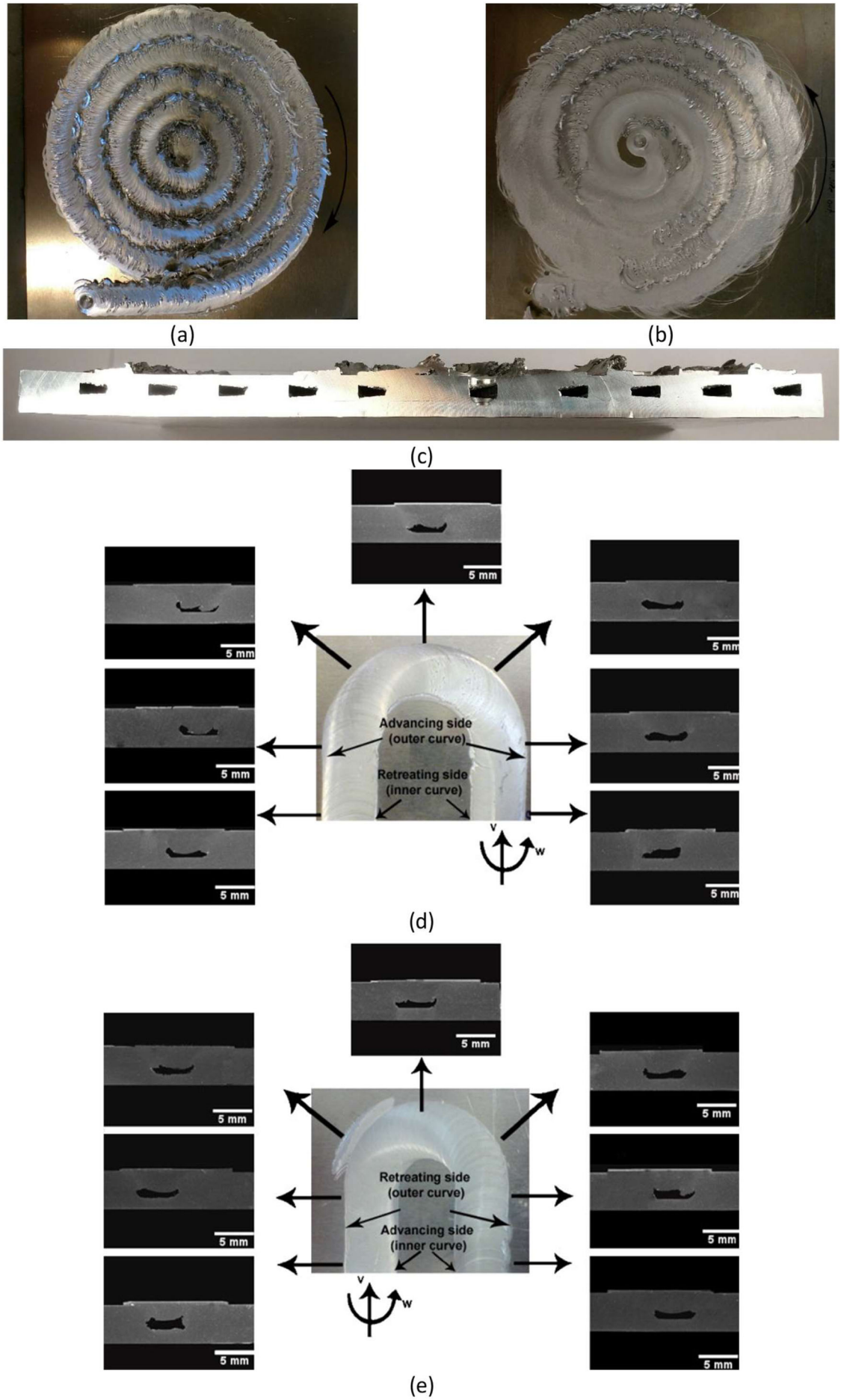
(a)
(b)
(c)
5 mm
Advancing side
(outer curve)
Retreating side
(inner curve)
v
w
(d)
Retreating side
(outer curve)
Advancing side
(inner curve)
(e)

3.5. Channel path and travel direction

FSC can produce conformal subsurfaced channels following an intricate path within a single manufacturing step. Intricate paths such as spiral (refer Figure 15a–c), serpentine (refer Figure 15d–e) and curvy bends, right angle bends or any other complex shape,[86–89] are possible to fabricate using friction stir-based channeling with continuous and uniform type of channel formation. This provides flexibility in design for various type of compact heat exchangers and for other possible applications mentioned in section Introduction. The uniformity of channel throughout the path with aforementioned intricate profiles affects the performance of the heat exchanger (such as the pressure drop and cooling efficiency). The channel's size and shape fabricated by friction stir-based channeling are greatly influenced by travel direction of tool's path. In case of complex shape such as serpentine profile and spiral profile, the curvature within the travel path affects the viscoplastic material flow that in turn influences uniformity of channel. The example of the channel's continuity and variations in size and shape across the spiral, curved and straight path are shown in Figure 15. The material flow of advancing side and retreating side is different, and therefore, the channel formation (in terms of size and shape) is influenced by tool's travel path. In case of serpentine path, the advancing side and retreating side are changed from the curvature of the path, which subsequently changes size and shape of channel. In the curvature region for the variant of FSC with shoulder workpiece clearance, the material extraction is improper that in turn results in small size of channel. The direction of tool's travel also influences channel formation as can be seen from Figure 15d,e. The material is moved from either inner curve to outer curve (Figure 15d) or outer curve to inner curve (Figure 15e) that depends on the travel direction of tool .[67]. In these two cases, the advancing side and retreating side are different for inner curve and outer curve. Balasubramanian et al.[16] mentioned that the material movement caused by advancing side (i.e. outer curve to inner curve; Figure 15d) provides better closing of channel due to enhanced forging force as compared to material movement from inner curve to outer curve, in case of FSC with shoulder-workpiece clearance. The differences in the material flow at advancing side and retreating side within the same cross-section is also observed because of differences in shearing action and subsequent influence on material movement across both the sides (refer section of material flow and microstructural features for more details).

Comparing the continuity of the channel, the channel size and shape are more uniform in case of FSC without shoulder-workpiece clearance and HFSC as compared to FSC with shoulder-workpiece clearance and FSC with tilt angle and toe flash. Refer Figure 15a–c and d–e for comparison of channel formation between HFSC and FSC with shoulder-workpiece clearance, respectively. In case of FSC without shoulder-workpiece clearance and HFSC, the channel formation is well controlled in cold conditions with highly viscous material movement. Due to higher viscosity in material flow during processing, the downward vertical movement (i.e. toward channel from workpiece) of material is only restricted to limited depth for channel ceiling formation, which results in larger, wider and more uniform channel formation throughout the travel path in case of FSC without shoulder-workpiece clearance and HFSC. However, minor variations in the channel size and shape can be resulted with FSC without shoulder-workpiece clearance and HFSC, as the material flow is always influenced by travel direction and other dynamic changes during processing of channel in case of friction stir-based channeling.[51,67,75] The examples of channel variations across the curved path are presented in Figures 16 and 17 for the case of HFSC and FSC with tilt angle and toe flash, respectively. Figures 16 and 17 show that the change in travel direction results in mirror effect of channel's shape and size, wherein the retreating side channel ceiling side of the channel form rougher surfaces. The shearing action is originated at advancing side from tool's probe that causes smother surface formation as compared to other surfaces.

3.6. Equipment and process control systems

The equipment used for friction stir-based channeling is similar like FSWP that works on similar process principle of solid-state processing. FSWP is already explored with different type of machines such as vertical milling machine, modified vertical milling machine, numerically controlled machine, computer numerically controlled (CNC) machine and robotic machine.[5] Programmable logic controller (PLC), programmable automation controller (PAC) and CNC

Figure 15. Complex path profiles manufactured by friction stir-based channeling: spiral profiles[49] (a) inward to outward movement path by tool, (b) outward to inward movement path by tool, (c) channel's continuity with cross-section of (b); serpentine profile's curved paths[60] with the advancing side on (d) outer curve and (e) inner curve.[67]

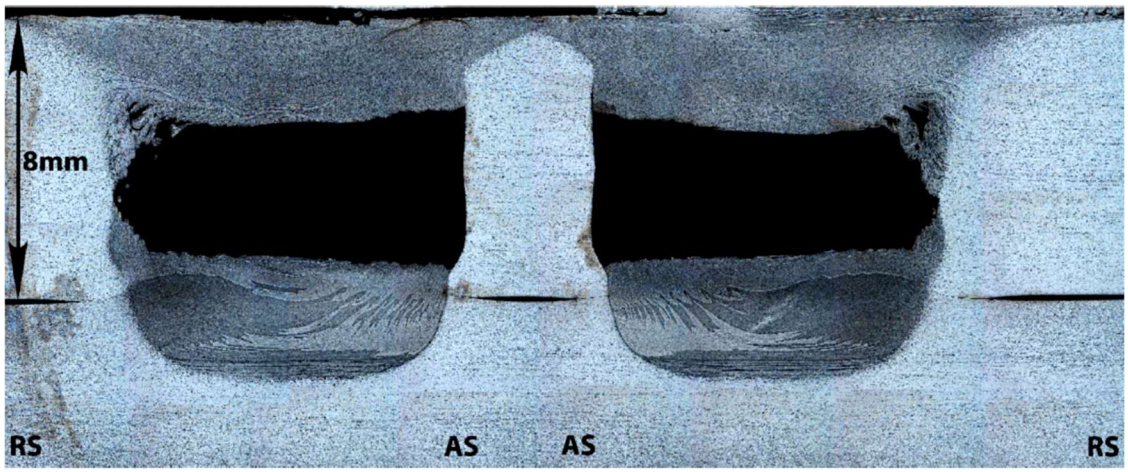

Figure 16. Channel continuity across the S shaped curved path in case of hybrid friction stir channeling (HFSC).[51]

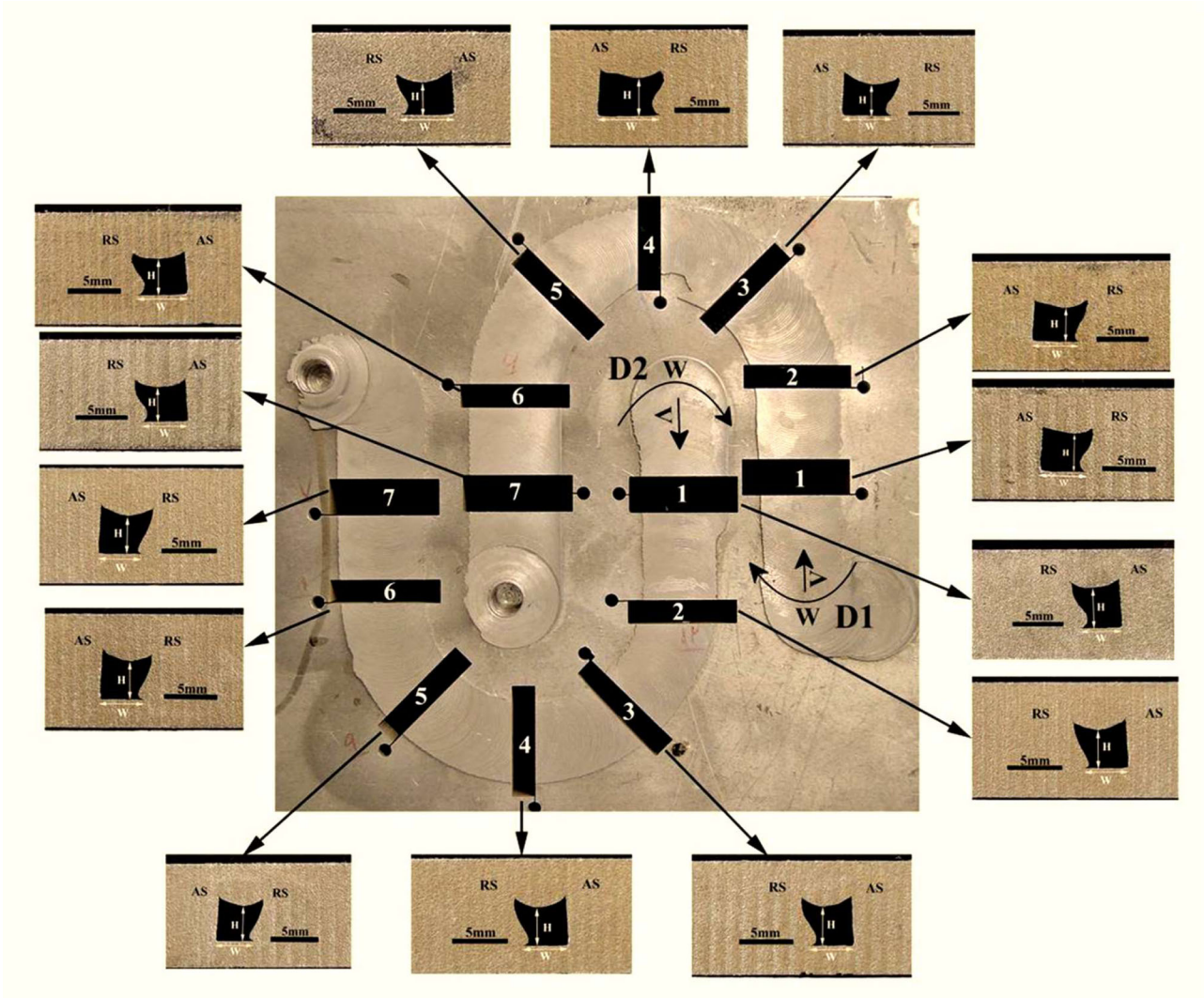

Figure 17. Channel continuity across the U type curve path in case of FSC with tilt angle and toe flash.[75]

are some of the features that are used for FSWP, which enables useful features such as acquisition of data, real time force or position control, real time monitoring, programmable path capabilities, orientations in different axis and automations.[89] Each of these controllers consists of different features, in terms

of capabilities and its working.[89] The friction stir-based channeling machine requires a setup that can follow complex paths with real time feedback system of position control or force control and data acquisition so that the channels with complex path profiles (such as serpentine or any other complex curved profile) can be produced. In case of application for straight channel, a single direction of tool's travel or workpiece's travel is sufficient. During the channel processing phase, it is important to keep a control on axial forging force and vertical axial position of the tool using closed loop control system (that is based on position control or force control), as discussed in the section of *Forces and torque during processing*. In case of axial force control system, the force changes in an incremental way while the position of the tool relies on machine stiffness. Besides, the axial position of the tool changes incrementally while the force relies on machine stiffness in case of axial position control system. In case of friction stir-based channeling, axial position control is recommended.

3.7. Other parameters and conditions

There are many other parameters that influence the precision, continuity and variations in formation of channel. Type of equipment, cooling system of tool, active usage of machine, freshness of the tool's features, tool wear, fixture design, fixture material, environmental conditions, type of backing plate, dwell time, plunge time and channel path configurations are some of those other parameters that also affects variations in channel formation.[51] The properties of workpiece materials and its dimensions play major role in friction stir-based channeling, as the plastic deformation of workpiece material governs material extraction capabilities for channel formation characteristics. So far, various aluminum alloys are subjected for the friction stir-based channeling (as summarized in Table 2).

4. Material flow and channel shape

Material flow during friction stir-based channeling decides the size, shape and features of the channel that subsequently affects the performance of the channel for the end applications. Various shape of channels such as rectangular, circular, oval, triangular and trapezoidal are obtained from friction stir-based channeling. These shapes are popular for different microchannel heat exchangers for different applications, which are conventionally fabricated using machining and subsequent mechanical fastening[71,90] or machining and welding. Different material flow characteristics and microstructural features are observed during processing of channel with different variants of FSC, which subsequently leads to formation of diverse size and shape of channel. The irregular nonuniform shape of the channel along the length increases pressure drop, hence, uniform shape of the channel along the length is desired for the application of heat exchanger. The pressure drops also increased when the hydraulic diameter of the channel increases within the same length of the channel. Similarly, the cooling efficiency is also depended on channel's size, shape and internal features. Therefore, optimum size and shape of channel with favorable internal surface features are required for better performance of channel.

Figure 18 presents cross-sectional view of channels, processed by different friction stir-based channeling techniques. It can be observed that different variants of friction stir-based channeling resulted in different channel formation characteristics with distinct size and shape of channel due to different material flow characteristics. Figure 18a shows cross-section of channel fabricated with variant of FSC with shoulder-workpiece clearance resulted in elliptical or oval shaped channels, because the tool extracts limited amount of material from the vertical direction of the tool's z-axis. The swirling action is stronger at the center and less at the sides when limited amount of material is extracted with conventional tools, which subsequently results in elliptical shape of channel. However, the channel shape can be improved controlling process parameters. For example, Pandya et al.[70] obtained the shape of the channel as nearly rectangle as shown in Figure 18b for a variant of FSC with shoulder-workpiece clearance. The material flow in case of FSC with shoulder-workpiece clearance lead to different regions around the channel such as probe influenced regions on the advancing and retreating sides and bottom side of the probe (resulted due to shearing action and material extraction) and shoulder influenced region (resulted due to forging action). In FSC with shoulder-workpiece clearance, the volume of the channel can be identified based on volume of deposited material at the clearance between shoulder and workpiece. Therefore, the channel size is limited (such as 10.90 mm^2 summarized in Table 2), with small volume constraint between shoulder workpiece clearance in case of variant of FSC with shoulder-workpiece clearance. Maximum clearance between shoulder and workpiece is observed as large as 1.2 mm in published literature (Table 2).

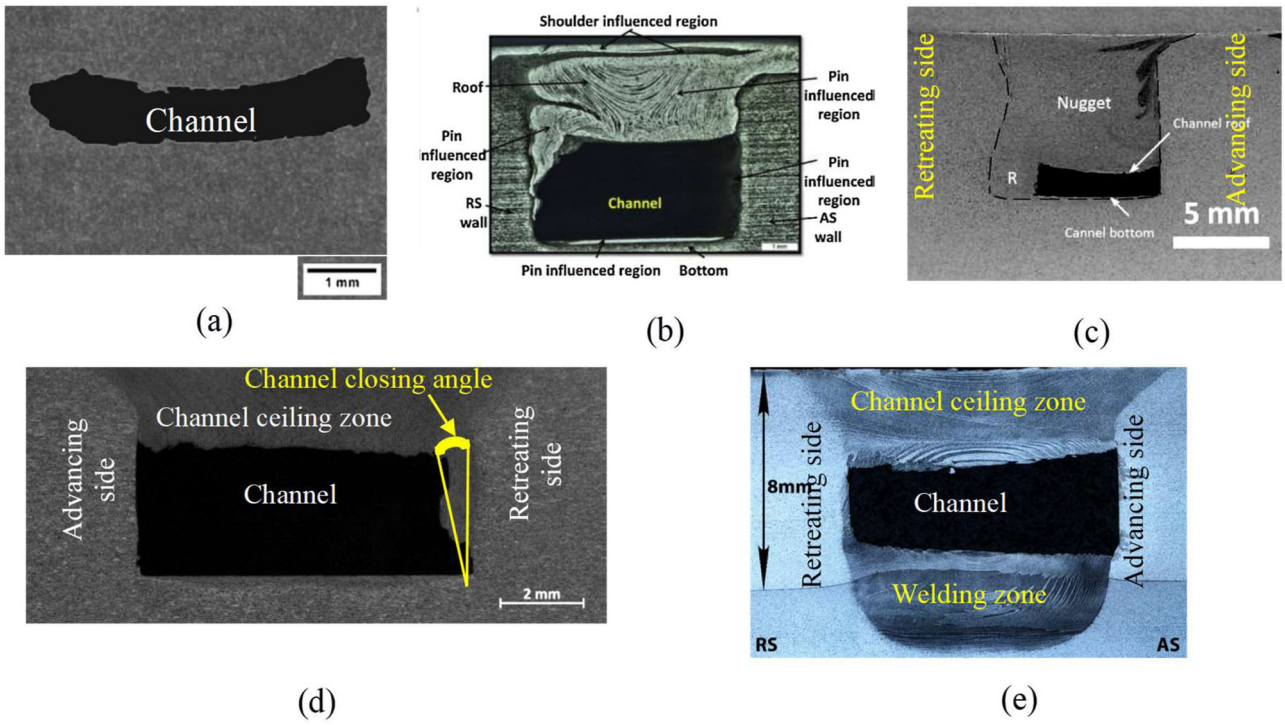

Figure 18. Cross-section of channel under different variants of friction stir-based channeling (a)[67] and (b)[70] FSC with shoulder-workpiece clearance, (c) FSC with tilt angle and toe flash,[73] (d) FSC without shoulder-workpiece clearance[52] and (e) HFSC.[51]

Figure 18c presents cross-section of channel processed by FSC with tilt angle and toe flash, wherein the channel shape is in between trapezoidal and rectangular shape.[73] Rashidi and Mostafapour[41,74] claimed that rectangular channel formation is possible with FSC with tilt angle and toe flash variant. Nevertheless, the rectangle shape of channel cannot be uniform and continuous in FSC with tilt angle and toe flash, as the tool is titled, and hence, material deposition is subjected to an angle. The rectangular type of shape is obtained in the channel of HFSC (Figure 16) while trapezoidal type of shape is obtained in FSC with tilt angle and toe flash channel (Figure 17). In FSC with tilt angle and toe flash variant, the width of channel is not equal to probe diameter unlike variants of FSC without shoulder workpiece clearance and HFSC, as the material on the retreating side is not fully sheared due to tool's tilt angle. The maximum channel's width of 6.82 mm and height of 2.62 mm are reported in case of FSC with tilt angle and toe flash (Table 2).

Figure 18d,e show cross-section of channels made by FSC without shoulder-workpiece clearance and HFSC, respectively. In these variants, the amount of material extracted in form of self-detachable flash is correlated to volume of the channel. The larger volume of channel can be obtained when large amount of self-detachable flash is extracted from the workpiece material during processing. Channel ceiling zone is created by forging action caused by shoulder's features, wherein the material movement is in the opposite direction of self-detachable flash's movement (i.e. downward toward channel from shoulder). The excess amount of material extraction causes large but open channel, because no material is available to close the channel for ceiling zone. Therefore, controlled amount of material extraction is required that is effectively performed in case of FSC without shoulder-workpiece clearance and HFSC. Improper material flow of extraction and forging can cause defects (such as voids, cracks and holes) within the channel ceiling zone.

In case of HSFC, the welding zone is formed due to stirring and forging movement of material below the channel caused by welding probe features (Figure 9m). The processed zone of welding is like a bowl shape (Figure 18e), which is caused due to tapered welding features of tool's probe. Material mixing is depended on participation of materials from the workpieces, wherein the height of the welding probe and subsequent penetration in workpieces plays an important role for materials mixing. The bottom surface of channel in case of HFSC is affected by secondary features of material mixing that in turn results in rough and uneven surface as compared to FSC without shoulder-workpiece clearance.

It can be observed as common notice from all the variants of friction stir-based channeling techniques

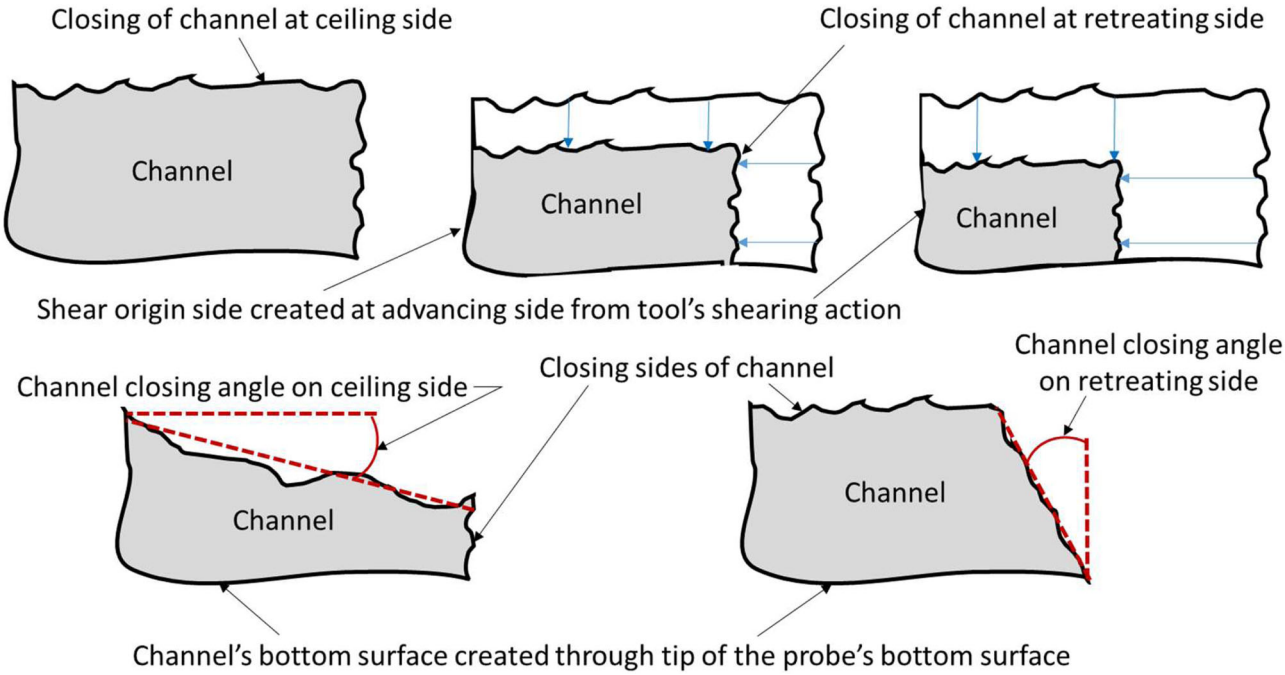

Figure 19. Channel formation in friction stir-based channeling (a) schematic of closing sides and shear sides and (b) channel closing angle.

that the channel wall of advancing side and channel wall of bottom surface are almost straight and relatively smooth, whereas the channel walls of retreating side and top ceiling surface are irregular and rough. The advancing side of channel is origin of shearing action from probe, whereas the bottom side of channel is stirring patterns of processing pitch from probe. The sheared material is deposited on retreating side and ceiling side of the channel. The retreating side and ceiling side serve as closing sides of the channel. Therefore, the size and shape of the channel is greatly governed by these closing sides of the channel as summarized in Figure 19a. The angle on retreating sidewall and ceiling surface of channel is governed by deposition of sheared material (that is referred as channel closing angle as shown in Figure 19b). The shape of the channel such as rectangle, trapezoidal, triangle and oval are governed by channel closing angle controlling the material deposition at retreating side and ceiling side of channel. The rectangular shape of the channel is obtained with least channel closing angle (i.e. zero), with controlled material extraction and subsequent deposition on retreating side and ceiling side of the channel.

5. Microstructural features

Friction stir-based channeling operates under the action of thermo-mechanical processing. The workpiece material experiences plastic deformation and recrystallization, similar like hot working that subsequently governs the microstructural features. Figure 20 shows general schematic representation of microstructural variations during friction stir-based channeling. The complex material flow under the action of thermo-mechanical processing leads various microstructural changes around the channel due to intense plastic deformation of material at elevated temperature (above the recrystallized temperature). Distinct microstructural zones such as ceiling zone/stir zone, HAZ, TMAZ and base material/unaffected zone can be observed from Figures 20 and 21 (example shows microstructures of FSC without shoulder-workpiece clearance).[51] The ceiling zone consists microstructure of recrystallized fine and equiaxed grains (see Figure 21b), caused due to recrystallization after intense plastic deformation. Similarly, recrystallized fine grains are observed at retreating side very close to the channel, where some of the deformed material is deposited during material extraction. However, this region is also influenced by heat in addition to mechanical deformation, and therefore, known as TMAZ, which also consists of partially recrystallized and distorted grains in addition to recrystallized grains. The small amount of material underneath of the channel and retreating side, in a very thin layer, is also influenced by shearing action of tool's probe that results in recrystallized grains at this region similar like ceiling zone, as shown in Figures 20d and 21d. The ceiling zone of the channel consist of two different features

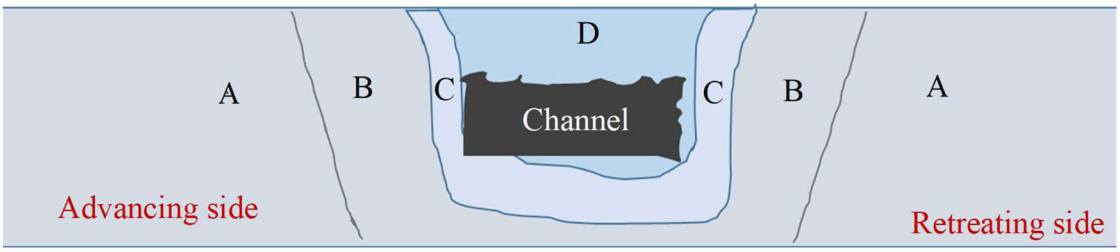

Figure 20. Schematic of microstructural regions during friction stir-based channeling, (a) base material, (b) heat affected zone (HAZ), (c) thermo mechanically affected zone (TMAZ) and (d) channel ceiling zone.

within recrystallized grains reflected through two different directions of material flow such as probe driven flow (toward tool from workpiece) and shoulder driven flow (toward workpiece from tool's probe). This different directional material flow behavior subsequently leads different grain orientation as can be seen from Figure 21c. In case of FSC with shoulder-workpiece clearance, the ceiling zone may consists of three different features such as (I) probe driven flow (Pandya et al.[70] named this zone as roof of probe influenced zone), (II) the shoulder driven flow similar to FSC without shoulder-workpiece clearance and (III) additional microstructure at shoulder-workpiece clearance (as can be seen in Figure 18b). In case of FSC with tilt angle and toe flash variant, the width of the channel is limited as the ceiling zone is restricted by lower swept action of probe.[40,41,73–75] In case of FSC without shoulder-workpiece clearance, the processing is carried out in cold conditions, whereas the same is carried out with hot conditions in case of FSC with tilt angle and toe flash and FSC with shoulder-workpiece clearance. This in turn results in different microstructures within processed regions even though recrystallized phenomenon is involved for each variant.

The TMAZ is formed due to combined thermal effects and mechanical deformation of the workpieces besides the channel and stirring region, wherein partially recrystallized grains are formed (as can be seen from Figure 21a,c,d). TMAZ is formed adjacent to channel and ceiling zone, wherein the heat is conducted from processed region with partial mechanical deformation influenced by shearing action that in turn leads to partially recrystallized and distorted grains within this zone. Some regions of TMAZ are consisting of elongated grains as compared to the grains of the ceiling zone (see Figure 21a,c,d). As the material deposition is on retreating side, the elongated grains of TMAZ on retreating side are slightly distorted than the advancing side grains. Although, these conditions such as elongated grains and distorted grains are depended on degree of deformation and heat conducted during processing. The HAZ is adjacent to the TMAZ that experiences only thermal effects without any interruption by mechanical deformation of material. As the friction stir-based channeling is recommended to operate in cold conditions in case of FSC without shoulder-workpiece clearance, the HAZ is expected to be very small or no HAZ formation. Therefore, in majority of literature belongs to FSC without shoulder-workpiece clearance variant, HAZ is not reported. Conversely, HAZ may be larger and significant in case of FSC with shoulder-workpiece clearance and FSC with tilt angle and toe flash, as these processes are recommended to be operated at high heat input conditions. Nevertheless, no quantification regarding HAZ comparison or any other zones is performed within available literature. The unaffected zone is microstructure of the base material, which is neither affected by heat nor by mechanical deformation.

In HFSC, the weld zone consists of bowl like shape below the channel as can be seen from macrograph (Figure 18e). The welding zone experiences stirring of plastically deformed material, wherein the grain refinement and recrystallization are involved to cause fine equiaxed grains of microstructure. As mentioned, the channel ceiling zone also consists of recrystallized fine equiaxed grains of microstructure, which is governed by material extraction and forging after plastic deformation of material. Figure 22a,b show microstructures of ceiling zone and weld zone, respectively. The grain refinement and dynamic recrystallization can be observed without any major distinction in microstructural features in both the images.[57] However, quantified data related to grain size and respective microstructural information are not reported in the literature. The welding zone is formed after the material mixing of workpieces, wherein different material mixing features such as hook like effect, film like flaws and banned type structures are commonly observed at the joining interface between workpiece materials. The materials mixing with film like flaws is shown in Figure 22c,d, in case of welding zone of HFSC.[51]

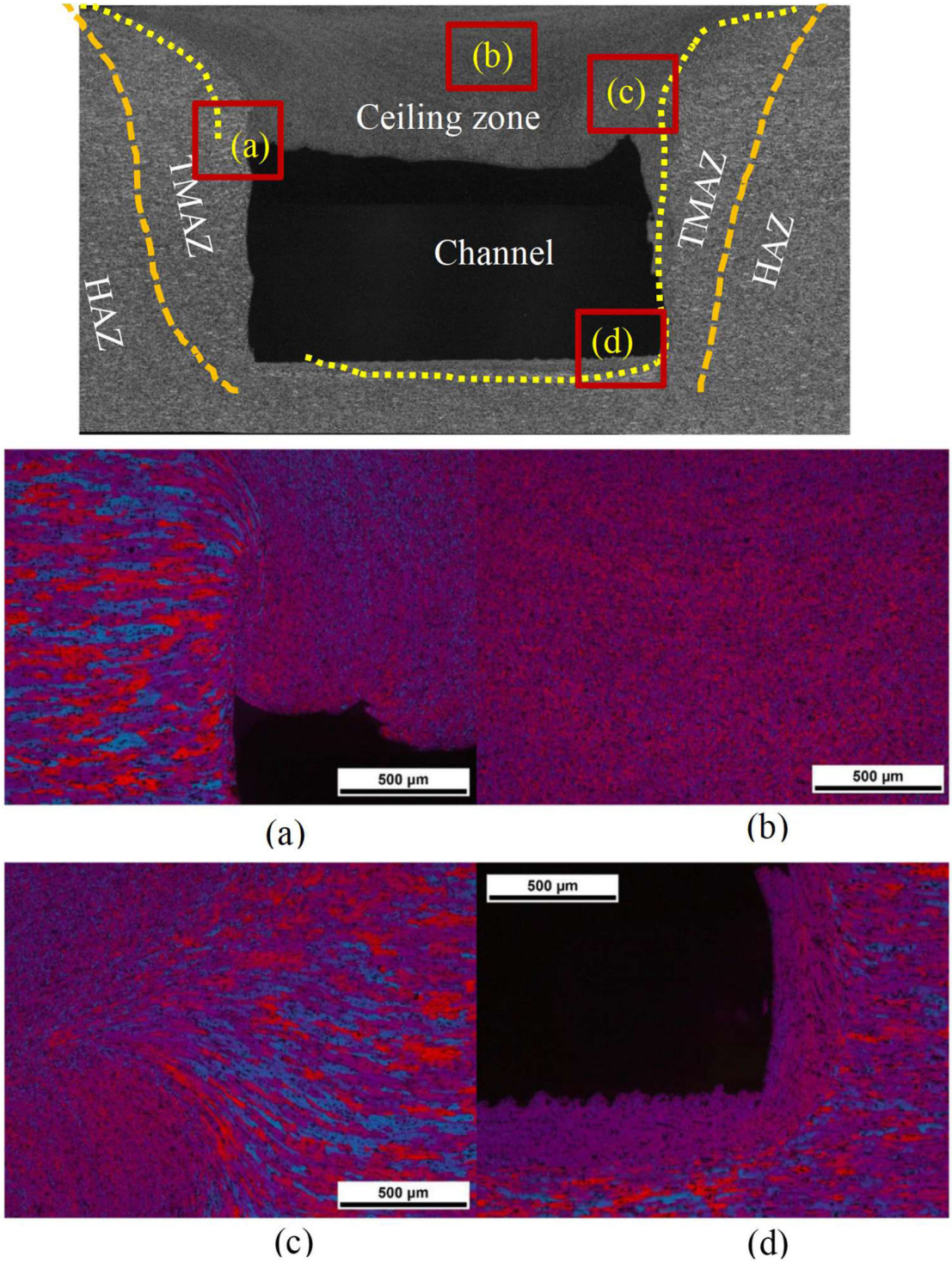

Figure 21. Microstructural features (a) channel-ceiling zone-TMAZ of advancing side, (b) ceiling zone (c) ceiling zone-TMAZ of retreating side (d) channel-deposition at retreating side-TMAZ of retreating side.[57]

6. Properties and performance of channels

The channel manufactured after friction stir-based channeling is investigated for channel's properties and performance using different testing and characterization methods such as hardness measurements across the channel, cooling efficiency of channel, pressure drop of working fluid within channel, tensile testing, bending and fatigue assessment during bending test. The performance of channels for fluid flow and thermal management system is depended on channel's surface roughness, size and shape of the channel. As

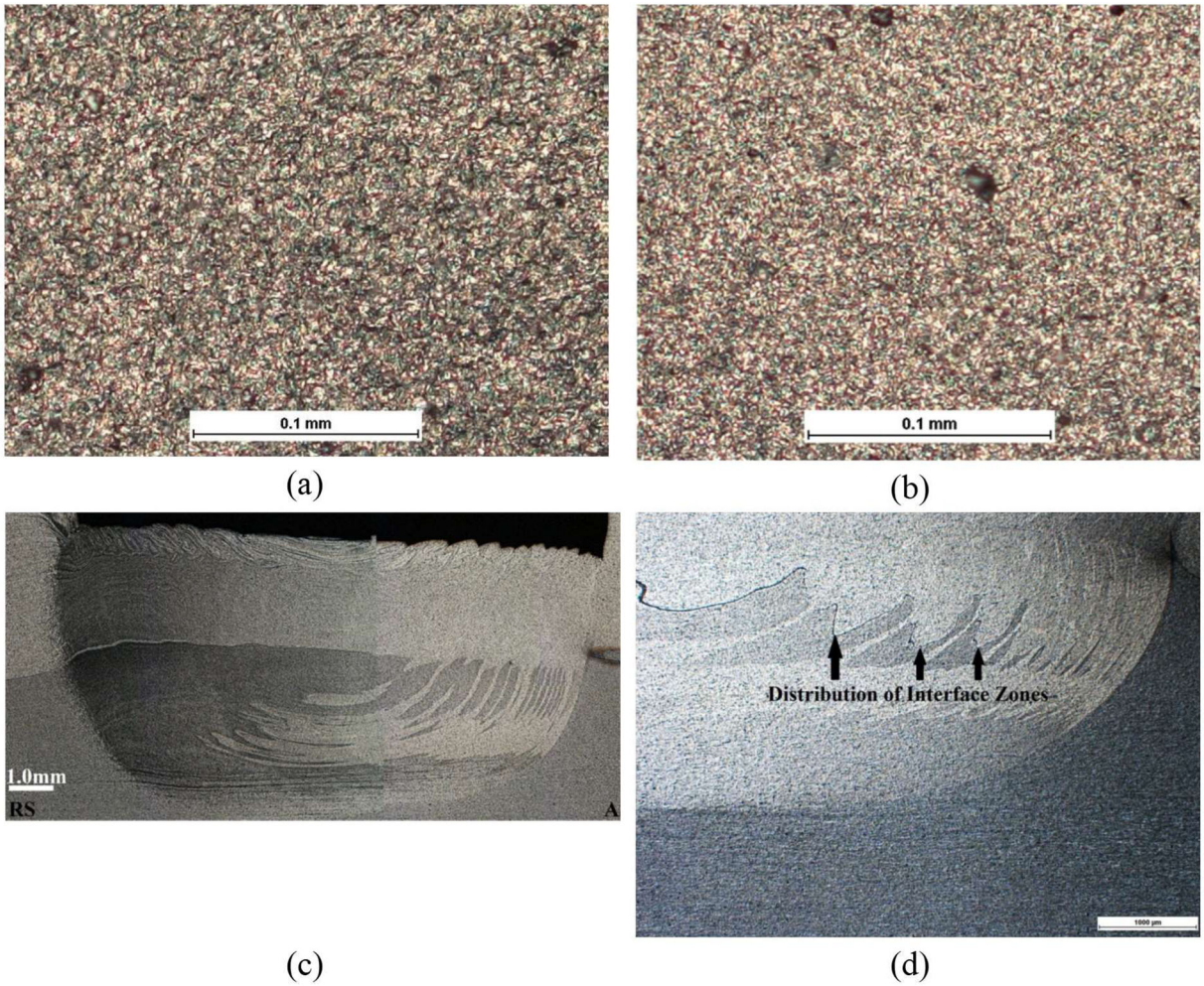

Figure 22. Microstructures of hybrid friction stir channeling (HFSC) (a) ceiling zone,[63] (b) weld zone,[63] (c) weld zone-hook like effect[51] and (d) weld zone-film like flaws.[51]

discussed, friction stir-based channeling provides great solution of subsurface channel manufacturing with an effective surface roughness and channel dimensions to better thermal management.

6.1. Surface features and performance

The surface features and dimensions of channel are important for thermal management performance, as it influences heat transfer efficiency and pressure drop of working fluid. Friction stir-based channeling is consisting of unique factor of channel fabrication with rough wall surfaces (as shown in Figure 23). In friction stir-based channeling, each wall of the channel is resulted with unique and distinct surface roughness features.[62,57,66,70,77] Figure 23 shows differences in surface roughness within channel's walls.[57,70,77] These differences in surface roughness are greatly influenced by the processing characteristics of friction stir-based channeling.

In case of friction stir-based channeling, the wall of channel's top surface (i.e. ceiling side surface) is roughest surface as compared to other three sides. The surface of the channel ceiling zone is created through material deposition to close the channel, wherein the deposited material is hanging on the channel without any support from channel side. This process of closing of channel by material deposition is dynamic with viscoplastic material movement and its consolidation. Therefore, the channel ceiling surface is also uneven with higher surface roughness. The wall of the channel at retreating side acts as second roughest surface after channel ceiling surface. The retreating side of channel is an another the closing side of the channel, where some of the material is deposited during material extraction. Small amount of material loses its momentum during material extraction from advancing side to retreating and then toward tool that in turn results in thin layer of material deposition at retreating side. Therefore, the retreating side of

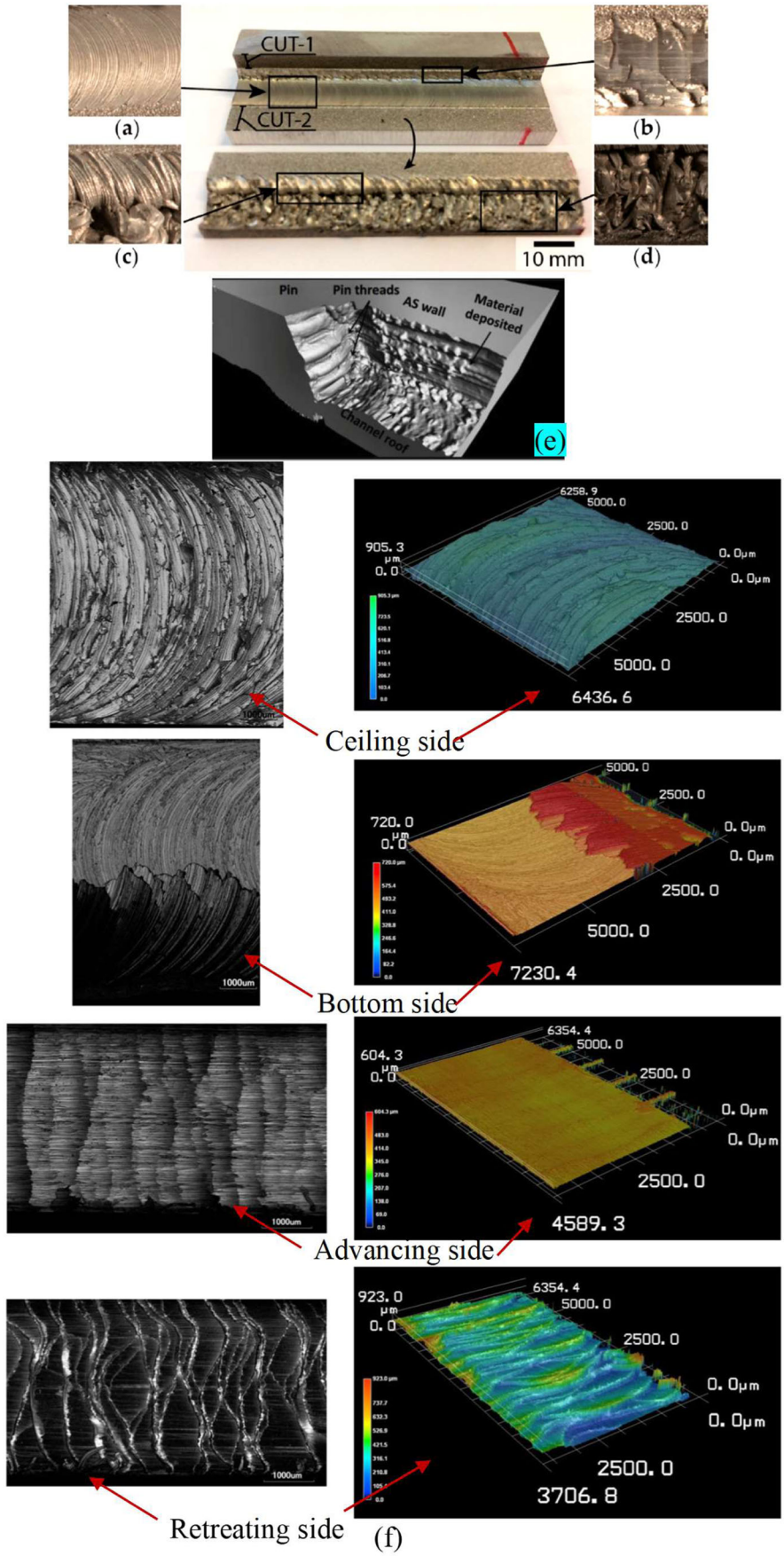

Figure 23. Surface features of channel manufactured by friction stir channeling (a–d) cross-section of channel with four different sides,[77] (e) X-ray microcomputed tomography of channel,[70] (f) Channel surfaces and its confocal laser scanning microscopy for channel.[57]

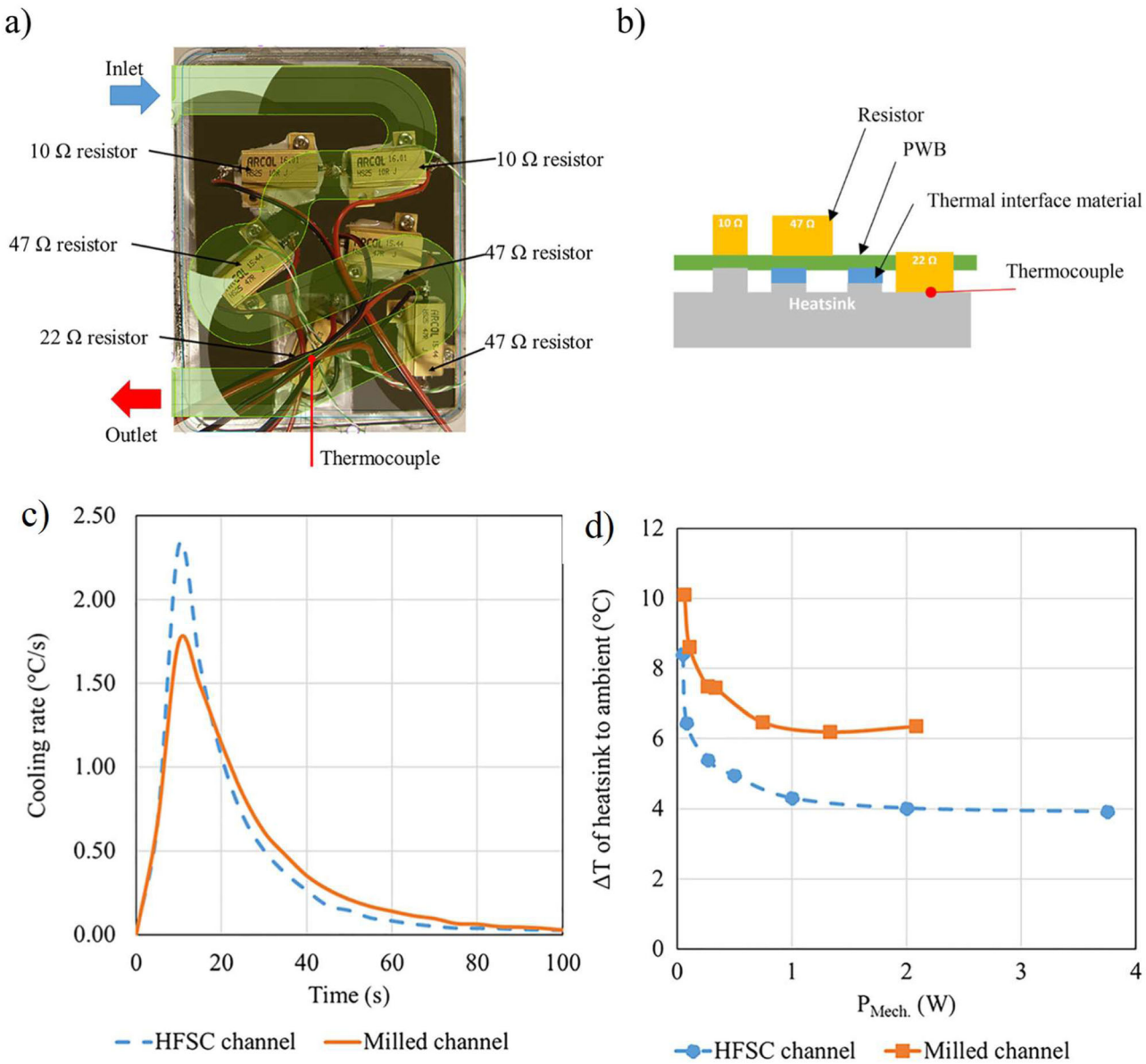

Figure 24. Performance of channels produced by FSC and milling for electronic device with liquid working fluid, (a) and (b) thermocouple locations, (c) transient cooling performance of cooling rate vs. time and (d) heat sink temperature vs. mechanical power.[66]

channel is resulted from deposited material where higher surface roughness is obtained. Both of these surfaces (of ceiling zone and retreating side) are resulted with wavy surfaces with high peaks and valleys after consolidation followed by viscoplastic material flow. On the other side, the surface of channel on advancing side is formed by strong shearing action, as this side acts as origin of shearing action by probe. The deformed material is fully extracted from advancing side to outer surface of workpiece through retreating side that results into smoothest channel surface at advancing side. The bottom side of the channel's surface is affected by probe's bottom surface. Therefore, bottom surface of the channel is left with probe's marking. This marking impression is matching with processing pitch of the tool. The bottom surface of channel is also consisting rough surface with processing marks on it. The surface roughness of bottom surface of channel is higher as compared to advancing side surface, and less than ceiling side surface and retreating side surface of channel. The surface roughness of retreating side surface and ceiling side surface is nonuniform throughout the length of the channel due to dynamic variations in material extraction and consequent deposition along the length of the channel. Karvinen et al.[66] found that channel produced by HFSC is resulted with very high surface roughness, such as 20 times higher for ceiling surface and 10

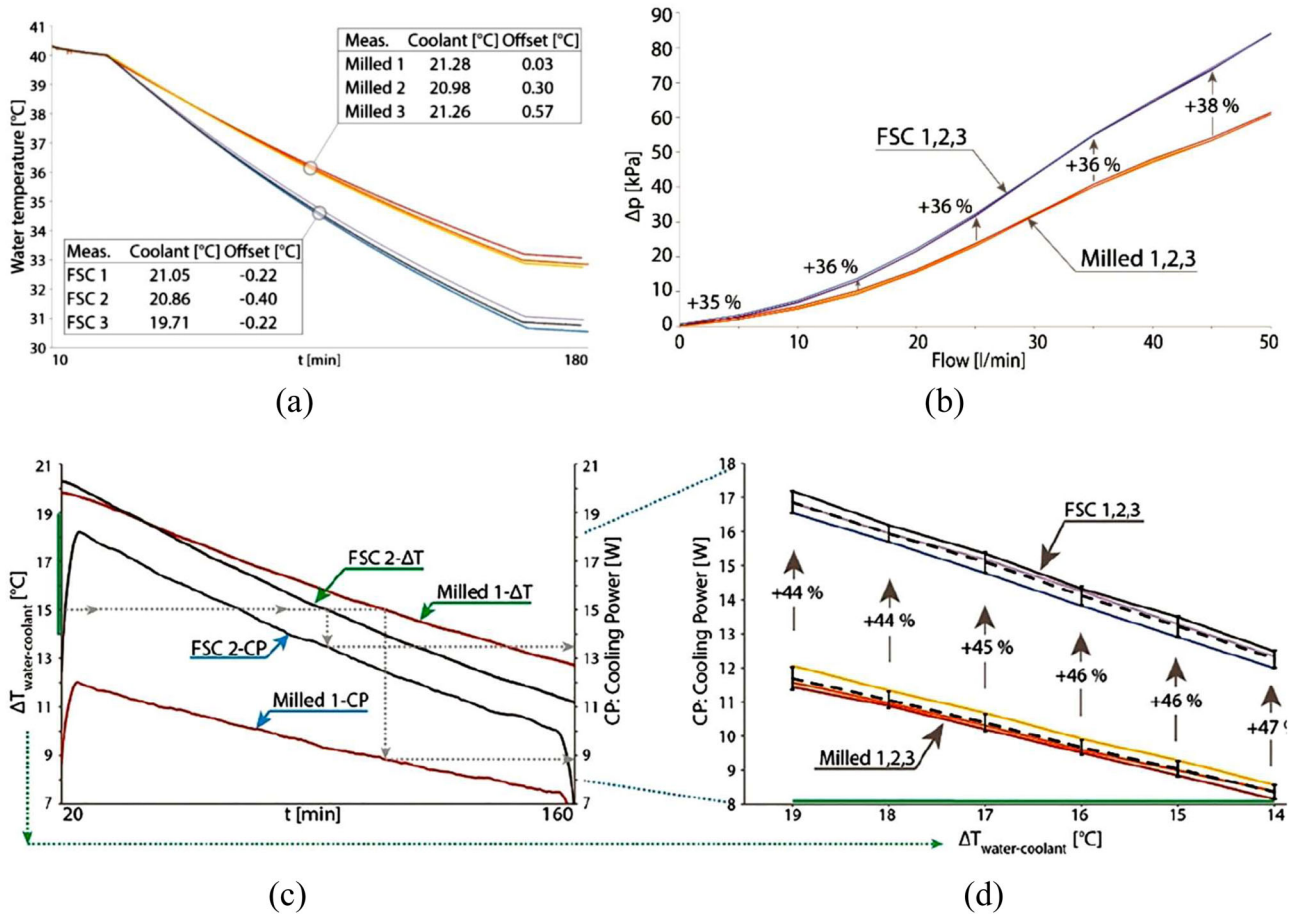

Figure 25. Thermal performance of channels produced by FSC and milling with air as working fluid, (a) calorimeter water temperature differences with time, (b) pressure differences with flow rate, (c) cooling power with similar thermal conditions with respect to time and temperature and (d) cooling power with similar temperature differences.[91]

times higher for bottom surface as compared to the channel fabricated by milling operation. Quantitative summary on surface roughness of channels fabricated by different friction stir-based channeling in presented in Table 2.

The fluid flow characteristics of working fluid inside the channel (such as laminar or turbulent flow of fluid) are greatly influenced rough surfaces of the channel. This fluid flow characteristics affect thermal convection and conduction resistance, rate of cooling and cooling efficiency. Karvinen et al.[66] tested channels manufactured by HFSC and milling, for thermal management application of electronic device with multiple heat sources as shown in Figure 24a,b. They found that channels fabricated by HFSC are better for thermal management performances such as 30% to 40% lower steady state temperature and 33% higher cooling rate during the transient period (refer Figure 24c,d), as compared to channels fabricated by milling (with similar path and dimensions). It is also suggested that, improved performance of HFSC channels results in extending the life of electronic components that undergo complex and demanding heat loading cycles during service. Karvinen et al.[77] concluded that channels produced by FSC without shoulder-workpiece clearance improve performance by 45% of heat transfer capacity with turbulent air cooling as compared to the milled channels, despite of increased pressure loss of 36%. Salminen et al.[91] found that channels produced by FSC without shoulder-workpiece clearance are better in terms of heat transfer rate and cooling power ability despite of high pressure difference, as compared to channel produced by milling (Figure 25). Salimi et al.[71] used different FSC tool designs to produce channels with different surface roughness. They found that channels having mean surface roughness of 6.11 micron are better in terms of performance, wherein laminar and turbulence fluid flow resistance, laminar and turbulence convection heat transfer resistance and conduction heat transfer resistance are considered.

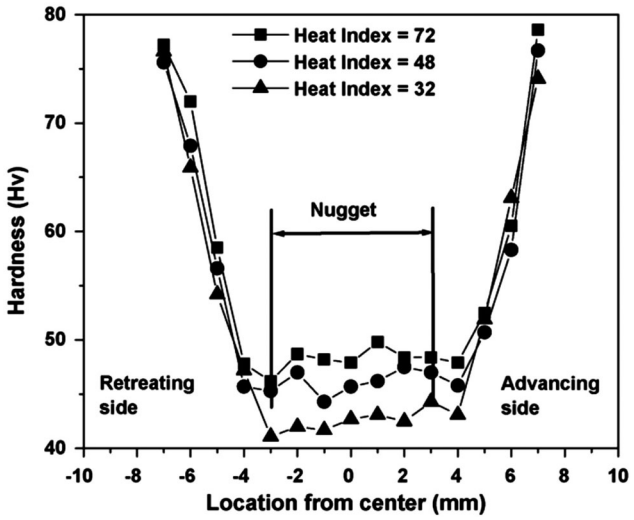

Figure 26. Hardness measurements in the cross-section of channel ceiling zone in case of FSC with shoulder-workpiece clearance.[16]

In the same investigation, it is found that the very high surface roughness increases pressure drop that in turn leads to less efficient heat exchanger arrangement.[71] Therefore, intermediate surface roughness of channel is required for desired Reynold's number to govern optimum turbulent flow of working fluid in channel along with enhanced heat transfer efficiency. Pandya et al.[72] found that effective axial wall conduction in case of channel produced by FSC greatly enhances the heat transfer and fluid flow characteristics due to higher surface roughness within channel's walls.

6.2. Mechanical properties

The mechanical properties and structural integrity of the channel are important for applications experiencing loading conditions.

6.2.1. Hardness

The hardness of processed zones around the channel is influenced by microstructural differences of processed regions. Balasubramanian et al.[16,67] observed hardness variations at the middle of the ceiling zone (Figure 26), wherein the hardness is decreased compare to the base material. This decreased in hardness is due to either grain coarsening effect or dissolution of precipitates resulted to strengthening due to strong stirring action during processing in case of FSC with shoulder-workpiece clearance. The grain coarsening is expected in this variant due to processing conditions in high heat input with low pressure consolidation by shoulder-workpiece clearance, whereas higher hardness in ceiling zone is observed in other variants of HFSC and FSC without shoulder-workpiece clearance. The hardness variations across the cross-section are mapped in literature of [57, 66, 77] as shown in Figure 27 for variants of HFSC and FSC without shoulder-workpiece clearance. On contrary to the hardness of ceiling zone in case of FSC with shoulder-workpiece clearance, it can be seen that the hardness on the ceiling zone is higher as compared to the base material in both the cases of FSC without shoulder-workpiece clearance and HFSC. This is attributed due to higher grain refinement of ceiling zone caused by high strain rate of deformation in combination with cold processing conditions that too with higher forging action caused by contacting shoulder surface to workpiece in the variant of FSC without shoulder-workpiece clearance. Figure 27 shows that the hardness of the ceiling zone is varying from top to bottom within the same processed zones. Higher hardness at shoulder forging region of ceiling zone (i.e. top portion of ceiling zone) and at the retreating side of material deposition zone can be seen from Figure 27a, which is due to intense grain refinement resulted in these regions. In case of HFSC, increased hardness is observed at the weld zone as can be seen from Figure 27c. This is due to similar effect of intense stirring resulted in grain refinement, but for mixing with downward movement of materials. This can be correlated with similar microstructures of stirring effects mentioned in the section of Microstructural features. Figure 27 shows that resulted in the TMAZ is resulted with lowest hardness that is may be due to partial recrystallization and large partially deformed grains.

6.2.2. Bending behavior

To assess the bending behavior, four-point bending test is performed in the vicinity of the processed channel. The bending strength of the friction stir channeled specimens is depending upon size and shape of the processed channel as well as presence of the defects such as cracks, voids in the ceiling zone or any other zones. Figure 28 shows the load-displacement curve of four-point bending test performed for four different channels (of U1, U2, L1 and L2 in Figure 28), that are processed by FSC without shoulder-workpiece clearance. The maximum bending strength and higher elongation can be seen in case of U1 that is consisting of highest ceiling area and smallest channel size. In case of U2, the decreased bending strength is observed as compared to U1 specimen. However, in this case, the size of channel is not so large as compared to U1, but defects such as voids and cracks in the ceiling zone may have resulted with

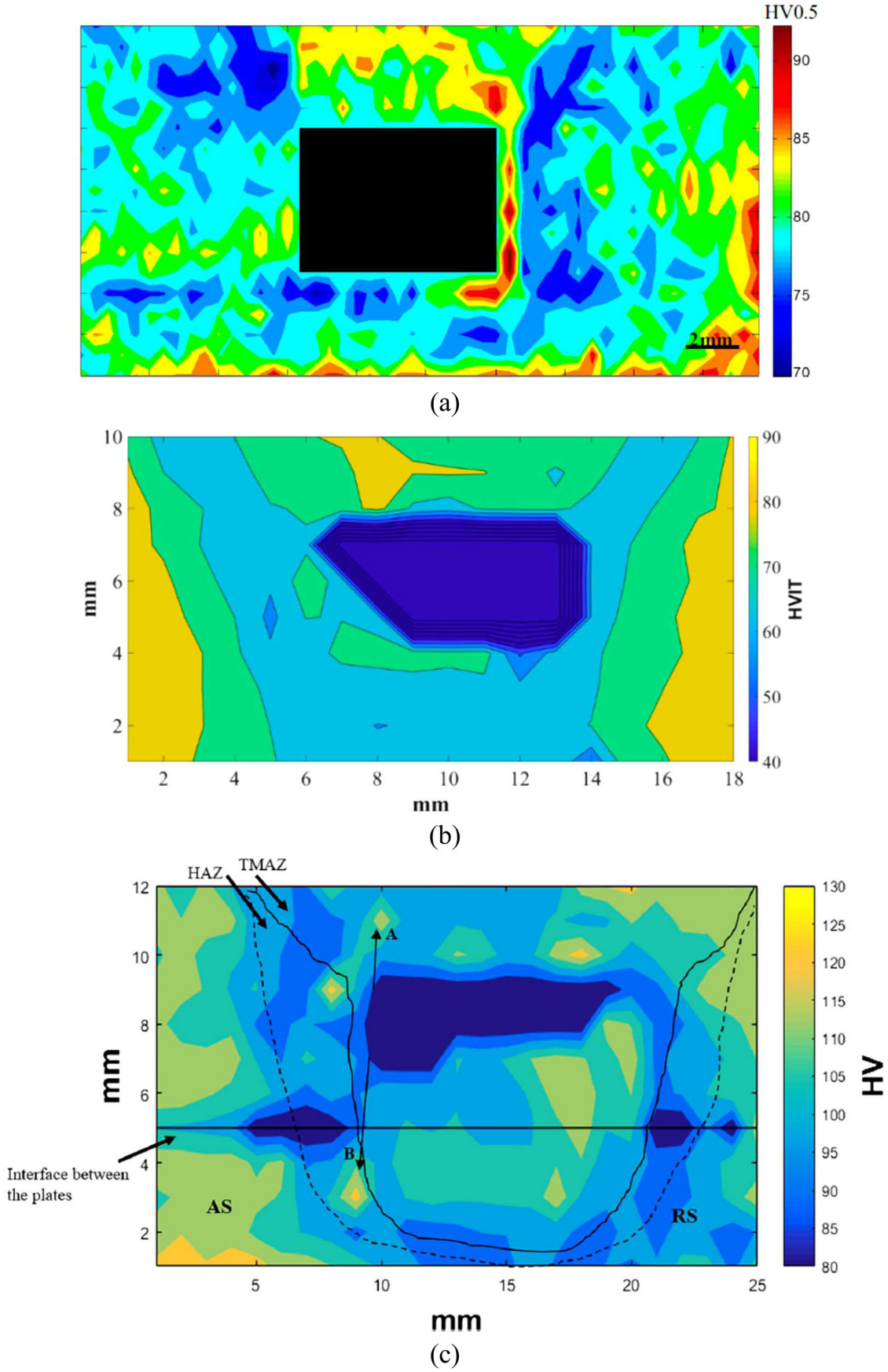

Figure 27. Hardness measurements all over the cross-section around the channels (a)[57] and (b)[77] FSC without shoulder-workpiece clearance and (c) hybrid friction stir channeling (HFSC).[66]

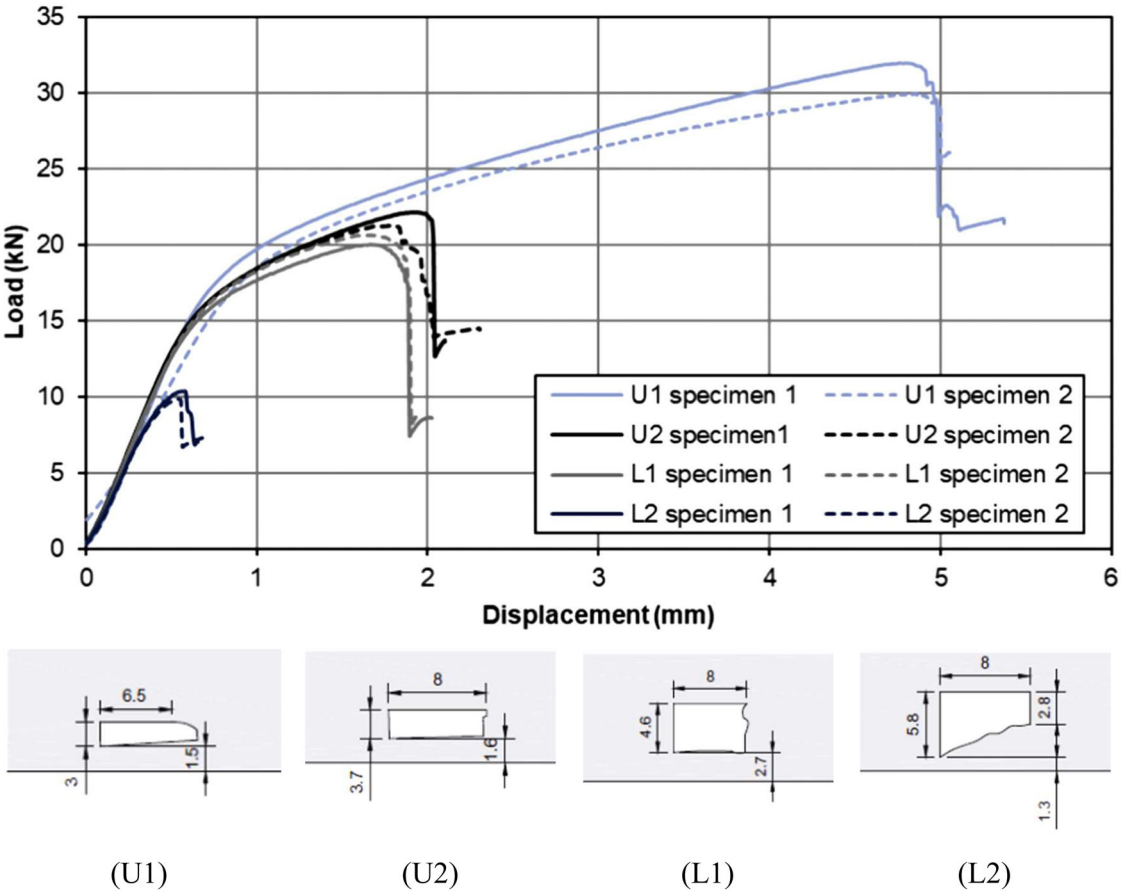

Figure 28. Load-displacement bending curve and corresponding channel size.[53]

decreased bending strength. These defects can be avoided with enhanced material flow through optimum channel processing conditions. The lowest fracture load during bending test is reported for trapezoidal type of shape and consisting of biggest channel in case of L2. It can be summarized that the size and shape of the channel influence fracture load during bending. Large ceiling zone of channel leads higher fracture load during bending. However, defects in larger ceiling zone lead to smaller fracture load during bending.

6.2.3. Fatigue

The fatigue strength of defect free FSCed specimen is always lower as compared to the base material due to the presence of channel where no material is present. The fatigue crack initiation is always from the channel's area due to stress concentration, and that propagates from ceiling zone or from material below the channel, depending on size, shape and presence of defects. The crack propagation period increases with an increase in area of channel ceiling.[43] The fatigue crack initiation time is found larger than the crack propagation time in in case of [43, 53]. The presence of defect such as voids on the ceiling side results in worst fatigue performance, wherein the defect acts as notch during fatigue testing. The stresses are high at this notch that in turn results in fatigue failure within lower number of loading cycles, as reported in [43, 53]. In the literature of [54], it is found that the fatigue strength of FSC specimens generally decreases at an elevated temperatures as thermally activated elements and time depended factors are applied in combination. Vidal et al.[54] performed fatigue testing using four point bending test at elevated temperature of 200 °C, wherein the fatigue strength of FSCed specimens significantly decreased as compared to testing performed at room temperature. They observed that the fracture of FSCed specimen is occurred from the interface between ceiling zone and TMAZ during the fatigue test (Figure 29a,b). The crack initiation (shown by point 1) is due to the transition of coarse grains from TMAZ to recrystallized fine grains of ceiling zone. Line 2 in Figure 29 show that the fracture is propagating from advancing side of the channel (Figure 29a) or retreating side of the channel (Figure

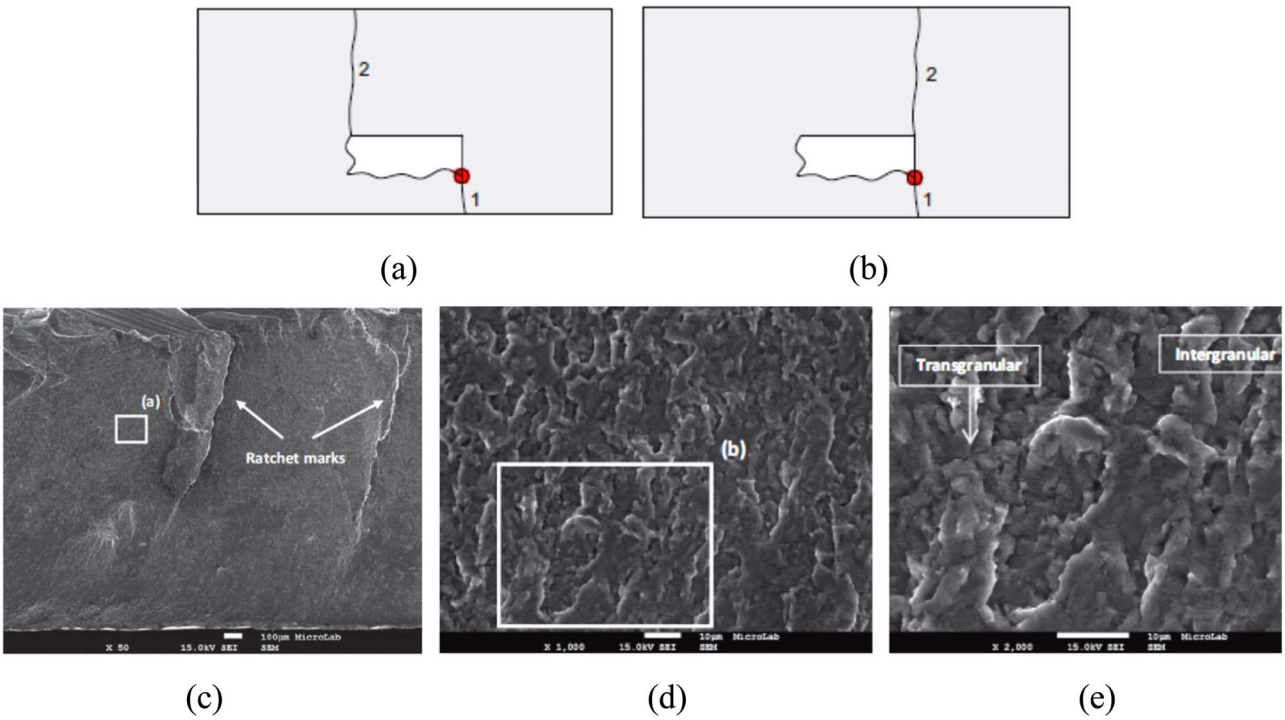

Figure 29. Four point bending fatigue test (a) and (b) crack initiation and propagation and (c), (d) and (e) fracture surfaces.[43]

29a). The fatigue fracture is from cross-surfaces (i.e. line 2 at advancing side as shown in Figure 29a), when the channel is nearly rectangular shape such as Figure 28 (U2) and (L1). Besides, the fracture occurs linearly (i.e. line 2 at retreating side as shown in Figure 29b) when the channel is nonrectangular shape consisting of higher channel closing angles like Figure 28 (U1) and (L2). The fracture surfaces of four point bending are found with mixed fracture of intergranular decohesion and trans granular cracking as shown in Figure 29c–e, mostly with flat surfaces in line with its slip phenomena of FCC fracture.

6.2.4. Tensile properties

The ultimate tensile strength is less than the base material when tensile testing is performed with channel existed specimen (as shown in Figure 30a). For the same specimen, the difference of yield strength and elongation in the specimen of channel is found less as compared to the base material.[54] They observed fracture surfaces with dimples after tensile testing as can be seen from Figure 30c,d, which indicate ductile fracture. During tensile testing, the fracture initiates from the interface between advancing side and ceiling zone as shown in Figure 30b. The fracture initiation during mechanical testing is depended on the channel's shape and size as mentioned in previous section shown by Figure 29a,b. Figure 30b shows sharp corner between ceiling zone and advancing side that is responsible for the stress concentration during tensile testing, and subsequently resulted in crack initiation point. Balasubramanina et al.[67] performed tensile testing only considering ceiling zone without channel as a part of specimen for testing, for a sample processed by FSC with shoulder-workpiece clearance. They found that the ultimate tensile strength and yield strength of channel's ceiling zone are observed 60% more than base material.

6.2.5. Leakproof testing

The leakproof testing is a nondestructive type testing to identify leakage from processed zone for fluid flow applications. The leakproof testing is carried out by working fluid of either liquid or gas or both, depending upon the application of channels. The channels are filled with specified fluid at desired working pressure or more than desired working pressure, for determined time duration to assess the leakproof ability of channels.

Vidal et al.[44] performed pneumatic leakproof test for the processed channels using air as working fluid inside the channel at internal pressure of 100 bar, wherein helium gas is applied on outer surface of the channels to identify leakage of air from the channel to outer surface. In some of the FSC fabricated channels of [44], the leak location is mainly identified from advancing side of ceiling zone. This shows that the channels fabricated by FSC are weak from advancing side of the ceiling zone. This is due to material flow phenomena in case of friction stir-based channeling.

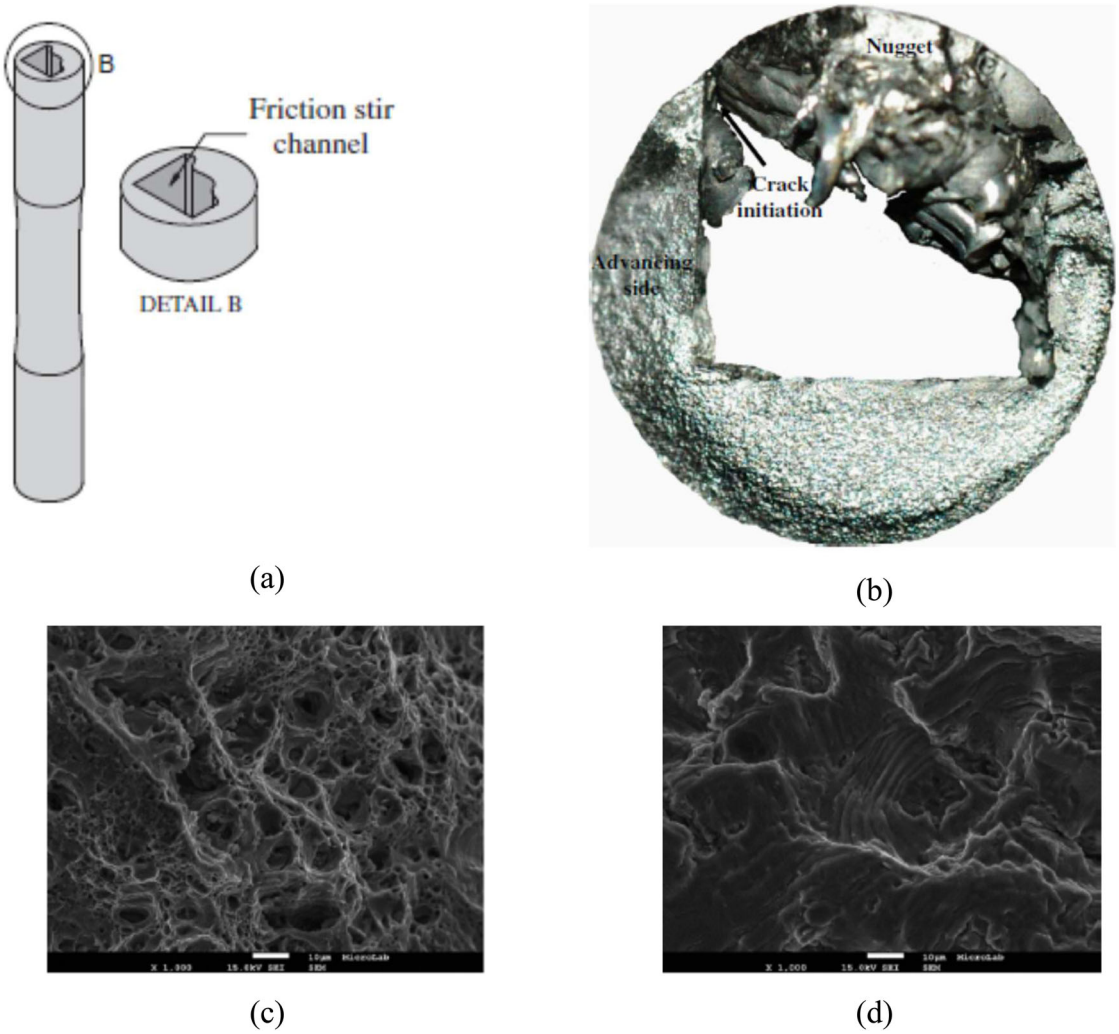

Figure 30. (a) Tensile specimen, (b) fracture initiation image, (c, d) fractured surface.[46]

The advancing side of ceiling zone is formed at last by deposition of the extracted material along with forging action. Inadequate forging during processing of friction stir-based channeling may lead to improper bonding lead to lack of consolidation to close the ceiling zone at the advancing side, as it is formed lastly when material deposition occurs. Friction stir-based channeling can produced structurally stiffed subsurface channels that can able to sustain high internal pressure of working fluid. Aleni et al.[78] performed hydraulic test and pneumatic test using internal pressure of 100 bar, wherein channels sustained the pressure without any leak. The channels fabricated by Karvinen et al.[66] resisted internal pressure up to 380 bar for a long period of time.

7. Outlook and way forward

The comprehensive review on friction stir-based channeling is presented, addressing the fundamentals on process description of different variants of friction stir-based channeling, tool designs, process parameters, channel formation characteristics, channel performance, microstructural features and mechanical properties of processed regions. The friction stir-based channeling is a novel channel manufacturing technique, under the category of solid-state processing, applied to produce conformal subsurfaced channels within single manufacturing step. In friction stir-based channeling, different variants such as FSC with shoulder-workpiece clearance, FSC with tilt angle and toe flash, FSC without shoulder workpiece clearance and SSFSC are developed with process variations by tool design and parametric conditions. Recent development of friction stir-based channeling is hybrid friction stir channeling, wherein solid-state processing enabling simultaneous channeling and welding is performed within single manufacturing step.

The channels fabrication by friction stir-based channeling find popular application to manufacture

compact size of heat exchangers for different thermal management systems. Friction stir-based channeling has great potential for industrialization for variety of applications within thermal management systems as well as fabrication of composites with channels, channels with metallic structures for electric cables, structurally inbuilt hollow paths for nondestructive testing wires, hollow panels and structures for light weight assemblies and composite materials with channels filled with secondary material. Friction stir-based channeling is consisting unique ability to produce rough wall surfaces of channels that benefits to enhanced cooling efficiency for heat transfer applications.

This review presents extensive information on variants of friction stir-based channeling. The processing variants of channels influences size, shape and surface roughness of the channels, which in turn govern performance of channels by fluid flow characteristics, thermal performances, variation in microstructural features and mechanical properties of processed regions. The tool design and features on probe and shoulder govern channel's size, shape and surface roughness of the channel. Combination of process parameters such as rotational speed, travel speed, tilt angle and shoulder-workpiece clearance, channel processing path and configurations and forces and torque during processing plays a critical role in case of friction stir-based channeling, wherein additional factors such as equipment and control systems, workpiece material properties, workpiece thickness, tool wear, fixture design and material, environmental conditions, dwell time and plunge time also influences operation of channel manufacturing. Continuous formation of conformal channel with uniform size and shape with higher surface roughness is possible to produce using controlled processing of friction stir-based channeling.

As a future prospective, the friction stir channeling can be explored to other range of heat exchangers by varying the size and shape of the channels. The stability and uniformity of channel formation in extremely complex and long path can also be considered as an area of futuristic research and applications. So far, the friction stir-based channeling is applied to aluminum and its alloys due to its excellent viscoplastic behavior. Other materials such as copper, magnesium, titanium, stainless steels, plastics and composites, can be explored with friction stir-based channeling for range of upcoming applications. Multimaterial processing using hybrid friction stir channeling can be explored for novel engineering applications considering large open research questions and novel solutions. Developments in equipment, fixture and tool materials in friction stir-based channeling can also be viewed as futuristic area of expansion for research and engineering applications. The concept of channel manufacturing can be extended to open wide window for other configurations and complex paths such as cylindrical components, uneven thicknesses and processing within different planes.

Funding

Authors would like to express their gratitude of thanks to EIT Manufacturing-European union for AeroMC2-20130_2020 project funding. Kush Mehta would like to thank School of Engineering, Aalto University-Finland for providing funding through postdoctoral researcher's scholarship.

ORCID

Kush P. Mehta http://orcid.org/0000-0001-6158-8627

References

1. Mehta, K. Advanced Joining and Welding Techniques: An Overview. In *Advanced Manufacturing Technologies. Materials Forming, Machining and Tribology*; Gupta, K., Ed. Springer International Publishing AG: Birkhäuser Verlag AG, Springer, Cham.; 2017; pp 101–136. doi:10.1007/978-3-319-56099-1
2. Vilaça, P.; Thomas, W. Friction Stir Welding Technology. In *Structural Connections for Lightweight Metallic Structures. Advanced Structured Materials*; Moreira, P. M. G. P., Da Silva, L. F. M., Paulo de C. M. S. T., Eds. Springer International Publishing AG: Birkhäuser Verlag AG, Springer, Cham; 2011; pp 85–124. doi:10.1007/8611
3. Mehta, K. P. A Review on Friction-Based Joining of Dissimilar Aluminum – Steel Joints. *J. Mater. Res.* 2019, *34*, 78–96. doi:10.1557/jmr.2018.332
4. Mehta, K. P.; Badheka, V. J. A Review on Dissimilar Friction Stir Welding of Copper to Aluminum: Process, Properties, and Variants. *Mater. Manuf. Process.* 2016, *31*, 233–254. doi:10.1080/10426914.2015.1025971
5. Gandra, J.; Krohn, H.; Miranda, R. M.; Vilaça, P.; Quintino, L.; Santos, J. F. Friction Surfacing — A Review. *J. Mater. Process. Technol.* 2014, *214*, 1062–1093. doi:10.1016/j.jmatprotec.2013.12.008
6. Kulekci, M. K.; Esme, U.; Buldum, B. Critical Analysis of Friction Stir-Based Manufacturing Processes. *Int. J. Adv. Manuf. Technol.* 2016, *85*, 1687–1712. doi:10.1007/s00170-015-8071-5
7. Padhy, G. K.; Wu, C. S.; Gao, S. Friction Stir Based Welding and Processing Technologies - Processes, Parameters, Microstructures and Applications: A Review. *J. Mater. Sci. Technol.* 2018, *34*, 1–38. doi:10.1016/j.jmst.2017.11.029

8. Thomas, W.; Nicholas, E.; Watts, E.; Staines, D. Friciton Based Welding Technology for Aluminum. *MSF*. 2002, *396–402*, 1543–1548. doi:10.4028/www.scientific.net/MSF.396-402.1543
9. Vilaça, P.; Gandra, J.; Vidal, C. Linear Friction Based Processing Technologies for Aluminum Alloys: Surfacing, Stir Welding and Stir Channeling. In *Aluminium Alloys - New Trends in Fabrication and Applications*; Zaki, A., Ed. InTech: Rijeka, Croatia; 2012; pp 159–197. doi:10.5772/52026
10. TWI Ltd. Structural Thermal Management by Friction Stir Channelling, 2019. https://www.twi-global.com/media-and-events/press-releases/2019/structural-thermal-management-by-friction-stir-channelling (accessed June 02, 2020).
11. Gandra, J.; Stocks, T. Integrating Thermal Management Networks in Structures by Friction Stir Channelling, 2019. https://www.twi-global.com/what-we-do/research-and-technology/current-research-programmes/joint-industry-projects/integrating-thermal-management-networks-in-structures-by-friction-stir-channelling (accessed June 02, 2020).
12. Gandra, J. Friction Stir Channelling: A Leaner Method of Manufacturing Heat Exchangers for Aerospace. AEROMAT19 30th Conference and Exposition, ASM International, May 6–8, 2019.
13. Simulation, S.; Annealing, T.; Furnaces, V. Hydra Cool Water Cooling system, 2018. https://www.lesker.com/newweb/manufacturing/hydracool.cfm (accessed June 02, 2020).
14. Kandlikar, S. G.; Grande, W. J. Evaluation of Single Phase Flow in Microchannels for High Heat Flux Chip Cooling — Thermohydraulic Performance Enhancement. *Heat Transf. Eng.* 2004, *25*, 5–16. doi:10.1080/01457630490519772
15. Mehendale, S. S.; Jacobi, A. M.; Shah, R. K. Fluid Flow and Heat Transfer at Micro- and Meso-Scales with Application to Heat Exchanger Design. *Appl. Mech. Rev.* 2000, *53*, 175–193. doi:10.1115/1.3097347
16. Balasubramanian, N. Friction Stir Channeling: An Innovative Technique for Heat Exchanger Manufacturing. Doctoral Thesis, Missouri University of Science and Technology, USA, 2008. https://scholarsmine.mst.edu/doctoral_dissertations/1884 (accessed June 02, 2020).
17. Mehta, K. P.; Badheka, V. J. Hybrid Approaches of Assisted Heating and Cooling for Friction Stir Welding of Copper to Aluminum Joints. *J. Mater. Process. Technol.* 2017, *239*, 336–345. doi:10.1016/j.jmatprotec.2016.08.037
18. Mehta, K. P.; Carlone, P.; Astarita, A.; Scherillo, F.; Rubino, F.; Vora, P. Conventional and Cooling Assisted Friction Stir Welding of AA6061 and AZ31B Alloys. *Mater. Sci. Eng. A* 2019, *759*, 252–261. doi:10.1016/j.msea.2019.04.120
19. Mehta, K. P.; Badheka, V. J.; Mehta, K. P.; Badheka, V. J. Effects of Tilt Angle on the Properties of Dissimilar Friction Stir Welding Copper to Aluminum. *Mater. Manuf. Process.* 2016, *31*, 255–263. doi:10.1080/10426914.2014.994754
20. Mehta, K. P.; Badheka, V. J. Influence of Tool Design and Process Parameters on Dissimilar Friction Stir Welding of Copper to AA6061-T651 Joints. *Int. J. Adv. Manuf. Technol.* 2015, *80*, 2073–2082. doi:10.1007/s00170-015-7176-1
21. Patel, N. P.; Parlikar, P.; Dhari, R. S.; Mehta, K.; Pandya, M. Numerical Modelling on Cooling Assisted Friction Stir Welding of Dissimilar Al-Cu Joint. *J. Manuf. Process.* 2019, *47*, 98–109. doi:10.1016/j.jmapro.2019.09.020
22. Mehta, K. P.; Badheka, V. J. Influence of Tool Pin Design on Properties of Dissimilar Copper to Aluminum Friction Stir Welding. *Trans. Nonferrous Met. Soc. China* 2017, *27*, 36–54. doi:10.1016/S1003-6326(17)60005-0
23. Vilaça, P.; Quintino, L.; dos Santos, J. F. iSTIR — Analytical Thermal Model for Friction Stir Welding. *J. Mater. Process. Technol.* 2005, *169*, 452–465. doi:10.1016/j.jmatprotec.2004.12.016
24. Ma, Z. Y.; Feng, A. H.; Chen, D. L.; Shen, J. Recent Advances in Friction Stir Welding/Processing of Aluminum Alloys: Microstructural Evolution and Mechanical Properties. *Crit. Rev. Solid State Mater. Sci.* 2018, *43*, 269–333. doi:10.1080/10408436.2017.1358145
25. Vyas, H.; Mehta, K. P. Effect of Multi Pass Friction Stir Processing on Surface Modification and Properties of Aluminum Alloy 6061. *KEM.* 2019, *813*, 404–410. doi:10.4028/www.scientific.net/KEM.813.404
26. Santos, T. G.; Lopes, N.; Machado, M.; Vilac, P.; Miranda, R. M. Surface Reinforcement of AA5083-H111 by Friction Stir Processing Assisted by Electrical Current. *J. Mater. Process. Technol.* 2015, *216*, 375–380. doi:10.1016/j.jmatprotec.2014.10.005
27. Santos, T. G.; Miranda, R. M.; Vilaça, P.; Teixeira, J. P. Modification of Electrical Conductivity by Friction Stir Processing of Aluminum Alloys. *Int. J. Adv. Manuf. Technol.* 2011, *57*, 511–519. doi:10.1007/s00170-011-3308-4
28. Patel, V.; Li, W.; Vairis, A.; Badheka, V. Recent Development in Friction Stir Processing as a Solid-State Grain Refinement Technique: Microstructural Evolution and Property Enhancement. *Crit. Rev. Solid State Mater. Sci.* 2019, *44*, 378–426. doi:10.1080/10408436.2018.1490251
29. Rathee, S.; Maheshwari, S.; Siddiquee, A. N.; Srivastava, M. A Review of Recent Progress in Solid State Fabrication of Composites and Functionally Graded Systems via Friction Stir Processing. *Crit. Rev. Solid State Mater. Sci.* 2018, *43*, 334–366. doi:10.1080/10408436.2017.1358146
30. Arbegast, W. J. A Flow-Partitioned Deformation Zone Model for Defect Formation during Friction Stir Welding. *Scr. Mater.* 2008, *58*, 372–376. doi:10.1016/j.scriptamat.2007.10.031
31. Zettler, R.; Vugrin, T. Effects and Defects of Friction Stir Welds. In *Friction Stir Welding from Basics to Applications*; Lohwasser, D., Chen, Z., Eds. Woodhead Publishing: Sawston, Cambridge; 2003; pp 245–276. doi:10.1533/9781845697716.2.245
32. Santos, T.; Vilaça, P.; Quintino, L. Developments in NDT for Detecting Imperfections in Friction Stir Welds in Aluminium Alloys. *Weld. World* 2008, *52*, 30–37. doi:10.1007/BF03266666

33. Zhang, Y. N.; Cao, X.; Larose, S.; Wanjara, P.; Zhang, Y. N.; Cao, X.; Larose, S.; Wanjara, P. Review of Tools for Friction Stir Welding and Processing Review of Tools for Friction Stir Welding and Processing. *Can. Metall. Q.* 2012, *51*, 250–261. doi:10.1179/1879139512Y.0000000015
34. Mishra, R. S.; De, P. S.; Kumar, N. *Friction Stir Processing: Science and Engineering*. Springer Publishing: Cham, Switzerland; 2014. doi:10.1007/978-3-319-07043-8
35. Nandan, R.; Debroy, T.; Bhadeshia, H. K. D. H. Recent Advances in Friction Stir Welding – Process, Weldment Structure and Properties. *Prog. Mater. Sci.* 2008, *53*, 980–1023. doi:10.1016/j.pmatsci.2008.05.001
36. Givi, M. K. B.; Asadi, P. *Advances in Friction Stir Welding and Processing*. Woodhead Publishing: Sawston, Cambridge; 2014. doi:10.1016/B978-0-85709-454-4.50016-1
37. Kumar, N.; Yuan, W.; Mishra, R. S. *Friction Stir Welding of Dissimilar Alloys and Materials. A Volume in Friction Stir Welding and Processing Metallographer's Guide – Practises and Procedures for Irons and Steels*. Butterworth-Heinemann Publishing: Oxford, United Kingdom; 2015. doi:10.1016/C2014-0-01707-8
38. Mishra, R. S. Intergral Channels in Metal Components and Fabrication Thereof. *Patent Application Number* 2005, 6923362. US00B2.
39. Balasubramanian, N.; Mishra, R. S.; Krishnamurthy, K. Process Forces during Friction Stir Channeling in an Aluminum Alloy. *J. Mater. Process. Technol.* 2011, *211*, 305–311. doi:10.1016/j.jmatprotec.2010.10.005
40. Rashidi, A.; Mostafapour, A.; Rezazadeh, V.; Salahi, S. Channel Formation in Modified Friction Stir Channeling. *Appl. Mech. Mater.* 2013, *302*, 371–376. doi:10.4028/www.scientific.net/AMM.302.371
41. Rashidi, A.; Mostafapour, A. Influence of Machine Parameters on Material Flow Behavior during Channeling in Modified Friction Stir Channeling. *Int. J. Mater. Form.* 2016, *9*, 1–8. doi:10.1007/s12289-014-1193-8
42. Vidal, C.; Vilaça, P. Processo de Abertura de Canais Internos Contínuos em Componentes Maciços Sem Alteração da Cota de Superfície Processada e Respectiva Ferramenta Modular Ajustável. Patent publication number PT 105628 2012.
43. Vidal, C.; Infante, V.; Vilaça, P. Characterisation of Fatigue Fracture Surfaces of Friction Stir Channelling Specimens Tested at Different Temperatures. *Eng. Fail. Anal.* 2015, *56*, 204–215. doi:10.1016/j.engfailanal.2015.02.009
44. Vidal, C. Development and Mechanical Characterization of a New Manufacturing Technology: Friction Stir Channeling. Doctoral Thesis, Technical University of Lisbon, Lisbon, Portugal, 2015.
45. Vidal, C.; Infante, V.; Vilaça, P. Fatigue Behavior at Elevated Temperature of Friction Stir Channelling Solid Plates of AA5083-H111 Aluminium Alloy. *Int. J. Fatigue* 2014, *62*, 85–92. doi:10.1016/j.ijfatigue.2013.10.012
46. Vidal, C.; Infante, V.; Vilaça, P. Fatigue Assessment of Friction Stir Channels. *Int. J. Fatigue* 2014, *62*, 77–84. doi:10.1016/j.ijfatigue.2013.10.009
47. Vidal, C.; Infante, V.; Vilaça, P. Mechanical Characterization of Friction Stir Channels under Internal Pressure and in-Plane Bending. *KEM.* 2011, *488–489*, 105–108. www.scientific.net/KEM.488-489.105. doi:10.4028/
48. Vidal, C.; Infante, V.; Vilaça, P. Assessment of Performance Parameters for Friction Stir Channelling. Proceedings of the IIW 2011 International Conference on Global Trends in Joining, Cutting and Surfacing Technology, Chennai, India; 2011; pp 21–22.
49. Vidal, C.; Infante, V.; Vilaça, P. Effect of Microstructure on the Fatigue Behavior of a Friction Stirred Channel Aluminium Alloy. *Proc. Eng.* 2013, *66*, 264–273. doi:10.1016/j.proeng.2013.12.081
50. Vidal, C.; Infante, V.; Vilaça, P. Metallographic Characterization of Friction Stir Channels. *MSF.* 2012, *730–732*, 817–822. doi:10.4028/www.scientific.net/MSF.730-732.817
51. Nordal, D. Design, Development and Analysis of Tools for Hybrid Friction Stir Channeling. Masters Thesis, Aalto University, Finland, 2017. http://urn.fi/URN. NBN:fi:aalto-201707045989 (accesed June 02, 2020).
52. Vidal, C.; Baptista, R.; Infante, V. Numerical Simulation of the Fatigue Behavior of a Friction Stirred Channel Aluminium Alloy. 12th International Fatigue Congress (FATIGUE 2018), MATEC Web of Conferences, EDP Sciences. Vol. 165, 2018; p 21008. doi:10.1051/matecconf/201816521008
53. Vidal, C.; Baptista, R.; Infante, V. Experimental and Numerical Investigation on the Fatigue Behavior of Friction Stirred Channel Plates. *Eng. Fail. Anal.* 2019, *103*, 57–69. doi:10.1016/j.engfailanal.2019.04.068
54. Vidal, C.; Infante, V. Role of Friction Stir Channel Geometry on the Fatigue Behavior of AA5083-H111 at 120 °C and 200 °C. *AMR.* 2014, *891–892*, 1494–1499. www.scientific.net/AMR.891-892.1494. doi:10.4028/
55. Vidal, C.; Infante, V.; Lage, Y.; Vilaça, P. Modelling Microstructural Effects on the Mechanical Behavior of a Friction Stirred Channel Aluminium Alloy. *KEM.* 2013, *577–578*, 37–40. www.scientific.net/KEM.577-578.37. doi:10.4028/
56. Vidal, C.; Infante, V.; Vilaça, P. Monitoring of the Mechanical Load and Thermal History during Friction Stir Channelling under Constant Position and Constant Force Control Modes. *J. Manuf. Process.* 2020, *49*, 323–334. doi:10.1016/j.jmapro.2019.11.01677
57. Vidal, C.; Infante, V.; Vilaça, P. Metallographic and Morphological Characterization of Sub-Surface Friction Stirred Channels Produced on AA5083-H111. *Int. J. Adv. Manuf. Technol.* 2019, *105*, 2215–2235. doi:10.1007/s00170-019-04459-7
58. Dasgupta, S. Modelling and Testing of Hybrid Channeling Plates for Thermal Management of Batteries for Electrical Vehicles. Masters Thesis, Aalto University, Finland, 2017. http://urn.fi/URN:NBN:fi:aalto-201712188188 (accessed June 02, 2020).

59. Tang, W.; Reynolds, A. P. Production of Wire via Friction Extrusion of Aluminum Alloy Machining Chips. *J. Mater. Process. Technol.* 2010, *210*, 2231–2237. doi:10.1016/j.jmatprotec.2010.08.010
60. Abbas, N. M.; Deng, X.; Reynolds, A. P. Compaction of Machining Chips: Extended Experiments and Modeling. *Mech. Mater.* 2020, *141*, 103249. doi:10.1016/j.mechmat.2019.103249
61. Gandra, J. Methods and Appratus for Creating Channels in Workpieces. Patent publication number WO 2018/083438 2018.
62. Vilaça, P.; Karvinen, H. Solid-State Production of a Channel and a Weld Joint in One Simultaneous Action by Stirring Multiple-Components and Partial Extraction of the Processed Material into Flash. Patent number FI 20160247 2016.
63. Yan, T.; Zhan, X.; Gao, Q.; Wang, F.; Ling, W. Influence of Laser Power on Molten Pool Flow Field of laser-MIG Hybrid Welded Invar Alloy. *Opt. Laser Technol.* 2021, *133*, 106539. doi:10.1016/j.optlastec.2020.106539
64. Mira, I. F. Modelling of Thermal Management by Hybrid Channeling. Masters Thesis, Aalto University, Finland, 2018. http://urn.fi/URN:NBN:fi:aalto-201806293864 (accessed June 02, 2020).
65. Karvinen, H.; Nordal, D.; Vilaça, P. Microstructural Characterization of the Stir Processed Zones of Cu-Al and Al-Al Plate Systems Manufactured by Hybrid Friction Stir Channeling. 12th lnternational Symposium on Friction Stir Welding, Candada, 2018; pp 1–18.
66. Karvinen, H.; Nordal, D.; Galkin, T.; Vilaça, P. Application of Hybrid Friction Stir Channeling Technique to Improve the Cooling Efficiency of Electronic Components. *Weld. World* 2018, *62*, 497–509. doi:10.1007/s40194-018-0576-8
67. Balasubramanian, N.; Mishra, R. S.; Krishnamurthy, K. Friction Stir Channeling: Characterization of the Channels. *J. Mater. Process. Technol.* 2009, *209*, 3696–3704. doi:10.1016/j.jmatprotec.2008.08.036
68. Balasubramanian, N.; Mishra, R. S. Development of a Mechanistic Model for Friction Stir Channeling. *J. Manuf. Sci. Eng.* 2016, *132*, 54504. doi:10.1115/1.4002453
69. Balasubramanian, N.; Krishnamurthy, K.; R. S. Mishra. Preliminary Study of Pressure Drop and Heat Transfer through a Friction Stir Channel. ASME 2007 International Mechanical Engineering Congress and Exposition, 2007; pp 933–939. doi:10.1115/IMECE2007-41634
70. Pandya, S.; Mishra, R. S.; Arora, A. Channel Formation during Friction Stir Channeling Process — A Material Flow Study Using X-Ray Micro-Computed Tomography and Optical Microscopy. *J. Manuf. Process.* 2019, *41*, 48–55. doi:10.1016/j.jmapro.2019.03.021
71. Salimi, S.; Haghpanahi, M.; Bahemmat, P. Fabrication of Cooling Channels Employing Worm Voids Caused by Friction Stir Based Process: Considering Cooling and Fluid Parameters. *J. Manuf. Process.* 2018, *35*, 61–70. doi:10.1016/j.jmapro.2018.07.016
72. Pandya, S.; Gurav, S.; Hedau, G.; Saha, S.; Arora, A. Effect of Axial Conduction in Integral Rough Friction Stir Channels: Experimental Thermo-Hydraulic Characteristics Analyses. *Heat Mass Transfer* 2020, *56*, 1725–1738. doi:10.6013/jbrewsoc-japan1915.62.477
73. Rashidi, A.; Mostafapour, A.; Salahi, S.; Rezazadeh, V. Modified Friction Stir Channeling: A Novel Technique for Fabrication of Friction Stir Channel. *AMM.* 2013, *302*, 365–370. www.scientific.net/AMM.302.365. doi:10.4028/
74. Rashidi, A.; Mostafapour, A. Influence of Tool Pin Geometry and Moving Paths of Tool on Channel Formation Mechanism in Modified Friction Stir Channeling Technique. *Int. J. Adv. Manuf. Technol.* 2015, *80*, 1087–1096. doi:10.1007/s00170-015-7049-7
75. Rashidi, A.; Mostafapour, A. Influence of Tool Geometry on the Channel Formation along the Linear and Non-Linear Channeling Using Modified Friction Stir Channeling. *Proc. Inst. Mech. Eng. Part B J. Eng. Manuf.* 2015, *231*, 1–10. doi:10.1177/0954405415598943
76. Ferraz, M. F. S. Friction Stir Channeling Industrial Applications Prototype Design and Production. Masters Thesis, University of Lisbon, Portugal, 2012. https://fenix.tecnico.ulisboa.pt/downloadFile/395144527870/Dissertacao_.pdf (accessed June 02, 2020)
77. Karvinen, H.; Aleni, A. H.; Salminen, P.; Minav, T.; Vilaça, P. Thermal Efficiency and Material Properties of Friction Stir Channelling Applied to Aluminium Alloy AA5083. *Energies* 2019, *12*, 1549. doi:10.3390/en1208
78. Aleni, A. H. Development of Technological Conditions and Applications of Friction Stir Channeling. Masters Thesis, Aalto University, Finland, 2014. http://urn.fi/URN:NBN:fi:aalto-201502191902 (accessed June 02, 2020).
79. Karvinen, H.; Nordal, D.; P. Vilaça, New Development and Testing of FSChanneling Technique: HybridFSC. 10th International Conference on Trends in Welding Research and 9th International Welding Symposium of Japan Welding Society (9WS). 2017; pp 376–379.
80. Karvinen, H.; Vilaça, P.; Nordal, D. A Non-Consumable Tool and a Process for Solid - State Production of a Channel and a Weld Joint, and a Structure of at Least Two Components Based on Originally Bulk Components of Similar, or Dissimilar, Materials. Patent publication number PCT/FI2017/050467 2019.
81. Gandra, J. Integration of Thermal Managements Networks into Aluminium Structures by Stationary Shoulder Friction Stir Channelling. *The 6th International Conference on Scientific and Technical Advances on Friction stir Welding & Processing* (FSWP'2019). 2019, Vol. 1. https://sites.uclouvain.be/fswp2019/presentations.php?ind=893 (accessed June 02, 2020).
82. Vilaça, P.; Karvinen, H. One-Action Simultaneous Production of Welding between Multiple Components and Internal Closed Channels within

the Processed Zone: Hybrid Friction Stir Channeling. Patent number FI 20160165 2016.
83. Cavaliere, P.; Squillace, A.; Panella, F. Effect of Welding Parameters on Mechanical and Microstructural Properties of AA6082 Joints Produced by Friction Stir Welding. *J. Mater. Process. Technol.* 2008, *200*, 364–372. doi:10.1016/j.jmatprotec.2007.09.050
84. Akinlabi, E. T.; Mahamood, R. M. *Solid-State Welding: Friction and Friction Stir Welding Processes*. Springer International Publishing: Cham, Switzerland. 2020. doi:10.1007/978-3-030-37015-2
85. Arici, A.; Selale, S. Effects of Tool Tilt Angle on Tensile Strength and Fracture Locations of Friction Stir Welding of Polyethylene. *Sci. Technol. Weld. Join* 2007, *12*, 536–539. doi:10.1179/174329307X173706
86. Snyder, B.; Li, K. T.; Wirtz, R. A. Heat Transfer Enhancement in a Serpentine Channel. *Int. J. Heat Mass Transf.* 1993, *36*, 2965–2976. doi:10.1016/0017-9310(93)90026-3
87. York, N.; Oosthuizen, P. H.; Austin, M. Channel-to-Channel Pressure Differences in Serpentine Minichannel Flow Systems. *Microscale Thermophys. Eng.* 2005, *9*, 49–48. doi:10.1080/10893950590913233
88. Li, B.; Chai, S.; Tian, F.; D. Y. Kwok, Interfacial Electrokinetic Effects on Fluid Flow in Microchannel by a Generalized Lattice Boltzmann Model. ASME 2003 1st International Conference on Microchannels and Minichannels, **2003**; pp 345–350. doi:10.1115/ICMM2003-1040
89. Zappia, T.; Smith, C.; Colligan, K.; Ostersehlte, H.; S. W. Kallee, Friction Stir Welding Equipment. In *Friction Stir Welding: From Basics to Applications*; Lohwasser, D., Chen, Z., Eds. Woodhead Publishing: Sawston, Cambridge; 2009; pp 73–117. doi:10.1533/9781845697716.1.74
90. Ohadi, M. M.; Choo, K.; Dessiatoun, S.; Cetegen, E. *In SpringerBriefs in Applied Sciences and Technology/SpringerBriefs in Thermal Engineering and Applied Science. Next Generation Microchannel Heat Exchangers*, Springer: Verlag New York; 2012. doi:10.1007/978-1-4614-0779-9
91. Salminen, P. Improving Mechanical and Thermal Design of New Energy Production Systems. Doctoral Thesis, Aalto University, Finland, 2017. https://aalto-doc.aalto.fi/handle/123456789/29058 (accessed June 02, 2020).
92. Singh, S.; Pal, K. Effect of Texture Evolution on Mechanical and Damping Properties of SiC/ZnAl 2 O 4/Al Composite through Friction Stir Processing. *J. Mater. Res. Technol.* 2019, *8*, 222–232. doi:10.1016/j.jmrt.2017.07.006
93. INTA Technologies, Brazed Metal & Ceramic to Metal Assemblies, 2020. http://www.intatech.com/brazed-metal-ceramic-assemblies.html (accessed June 02, 2020).
94. Drahansky, M.; Paridah, M.; Moradbak, A.; Mohamed, A.; Abdulwahab Taiwo Owolabi, F.; Asniza, M.; Abdul Khalid, S. H. Current Issues and Problems in the Joining of Ceramic to Metal. *Joining Technol.* 2016, *159–193*. doi:10.5772/64524
95. Cipriano, G. P.; Blaga, L. A.; dos Santos, J. F.; Vilaça, P.; Amancio-Filho, S. T. Fundamentals of Force-Controlled Friction Riveting: Part I-Joint Formation and Heat Development. *Materials (Basel)* 2018, *11*, 2294. doi:10.3390/ma11112294
96. Reitschuster, L.; Richter, D. Friction-Stir Welding Effectively Seals Aluminum Parts, 2018. https://www.spotlightmetal.com/friction-stir-welding-effectively-seals-aluminum-parts-a-725334 (accessed June 02, 2020).
97. Mishra, R. S.; Ma, Z. Y. Friction Stir Welding and Processing. *Mater. Sci. Eng. R Reports* 2005, *50*, 1–78. doi:10.1016/j.mser.2005.07.001
98. Nct Inc. Benefits of friction welding – product improvement 1, 2018. https://nctfrictionwelding.com (accessed June 02, 2020).
99. Givi, M. K. B.; Asadi, P. General Introduction. In *Advances in Friction-Stir Welding and Processing*. Woodhead Publishing Limited; Sawston, Cambridge, 2014; pp 1–19. doi:10.1533/9780857094551.1.
100. Lim, Y. C.; Warren, C. D.; Chen, J.; Feng, Z. Joining of Lightweight Dissimilar Materials by Friction Self-Piercing Riveting. In *Friction Stir Welding and Processing X*. Springer International Publishing: Cham, Switzerland; 2019; pp 189–195. doi:10.1007/978-3-030-05752-7.
101. Dehghan, S.; Ismail, M. I. S. B.; Mohd Ariffin, M. K. A. B.; Baharudin, B. T. H. T. B. Friction Drilling of Difficult-to-Machine Materials: Workpiece Microstructural Alterations and Tool Wear. *Metals (Basel)* 2019, *9*, 945. doi:10.3390/met9090945
102. Gerlich, A. P.; North, T. H. Friction Stir Spot Welding.*In Innov. Mater. Manuf. Fabr. Environ. Saf*; Schwartz, M., Ed.; Routledge & CRC Press, United Kingdom, 2010, 193–213. doi:10.1201/b10386.
103. Zelinski, P. How a Solid-State Process Stood Firm Until Additive's Moment, 2019. https://www.additivemanufacturing.media/blog/post/building-confidence-in-additive-manufacturing-for-tooling (accessed June 02, 2020).
104. Kevan, T. MELD Introduces Solid-State 3D Printing System, 2018. https://www.digitalengineering247.com/article/meld-manufacturing-introduces-solid-state-3d-system (accessed June 02, 2020).
105. Peels, J. Friction Stir Additive Manufacturing Used for Functionally Graded Components, 2017. https://3dprint.com/174645/friction-stir-am (accessed on June 02, 2020).
106. Shekh, A. Development of Friction Flash to Tube (F2T) and Application to S355 Grade Steel. Masters Thesis, Aalto University, Finland, 2017. https://aalto-doc.aalto.fi/handle/123456789/27081 (accessed June 02, 2020).
107. Meinhardt, C. P.; Chludzinski, M.; Ribeiro, R. F.; Rocha, C. L. F.; Santos, A. C. S.; Strohaecker, T. R. Evaluation of Friction Hydro-Pillar Processing Welding in Duplex Stainless Steels (UNS S31803). *J. Mater. Process. Technol.* 2017, *246*, 158–166. doi:10.1016/j.jmatprotec.2017.03.010